Efficient antisense targeting of Human Immunodeficiency Virus 1 (HIV-1) requires the Rev Response Element (RRE) and Rev protein

Alex Michael Ward
Indianapolis, Indiana

Bachelor of Arts, Reed College, 1998

A Dissertation presented to the Graduate Faculty
of the University of Virginia in Candidacy for the Degree of
Doctor of Philosophy

Department of Microbiology

University of Virginia
August, 2008
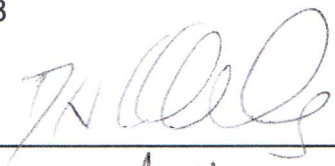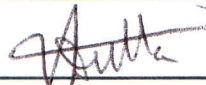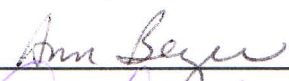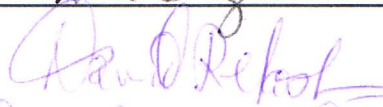
Abstract

An HIV-1-based vector expressing antisense RNA to *env* is currently in clinical trials. This vector has shown a remarkable ability to inhibit HIV-1 replication, in spite of the fact that therapeutic use of antisense RNAs has generally been disappointing. We decided to further analyze the basis for why the antisense inhibition is so efficient. To determine if co-targeting to common RNA export pathways made a significant contribution to efficient antisense inhibition, we constructed plasmid-based HIV-1 LTR-driven vectors that contained different export elements or no export element at all. The RNA expressed from these vectors was complementary to the HIV-1 *env* region and included either a Rev Response Element (RRE), which used the Rev/RRE export pathway, or a MPMV Constitutive Transport Element (CTE), which used the Tap/Nxf1 export pathway. The RRE-driven antisense RNA efficiently inhibited p24 production from an RRE-driven provirus, whereas the CTE-driven antisense inhibited only at higher concentrations. The vector without the export element failed to inhibit. The RRE-driven antisense also efficiently inhibited p24 production from a pNL4-3 provirus that uses the CTE for RNA export, indicating that cotargeting was not essential for efficient antisense inhibition. On the other hand, the CTE-driven antisense demonstrated a greater efficiency of antisense inhibition on the CTE-driven provirus than it did on the RRE-driven provirus, although in both cases the CTE-driven antisense was not as efficient as the RRE-driven antisense. Thus, efficient antisense inhibition required that the antisense RNA trafficked through

the Rev/RRE pathway. When RevM10-Tap and Nxt1 were coexpressed with RRE-driven provirus and antisense, forcing both the target and antisense RNA to use the Tap pathway, p24 production inhibited less efficiently. In fact, the RRE-driven antisense construct inhibited p24 production at similar levels as the CTE-driven construct.

Mechanistic studies demonstrated that nuclear retention does not contribute to antisense inhibition, since the GagPol and antisense RNA localized to the cytoplasmic fraction. We examined the stability of vector and GagPol target RNA to determine if degradation contributed to antisense inhibition and found that netiher vector nor target RNA was rapidly degraded. Since GagPol RNA efficiently localized to the cytoplasm and was not degraded in the presence of antisense RNA, we wanted to distinguish between an effect on protein levels and an effect on particle assembly and release. To do this, we examined protein expression levels from a provirus that produced GagPol Pr160 that could not be assembled into viral particles or released. We found that coexpression of the RRE-driven antisense led to reduced GagPol Pr160 levels, suggesting that the antisense RNA did not affect virus assembly or release, but rather protein levels. To determine if antisense expression had non-specific effects on protein expression, we assayed HIV-1 Nef expression from an RRE-driven provirus in the presence of antisense RNA. Nef is encoded by a multiply spliced HIV-1 RNA that does not contain the antisense target sequence, so specific antisense RNA inhibition would not be expected to reduce Nef levels. In the presence of RRE-

and CTE-driven antisense, Nef protein levels were not significantly reduced,

demonstrating that antisense inhibition is specific to RNA containing the target

sequence. Actively translated RNAs typically localize to the polyribosome. We

examined localization of the GagPol RNA to the polyribosome in the presence of

RRE-driven sense or antisense RNA. We found that there was no significant

difference in polyribosomal localization of GagPol RNA in the presence of sense

or antisense RNA. In addition, we determined that localization of the GagPol

RNA was specific to the polyribosome, since EDTA treatment abolished

localization. Our results demonstrate that antisense RNA expression leads to

reduced GagPol protein levels but not reduced localization to the polyribosome.

In addition, efficient antisense inhibition requires export of the antisense RNA via

the Rev/RRE pathway.

Acknowledgements

I would like to thank my mentors Drs. Lou Hammarskjöld and David Rekosh for their guidance and support during my training at UVA. I would also like to thank my committee members, past and present, Drs. Ann Beyer, Anindya Dutta, Ian Macara, Lucy Pemberton and Dean Kedes for their input, guidance and advice on this project. Many thanks to HamRek lab members past and present who provided training, reagents and support over the years. In particular, I would like to highlight the invaluable support of Dr. Yeou-Cherng Bor, or "The Closer". Other members I'd like to thank include Kate Hawley, Greg Singer, John Coyle, Li Jin, Sue Prasad, Jennifer Swartz, Ying Li, Yuming Xue, Joy Niesen-Morgenegg, Hua Cheng, Yukiko Misawa, Emily Sloan, Lafuno Mavhandu, Pascal Bessong, Gloria Bowers, Eileen Trainum and many others over the years. Thanks to all of my fellow Microbiology students for their support and discussions, in particular Colin de Bakker and Kurt Jensen. Thanks to all my other friends, non-Microbiology students and non-students alike, for being there whenever I needed you. Of course, I have to thank my parents and family for their support and not asking too many questions about when I'll finish. Many thanks to my wife, Dr. Meredith Calvert, my constant companion and confidante. I couldn't have done it without you.

Dedication

For Meredith and all my kitties, past and present.

Table of Contents

List of Figures

List of Tables

Chapter 1- Introduction

The Human Immunodeficiency Virus-1 and Acquired Immune Deficiency

Syndrome

An estimated 30 to 36 million people were living with Human Immunodeficiency Virus 1 (HIV-1) infection in 2007, with approximately two million new infections and nearly two million deaths from infection predicted per year (http://www.who.int/hiv/mediacentre/en/). The true number of new infections and AIDS-related deaths cannot be known due to logistical and technical challenges, as developing nations often lack the health infrastructure necessary to actively monitor infection rates. Social stigma can also discourage individuals from getting tested, even when there is an established health infrastructure (27).

HIV-1 has an incubation period of several months before antibodies to it can be consistently detected in infected individuals. In addition, the onset of AIDS following HIV-1 infection can occur anytime from several months to several years. Constant monitoring for new infections and the development of drug resistance is required in order to reduce the impact of AIDS on the lives and wellbeing of millions of individuals. While great advances have been made in understanding the basic biology and treatment of HIV-1, more work is necessary to identify new therapeutic targets, develop a protective vaccine and effectively prevent its spread (38, 71).

HIV-1 is a blood-borne pathogen typically transmitted through unprotected sex or needle sharing. The initial infection presents with flu-like symptoms that subside as the immune system controls the infection. However, patients eventually progress to Acquired Immune Deficiency Syndrome (AIDS) following the destruction of host CD4+ T cells, especially in the absence of treatment. Prior to the identification of HIV-1 as the causative agent of AIDS, patients typically presented with immune deficiency and death due to opportunistic infection (71).

Overview of Basic HIV-1 Biology

The General Problem

The following information is intended to provide a general overview of HIV-1 structure and biology. There are several excellent overviews in Field's Virology, with more current information presented in various reviews (2, 12, 26, 41, 43, 88). A virus faces several challenges in order to successfully produce progeny virion. At a basic cellular level, it is an obligate parasite. It must hijack the host cell to successfully produce viral enzymes and structural proteins required to form the virus particle. The virus must also package its genome encoding the necessary viral proteins for subsequent rounds of infection. Viral factors must interact with cellular proteins and take advantage of the host cell machinery to provide whatever components the virus cannot encode or carry. At

the same time, a virus must avoid detection by the host's immune system, which would prevent virus replication. Finally, the virus must be transmitted to new hosts for additional rounds of replication. For a general discussion of virus replication, please refer to Roizman and Palese in Field's Virology (116).

Virus Structure

HIV-1 is a Lentivirus of the family *Retroviridae* composed of an approximately 9 kilobase RNA genome encoding fifteen proteins (41). A pictorial representation of the virion structure and contents is presented in Figure 1. Each enveloped virion contains two copies of the RNA genome as well as the viral enzymes Protease (PR), Reverse Transcriptase (RT) and Integrase (IN).   Virions appear spherical with a conical core containing the RNA genomes, which interact with each other at their 5' ends.   The RNA genomes are bound by the Gag-derived nucleocapsid protein and tRNA *lys*, which acts as a primer for reverse transcription (145). The Env proteins, gp41 TM and gp120 SU, are generated by proteolytic cleavage of the gp160 Env precursor protein. The gp41 TM is incorporated into the viral envelope derived from the host cell membrane (88). The gp120 SU protein is bound to gp41 TM on the surface of the virus particle and binds to the HIV-1 cellular receptor.

The Virus Life Cycle
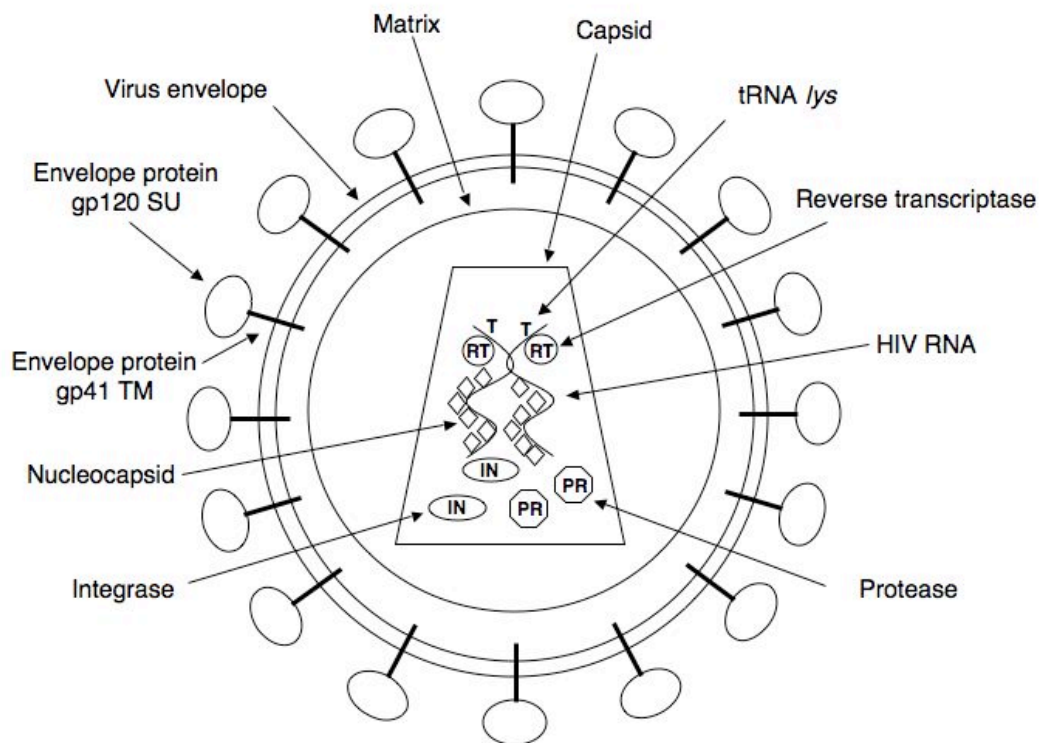
Figure 1: HIV-1 virion structure.

The major components of the HIV-1 virion are indicated. The conical virion core contains the HIV-1 enzymes RT, PR and IN, the RNA genomes and p7 NC. The two RNA genomes are associated with p7 NC protein and tRNA *lys*, which acts as a primer for reverse transcription. The core is encapsulated by the p17 MA proteins. The virion is enveloped by a membrane derived from the host cell that contains the gp41 TM Env protein, which is bound by the gp120 SU protein. The amounts of each component shown in this figure, excluding the RNA genomes are not representative of their actual amounts. Adapted from (88).

As schematized in Figure 2, the HIV-1 life cycle is made up of multiple intricate steps utilizing both the cellular machinery and virus-encoded factors. Briefly, the virus enters the host cell by binding to its cellular receptor, CD4, and a coreceptor, CCR5 or CXCR4 (5, 37). Following receptor binding, the HIV-1 Envelope protein undergoes a conformational change allowing fusion of the viral membrane to the host cell membrane, releasing the capsid into the host cell (18). After entering the host cell cytoplasm, the RNA genome is reverse transcribed into a DNA provirus, also called the pre-integration complex (PIC) (9, 157). The PIC is uncoated and translocated to the host nucleus, where it is integrated into the host genome by the viral IN enzyme (96, 157). The integrated provirus undergoes RNA polymerase II-mediated transcription and viral RNAs are exported from the nucleus for translation and/or packaging. Following translation of viral structural proteins, capsids are assembled at the host cell membrane, the viral RNA is packaged and immature virion are released from the host cell (2, 12, 43, 130). Following release from the host cell, the Gag precursor protein that makes up the immature virus capsid are cleaved by the viral protease to yield mature, infectious virus (26).

HIV-1 proteins and coding mRNAs

HIV-1 encodes fifteen proteins from an approximately 9 kb primary transcript. Several mechanisms contribute to this diversity of proteins obtained
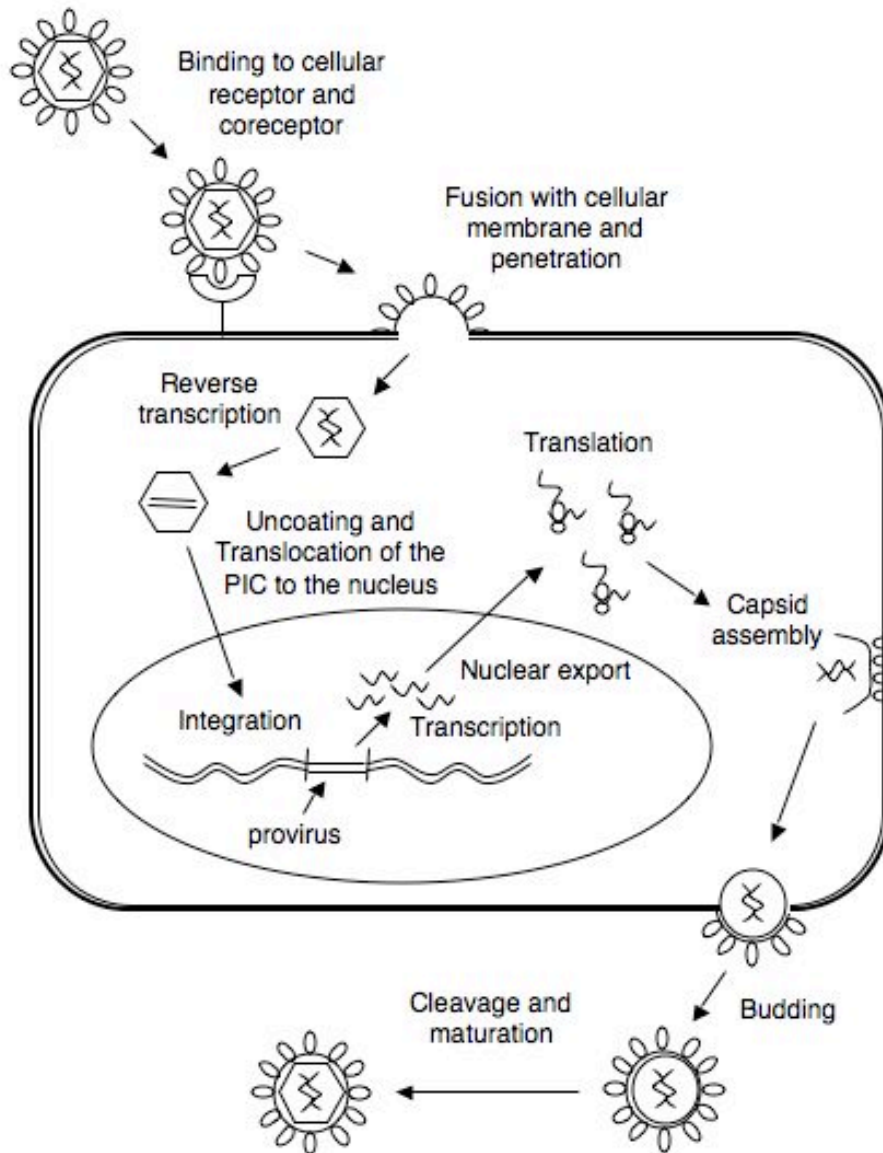
Figure 2: Diagram illustrating the HIV-1 life cycle

An infectious virion binds to the CD4 host cell receptor via the gp120 SU Env protein which undergoes a conformational change to associate with its coreceptor and fuse with the host cell membrane. Following entry, the virion core is uncoated and the RNA genome undergoes reverse transcription. The viral DNA is uncoated and translocated to the nucleus, where it integrates into the host genome. Following transcription, viral RNAs are exported to the cytoplasm and translated. Immature structural proteins assemble at the host cell membrane and package the viral RNA genome. Assembled capsids are budded from the host cell membrane, incorporating the Env proteins and released. Released virion undergo a maturation step that cleaves Gag into the CA, MA and NC proteins and give rise to infectious virion. Adapted from (26).

from relatively constrained coding sequence. The greatest diversity is derived from alternative splicing of the primary HIV-1 transcript, as depicted in Figure 3 (111). However, additional mechanisms, such as proteolytic cleaveage, ribosomal frameshifting and bicistronic messages maximize the use of the coding capacity (41).

The Gag and Pol proteins are derived from the unspliced 9 kb transcript and utilize proteolytic cleavage to generate the viral structural proteins and enzymes. The reading frame starts with the Gag polyprotein, which is cleaved by the viral Protease enzyme to give rise to the Matrix (MA), Capsid (CA), and Nucleocapsid (NC) (see Figure 3). The Pol proteins are derived from the GagPol Pr160 polyprotein, which is cleaved into the Gag proteins, as well as the viral enzymes Reverse Transcriptase (RT), Protease (PR) and Integrase (IN). The Pol coding sequence is located 3' of the Gag sequence, separated by an AU-rich region, which can cause a ribosomal frameshift. The majority of GagPol RNAs are translated into the Gag Pr55 protein only, but occasionally, the frameshift occurs, resulting in production of the GagPol Pr160 protein (106).

The Vpu and Env proteins are derived from a single mRNA, like all of the Gag and GagPol proteins, but a different mechanism is used to produce these two proteins from the same mRNA. The *vpu* coding sequence is located 5' to *env* in a different reading frame on the Vpu/Env mRNA (122). The *vpu* start codon is weak and the *env* start codon is strong, allowing ribosomal readthrough to occur. Thus, most of the time, the ribosome scans past the *vpu* start codon,
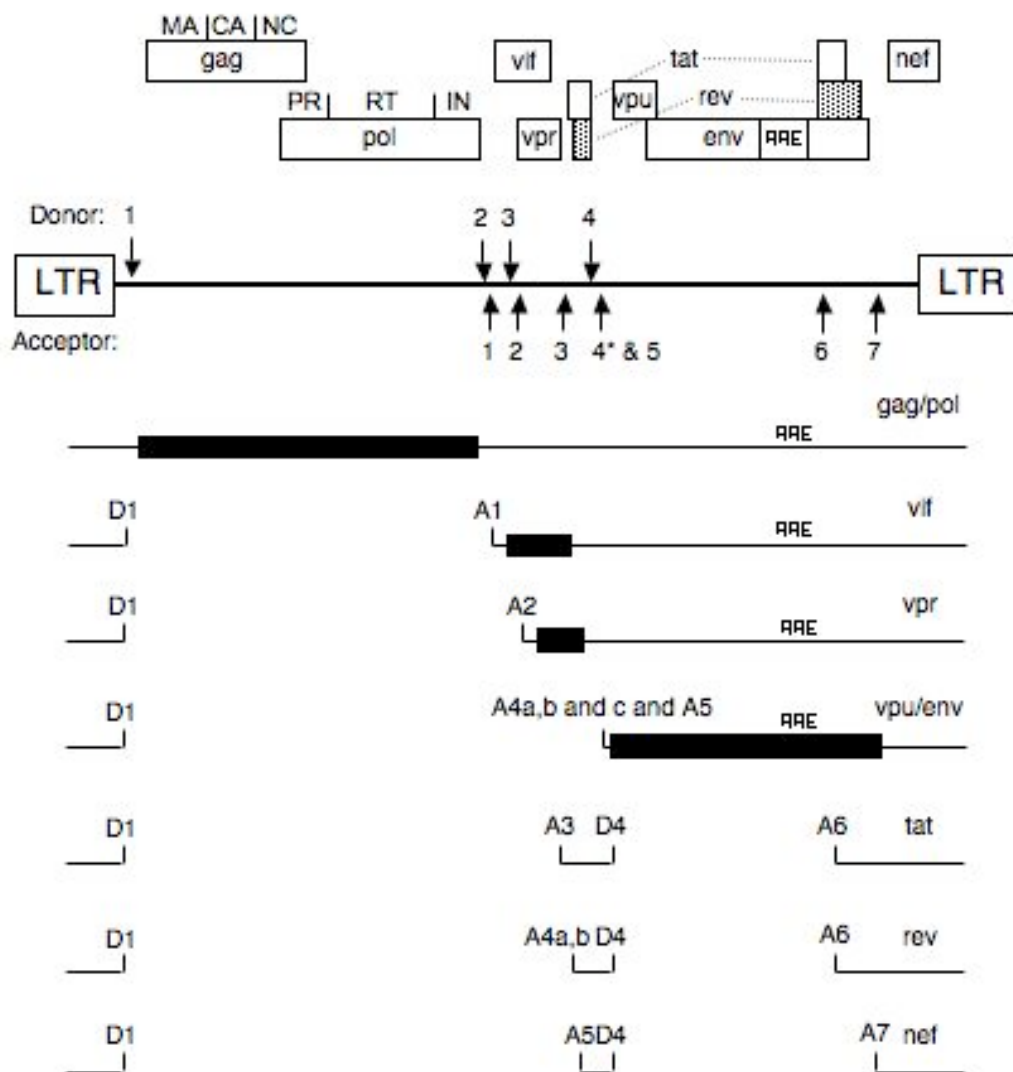
Figure 3: Diagram of alternative splicing pattern of HIV-1 RNAs

The HIV-1 open reading frames are illustrated by boxes and labeled according to their product. The primary HIV-1 transcript can be spliced using any of the Donor or Acceptor sites illustrated above. The predominant species of splice variants, their products and the splice donors and acceptors used to generate them are labeled. Solid boxes illustrate the approximate reading frame for proteins translated from unspliced or singly spliced RNAs.

continuing on to the *env* strong start codon, although in some cases, the Vpu

protein is translated. Experiments have shown that when the weak start codon is

mutated to become a strong start codon, only Vpu is produced from the Vpu/Env

RNA (3, 123).

The problem of intron retention

Alternative splicing of the primary HIV-1 transcript gives rise to multiple

species of RNA consisting of unspliced, singly spliced and multiply spliced

species. Figure 3 illustrates the alternative splice pattern of HIV-1 RNA. The

multiply spliced RNAs encode the Tat, Rev and Nef accessory proteins. The

singly spliced RNAs encode the Vif, Vpr and Vpu accessory proteins, as well as

the Env protein. The unspliced RNA encodes the Gag and GagPol proteins, in

addition to acting as the RNA genome for progeny virion (111). The challenge of

using this form of alternative splicing to allow gene expression is that unspliced

and incompletely spliced RNAs are typically retained in the nucleus and

eventually degraded (19, 125). HIV-1 has evolved a strategy to overcome

retention and promote the export of incompletely spliced viral RNA, relying on a

structured RNA element in the Env coding sequence, the Rev Response Element

(RRE), and the Rev accessory protein (36, 54, 91). Rev is derived from a

multiply spliced RNA, so the RNA is not subject to nuclear retention. Rev is a 19

kilodalton phosphoprotein containing an arginine-rich RNA binding domain

overlapping its nuclear localization domain. Rev also contains a nuclear export

sequence that binds to the Chromosomal Region Maintenance 1 protein (Crm1), which in turn recruits RanGTP in order to accomplish transport from the nucleus to the cytoplasm (40, 99). Figure 4 (left panel) illustrates the binding of Rev to the RRE and recruitment of Crm1 and RanGTP that facilitates nuclear export of RRE-containing RNAs.

Another example of a structured RNA element utilized for nuclear-cytoplasmic transport from the Retrovirus family is the Mason-Pfizer Monkey Virus Constitutive Transport Element (MPMV CTE). Unlike HIV-1, which uses a virus-encoded protein to accomplish RNA export, the MPMV CTE utilizes cellular proteins for transport (34, 108). The CTE is bound by the Tip (Tyrosine kinase-interacting protein) -associated protein/Nuclear export factor 1 (Tap/Nxf1) that functions with a cofactor, Nxt1/p15, to overcome nuclear retention of incompletely spliced RNAs (48, 51). In addition to accomplishing nuclear export of CTE-containing RNAs, Tap/Nxf1 and Nxt1 have been shown to enhance translation of CTE-containing RNAs (51, 62, 108). Whether Rev possesses similar translation functions has yet to be determined. Figure 4 (right panel) illustrates the binding of Tap/Nxf1 and its association with Nxt1 to accomplish RNA export and translation. The Crm1-specific inhibitor, Leptomycin B, inhibits Rev-mediated, but not Tap-mediated, RNA export, demonstrating that the Rev and Tap pathways are independent pathways of nuclear export (105). However, the CTE can substitute for the RRE for export in the context of an HIV-1 provirus (105, 161).
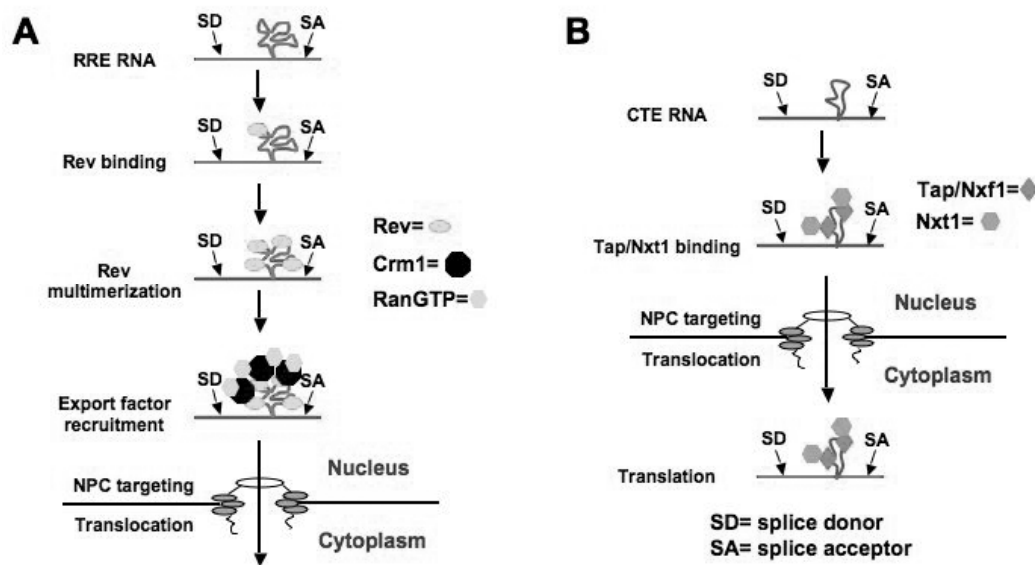
Figure 4: Two pathways for nuclear export of unspliced RNAs

(A) The HIV-1 Rev protein binds to a structured RNA element, the RRE, and recruits Crm1 to overcome nuclear retention. (B) The CTE relies on the cellular proteins Tap/Nxf1 and Nxt1 in order to overcome nuclear retention and enhance translation from CTE-containing RNAs.

An additional cofactor associated with the MPMV CTE is the Src-Associated in Mitosis 68 (Sam68) protein. Sam68 was identified as a substrate of Src tyrosine kinase during mitosis and is a member of the STAR (signal transduction and activation of RNA) family of proteins (42, 136, 137, 143). STAR proteins contain an hnRNP K homology and high affinity RNA binding domains and have been implicated in both translation and alternative splicing (60, 64, 132, 143). Sam68 increases polyribosomal localization and translation of CTE-containing RNAs and this function is regulated by phosphorylation by the Src homolog Sik/Brk (28).

Anti-HIV-1 Therapeutics and Drug Resistance

Following the identification of HIV-1 as the causative agent for AIDS by two separate research groups in France and the US, great strides were made in developing treatments. Many antiretroviral therapies have been developed since the beginning of the AIDS epidemic, listed in Table I, that have dramatically increased the time from HIV-1 infection to onset of AIDS (135). These therapies initially fell into two categories: Nucleoside analog Reverse Transcriptase Inhibitors (RTIs) and Protease Inhibitors (PIs), with the eventual development of Non-nucleoside RTIs. RTIs work by inhibiting the conversion of the RNA genome of HIV-1 into DNA, thus preventing its integration into the host genome. PIs prevent the proteolytic processing of immature progeny virion, rendering those

Table 1: FDA-approved drugs to treat HIV-1 infection
FDA-approved drugs to treat HIV-1 infection, including their targets, clinical names and mechanism of action (NIH AIDS Research and Reference Reagent Program and the Stanford University HIV Drug Resistance Database)

Class of drug	Target	Drug	Mechanism of action
Nucleoside/ nucleotide analog RT inhibitor	HIV-1 RT	D4T/Stavudine ddC/2'3'dideoxycytidine DDI/2'3' dideoxyinosine AZT/Zidovudine Abacavir 3TC/Lamivudine Tenofovir (-) FTC/ Emtricitabine Etravine	Inhibits RT activity by blocking DNA elongation
Non-nucleoside RT inhibitor	HIV-1 RT	Efavirenz Nevirapine	Binds catalytic site of RT, blocking activity
PR inhibitor	HIV-1 PR	Nelfinavir Ritonavir Atazanavir Sulfate, Saquinavir Indinavir sulfate Amprenavir Lopinavir Tipranavir Darunavir	Inhibits protease activity, resulting in immature, non-infectious virus
IN inhibitor	HIV-1 IN	Raltegravir/Isentress	Blocks HIV-1 IN activity, preventing integration into the host genome
Entry inhibitor	CCR5 coreceptor	Selzentry	Prevents entry by blocking access to the CCR5 HIV-1 coreceptor
Entry inhibitor	HIV-1 Env	Enfuvirtide (Fuzeon)	Prevents entry by blocking conformational change in Env that allows fusion of viral and cellular membranes

virion non- infectious. A recently approved drug targets the HIV-1 integrase (IN),

preventing integration of the DNA provirus into the host genome.

More recently, an additional class of treatment has been developed that

prevents fusion of the HIV-1 virion to the host cell membrane. It is a

peptidetherapy derived from an HIV-1 Envelope sequence that binds to the

Envelope

protein on infectious virion (55). The trade name for this peptide is Fuzeon, and

the generic name is enfuvirtide. Peptide binding prevents a conformational

change in Envelope required for fusion of the viral and cellular membranes,

preventing entry of the virion into the host cell. Another recently approved entry

inhibitor blocks access of Env to the CCR5 coreceptor (94).

All of the drugs described above target viral proteins and share a common

feature: HIV-1 can eventually develop resistance to the therapies (Stanford

University HIV Drug Resistance Database, http://hivdb.stanford.edu/). Anti-HIV-1

drugs are used in a triple drug combination, known as Highly Active Antiretroviral

Therapy (HAART), which typically employs RT and PR inhibitors (50). Initial

therapy controls HIV-1 infection, but the virus eventually accumulates mutations

that confer resistance to the drugs (93, 135). While additional drugs, such as

enfuvirtide or other entry inhibitors, provide a second line of defense, HIV-1 can

still develop resistance (85, 97). In fact, it is now known that certain subtypes

and clinical isolates already carry mutations that confer resistance to certain

therapies (23, 68).

Selective pressure from drug regimens helps select and maintain mutations in a viral population. Several mechanisms contribute to the generation of mutations that lead to drug resistance. A commonly attributed source of viral mutations are errors that occur during the reverse transcription step of replication. The HIV-1 RT has an error rate of approximately 1 nucleotide per 7000 *in vitro*, implying that RT can misincorporate one or more nucleotides per viral RNA template (61). Additional mechanisms for generating mutations can come from the host cell, due to the action of APOBEC (Apolipoprotein B mRNA-editing enzyme catalytic polypeptide-like) and ADAR (Adenosine deaminase that acts on RNA).

The APOBEC protein family catalyzes cytidine to uridine or thymidine editing of RNA and DNA sequences, respectively. APOBECs are a closely related family of enzymes differing primarily in substrate specificity. For instance, APOBEC3G has been implicated in editing of HIV-1 sequences, while APOBEC3A has been shown to edit Adeno-associated virus (AAV) DNA (6, 21). The related activation- induced deaminase (AID) contributes to antibody diversity by editing the immunoglobulin locus and inducing somatic hypermutation and class switch recombination (57). Overexpression of APOBEC3G has also been shown to antagonize miRNA inhibition, though editing activity is not required (59). While APOBEC is often described as an antiviral protein, it clearly has additional cellular functions.

HIV-1 has evolved an accessory protein, Vif, that specifically counteracts the effects of APOBEC3G. Studies with HIV-1 proviruses that did not express Vif demonstrated that certain cell lines were non-permissive for virus production in the absence of Vif. Using subtractive hybridization, CEM15 was identified as the restrictive factor and was later identified as APOBEC3G (127). APOBEC3G edits cytidine to thymidine on the negative DNA strand during reverse transcription, since sequence changes on the positive strand of HIV-1 proviral DNA only have guanosine to adenosine changes. Vif induces the ubiquitination of APOBEC3G, which targets it to the proteasome for degradation (128, 131). In addition, Vif antagonizes packaging of APOBEC3G in HIV-1 virion, though the degree to which it inhibits packaging differs from study to study (65, 100, 131). APOBEC3G is often described as a specific inhibitor of HIV-1 replication, but it is also possible that HIV-1 takes advantage of APOBEC activity to generate greater sequence diversity and has evolved the Vif accessory protein to modulate the amount of APOBEC3G packaged into virions or to regulate its activity. While hyperediting of HIV-1 RNA occurs in the absence of Vif, mutations in the deaminase domain of APOBEC3G do not substantially reduce its antiviral activity (100). This suggests that APOBEC3G may have an editing-independent function that prevents HIV-1 replication. Regardless, APOBEC3G editing activity is a potential mechanism for generating sequence diversity and developing drug resistance.

Another enzyme that can change the primary HIV-1 sequence is ADAR. Double-stranded RNA regions are subject to editing by ADAR, which catalyzes the deamination of adenosines to inosine. Inosines are recognized by the ribosome and reverse transcriptase as guanosine. ADARs have been described in many species from worms to humans (4). In humans, there are two isoforms of ADAR1, long and short, and one isoform of ADAR2. The two isoforms of ADAR1 are regulated by alternative promoters, with the long form being transcribed from an interferon-inducible promoter (45). In addition, while ADAR1-short and ADAR2 are nuclear proteins and have been shown to shuttle through the nucleolus, ADAR1-long can be found in the cytoplasm (32). This has led to the suggestion that ADAR1-long, at least, might have an antiviral function and several viral substrates have been described, including Hepatitis Delta, Polyoma virus and Human Immunodeficiency Virus (52, 75, 86, 126, 149). However, it is not clear in some cases whether editing has a deleterious effect, implying that editing could lead to greater viral diversity. The polyoma virus uses ADAR activity to shift from early to late transcription by taking advantage of the nuclear retention of inosine-containing RNAs (75). In contrast, the HIV-1 Rev protein can overcome nuclear retention of edited RNAs containing an RRE, suggesting that ADAR antiviral activity is not effective against all viruses (160).

More recently, ADAR activity has been shown to antagonize miRNA inhibition by editing pre-miRNA. ADAR editing prevents the processing of pre-miRNAs into miRNAs by Drosha and edited pre-miRNAs are degraded by

TudorSN nuclease (153). In addition to neurotransmission, ADAR may play a role in modulating miRNA metabolism and, in contrast to APOBEC, these roles are directly linked to RNA editing (153).

Drug resistance is a major challenge in developing anti-HIV-1 therapeutics. Nucleotide changes in viral sequences due to RT error or RNA editing quickly lead to escape mutants (85, 93, 97). Once a nucleotide change occurs, drugs become a selective agents for fixing drug resistance mutations in a patient's virus population. Other studies have demonstrated that drug resistance mutations are already present in HIV-1-infected individuals (23, 68). These mutations could complicate treatment, since drug resistant viruses would not be susceptible to all anti-HIV-1 therapies. In order to choose the most effective drug regimen, drug resistance mutations should be taken into account

Additional therapies are in development, and one recent focus of that research is to target the HIV-1 RNA directly, rather than viral proteins. Targeting viral RNA directly presents several challenges, including the possibility of drug resistance. As a result of APOBEC and ADAR activity, additional mutations can be accumulated in HIV-1 sequences that lead to drug resistance, complicating RNA-targeted strategies. While APOBEC and ADAR activity were described above as mechanisms for developing drug resistance, it is also possible that HIV-1 takes advantage of these enzymes for general virus evolution. Editing could contribute to increasing host susceptibility, cross-species infection or altering of tissue tropism.

RNA-targeted Therapeutics

As discussed above, many therapeutics have been developed to target specific HIV-1 proteins. Unfortunately, HIV-1 has demonstrated a keen ability to develop resistance to anti-HIV-1 drugs, even when used in combination. However, several therapeutic strategies are in development targeting HIV-1 RNA directly. Antisense oligonucleotides, ribozymes, small interfering RNAs (siRNAs) and long antisense RNAs are all tools being developed to inhibit HIV-1 replication. Targeting RNA directly has several advantages over targeting proteins. A single nucleotide change in the RNA sequence can lead to an amino acid change in RT or PR that confers drug resistance. However, antisense and siRNA-based strategies can tolerate some nucleotide changes. The size of the target sequence could be increased in order to prevent single nucleotide changes from reducing efficacy. Due to the overlapping reading frames in the HIV-1 genome, certain regions are less tolerant of mutation, restricting the ability of escape mutants to develop. The RNA genome is absolutely required for subsequent rounds of infection, and targeting viral RNA directly could prevent both production of structural proteins and packaging of the RNA genome.

Antisense oligonucleotides

Antisense oligonucleotides bind to complementary RNA sequences and inhibit translation of target RNAs (refer to Figure 5). In addition, antisense oligonucleotides can stimulate RNAse H activity, which recognizes and cleaves the RNA strand in DNA:RNA hybrids (29). To date, the only approved therapeutic using antisense oligonucleotide technology, Vitravene (Isis Pharmaceuticals), targets Cytomegalovirus and is used to control eye infections and prevent blindness in AIDS patients (31). There are several difficulties associated with the therapeutic use of antisense oligonucleotides. Vitravene must be delivered by injection directly into the eye, increasing the discomfort for the patient. The oligonucleotides are unstable, requiring multiple deliveries at a relatively high concentration to elicit significant therapeutic benefit. Antisense oligonucleotides are on average 20-30 nucleotides in length and require perfect complementarity for maximum inhibitory effect. As discussed above, HIV-1 has the ability to rapidly mutate, so sequence-specific targeting can be problematic if using a small target.

Ribozymes

Another technology for targeting RNA directly is ribozymes (refer to Figure 6). Ribozymes are catalytically active RNAs that can be engineered to target specific RNA sequences. RNA with catalytic activity was initially described in studies of Tetrahymena ribosomal RNA splicing. Kruger *et al.*, found that an *in vitro* transcribed ribosomal RNA could remove its intron in the absence of any
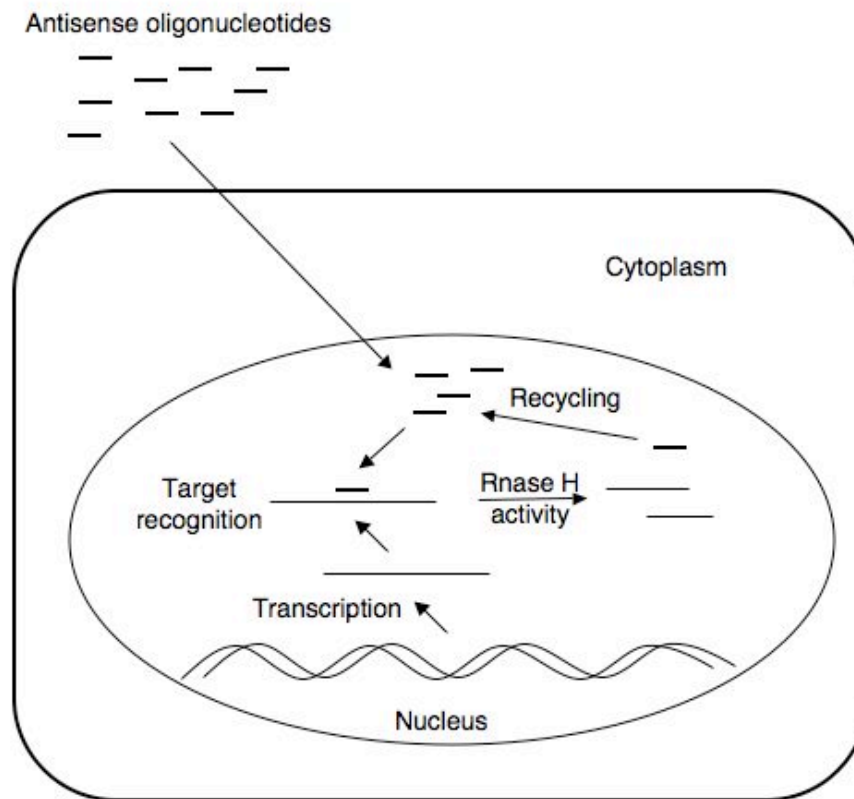
Figure 5: Mechanism of antisense oligonucleotide inhibition of gene expression.

Antisense oligonucleotides enter the nucleus of the cell and bind complementary target sequence. The DNA:RNA hybrid stimulates RNase H activity, which cleaves the target RNA. The antisense oligonucleotide is recycled for additional rounds of targeting. Figure adapted from (29).
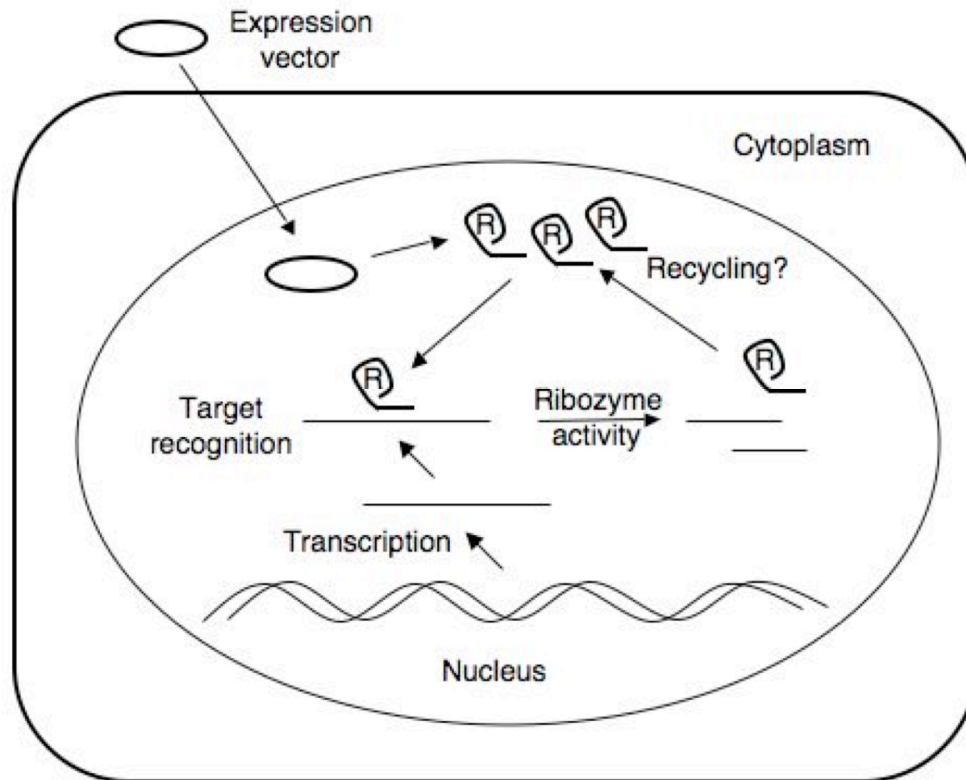
Figure 6: Mechanism of ribozyme inhibition of gene expression.

Ribozymes composed of an antisense tether sequence and catalytic RNA are transcribed from an expression vector. The antisense sequence recognizes its target sequence and the catalytic RNA cuts the target RNA, preventing expression. Note: ribozyme activity is not restricted to the cell nucleus. Figure is adapted from (69).

protein (73). Another RNA with catalytic activity was described in *Echerichia coli*

and *Bacillis subtilitis* by demonstrating that the RNA component of RNase P

could cleave tRNA precursors *in vitro* (49). Eventually, this work led to *in vitro*

strategies to select ribozymes that target defined sequences (134). Ribozymes

targeting the HIV-1 LTR, TAR, pol and env have been developed and are in

various stages of testing (10, 46, 112, 134, 151). While ribozymes have

demonstrated potent catalytic activity in vitro, their reliance on short recognition

sequences can cause difficulties similar to antisense oligonucleotides.

Small interfering and other small RNAs

The latest technology to enter development employs short interfering

RNAs (siRNAs), which have been used successfully in research for over a

decade, but have yet to be used in therapeutic applications. They were first

described in *C. elegans*, but homologous pathways have since been described in

D. melanogaster and mammals (15, 33, 39, 67). siRNAs are short RNA

sequences, 19-24 nucleotides in length, that persist in stable duplexes of

complementary strands. siRNAs can be generated from long double-stranded

and short hairpin RNAs (shRNA) by the RNase III enzyme Dicer. Synthetic

siRNAs can be added exogenously to tissue culture cells for targeted knockdown

of gene expression (33). The antisense strand of the siRNA anneals to

complementary sequence in a target mRNA, leading to translational silencing,

translational upregulation or degradation.

In addition to siRNA, other regulatory RNA molecules include microRNAs (miRNAs), Piwi-interacting RNAs (piRNAs) and Repeat-associated RNAs (rasiRNAs). These regulatory RNAs are generated from cellular transcripts that form hairpin structures and are initially processed by Drosha from primary-miRNAs (pri-miRNAs) to pre-miRNAs in the nucleus (78). These pre-miRNAs are exported from the nucleus to the cytoplasm by exportin-5, where they undergo final processing by Dicer (154). miRNAs typically target cellular mRNAs and are important in development, differentiation and oncogenesis (66). piRNAs and rasiRNAs regulate spermatogenesis and repress retrotransposition, preventing their expression and expansion in the host genome (118, 155). Uncontrolled retrotansposition has been implicated in cancer and neurodegenerative disease. While the origin and targets of these small RNAs differ, the mechanisms they use to regulate protein expression overlap. siRNAs can be designed to target specific RNAs either within coding sequences or in the 3' untranslated region (UTR) (39, 142). Perfectly complementary siRNAs stimulate the formation of the RNA-induced silencing complex (RISC) containing the Argonaute 2 (Ago2) protein, which has Slicer activity and cleaves the target RNA (84) (refer to Figure 7).

When the siRNA and target sequence are not perfectly complementary, pairing of the small RNA with target RNA stimulates the binding of Argonaute 1 (Ago1) protein and other factors such as RCK/p54, which inhibits translation of the RNA (24). In addition to translation repression, imperfect complementarity
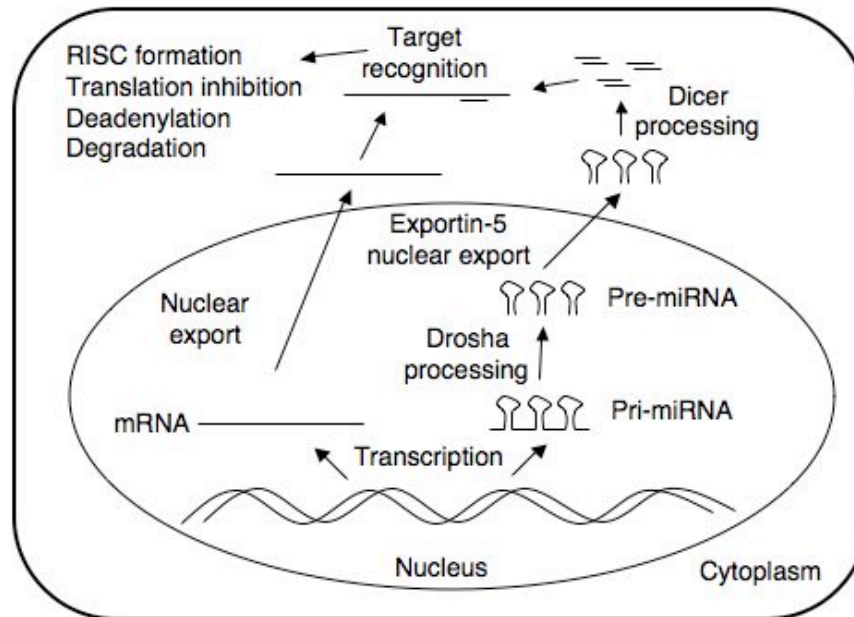
Figure 7: Mechanism of siRNA inhibition of gene expression.

siRNA introduced by native miRNA expression, expression vector, pre-processed siRNAs or shRNAs can be used to inhibit gene expression. Native miRNA is transcribed into tandem hairpins that are processed into individual hairpins by Drosha and transported to the cytoplasm by Exportin-5. Hairpins are processed by Dicer into siRNAs, which anneal to target RNAs. Annealing of the antisense siRNA strand to target RNA induces formation of the RISC complex. If the antisense and target RNA are perfectly complementary, Ago2 cleaves the target RNA, leading to degradation. If the antisense and target RNA are not perfectly complementary, translation from the target RNA is inhibited and the RNA can be degraded following deadenylation.

can lead to target degradation through deadenylation or decapping, followed by exonucleolytic digestion (150). An example of miRNA regulation comes from *C. elegans*, where let7 miRNAs control differentiation and development. Let7 miRNAs regulate expression of lin41 and other genes by binding to target sites in the 3' UTR of their mRNAs. In the absence of let7 miRNA, larvae failed to differentiate into adult cells, while overexpression of let7 miRNA led to early differentiation of larval cells to adult fates (114). Multiple targets have been identified in *C. elegans*, as well as humans, that contain target sequences in their 3' UTR with imperfect complementarity to let7 miRNAs (79). In addition, multiple let7 variants have been identified by sequence similarity with different functions in development (1).

While there has been significant biochemical characterization of RISC complex activity, less is known about the mechanism of miRNA-mediated translation control. Targeted RNAs still localize to the polysome, but are not translated into their corresponding proteins, suggesting inhibition occurs post-initiation (92, 98, 102). An alternative hypothesis is that miRNA-targeted mRNAs enter pseudo-polysomes, which are thought to be more closely related to P/GW bodies (138). However, it is difficult to distinguish between the polysome and pseudo-polysome in these cases, since the former studies were performed in human cell lines and the latter study was performed in Drosophila cell-free extracts.

Another mechanism for translation inhibition involves Ago2, which was recently shown to have m(7)G cap-binding activity (70). Based on this result, Ago2 binding to a miRNA-targeted mRNA competes with eIF4E for m(7)G cap-binding, preventing translation initiation. It is not clear at this time which mechanism is more important for translation inhibition. However, recent work by Eulalio *et al*. has questioned the importance of cap binding for miRNA inhibition (35). Mutations in the predicted cap-binding motif of Ago1 abolished miRNA inhibition, but the mutations also abolished interaction with GW182. GW182 associates with cytoplasmic foci and is required for miRNA inhibition to occur (113). Depleting GW182 or overexpressing the Ago1 binding domain of GW182 also abolished miRNA inhibition, implying that Ago1-mediated miRNA inhibition relied on interaction with GW182 and not cap binding. Additional work will be required to determine the mechanism or mechanisms of miRNA-mediated translation repression.

Interestingly, miRNA inhibition can be subject to regulation. Vasudevan *et al*. demonstrated that translation of miRNA-targeted RNAs is upregulated under stress conditions or cell cycle arrest, suggesting that the inhibition is reversible under certain conditions (141). Plasticity is important for development and differentiation, so, in some ways, the reversibility of miRNA-mediated repression is not surprising. This could have important implications for the design and development of siRNA-based therapeutics.

In addition to stress and cell cycle regulation, APOBEC3G has been shown to reverse miRNA-mediated inhibition (59). Overexpression of many members of the APOBEC family reversed miRNA inhibition of luciferase reporters. In addition, APOBEC overexpression led to the relocalization of the luciferase RNAs to polysomes. ADAR editing also has the potential to prevent miRNA inhibition, since it targets double-stranded RNA regions (153). ADAR editing of pre-miRNA has been demonstrated and leads to the degradation of pre-miRNAs. In addition, in ADAR null mouse embryonic fibroblasts, siRNA-mediated inhibition has been shown to be more effective than in wildtype parental cells, implying that RNAi and ADAR editing may antagonize one another (101).

While siRNA technology has proven to be a powerful tool for genetic dissection in higher eukaryotes, it relies on short target sequences. Mutations in the target sequence could cause a potent siRNA effect to become a less potent miRNA effect or lose any siRNA effect completely. Attempts to inhibit HIV-1 replication with shRNAs targeting *tat* rapidly gave rise to resistant mutants, suggesting that more highly conserved regions would make better siRNA targets (7). However, long-term passage of HIV-1 in the presence of an shRNA targeting the *env* and *rev* region eventually gave rise to mutants that were replication competent and resistant to siRNA inhibition (124). While these sequences were more restricted due to their overlapping coding sequences, they still gave rise to resistant mutants.

Long double-stranded antisense RNA

Long double-stranded antisense RNAs are another means for targeting specific sequences and the VIRxSYS corporation, as described in Lu *et al.*, demonstrated the potential of long antisense RNA for therapeutic use (86). The VIRxSYS corporation developed an HIV-1-derived lentiviral vector system for transducing patient CD34+ cells with a construct expressing a 937 bp antisense RNA complementary to the HIV-1 *env* coding sequence. The construct was derived from the HIV-1 pNL4-3 provirus and contains, from the 5' end to 3', the 5' Long Terminal Repeat (LTR), a portion of *gag* that contains a 5' splice donor (SD), packaging signal (ψ), and central polypurine tract (cPPT), a 937 bp fragment of *env* in the antisense orientation, the RRE, a 3' splice acceptor (SA), and the 3' LTR. This construct was packaged into infectious viral particles by coexpressing HIV-1 Gag and GagPol proteins and pseudotyping with VSV-G protein (86). Pseudotyping with the VSV-G protein allows virus entry via a low-pH endosomal mechanism (20, 152).

In the VIRxSYS study, CD4 cells were isolated from patient bone marrow and transduced using the lentiviral vector. HIV-1 infecting these cells would provide Tat and Rev *in trans*, and induce expression of the antisense RNA which would be expected to lead to inhibition of HIV-1 replication. After confirming transduction, cells were expanded and reintroduced into patient bone marrow. In Phase I clinical trials, five patients who were not responsive to conventional anti-

HIV-1 therapy demonstrated no adverse effects from the therapy and four patients showed improved immune function (81).

While it is not clear whether the antisense RNA uses a mechanism of inhibition similar to antisense oligonucleotides, siRNA, or both, this technology has demonstrated great potential as an anti-HIV-1 therapeutic. This is surprising in light of the disappointing results from previous attempts to use antisense as a therapeutic (56, 80). The strategy avoids some of the pitfalls associated with antisense oligonucleotides and siRNAs, since it targets a long region of RNA. Mutation of the target region would not necessarily reduce the antisense effect. If mutations occurred within one part of the target region, other regions would maintain their original sequence, allowing continued targeting. In fact, attempts to generate a resistant virus after long-term passaging did not result in replication competent mutants. However, a subset of viruses passaged in the presence of the antisense construct and recovered from cell media supernatant contained mutations in their RNA consistent with ADAR editing (86). As discussed in the previous section, ADAR editing may antagonize miRNA inhibition (153). Thus, it is possible that ADAR is antagonizing antisense inhibition of HIV-1 replication. While a role for ADAR in the process of antisense inhibition cannot be ruled out, it seems likely that additional mechanisms contribute to efficient antisense inhibition.

Some insight into the mechanism of antisense inhibition might be gained from viral and cellular examples of antisense transcription. Natural antisense

transcription has been reported for HIV-1 that results in a transcript antisense to the *env* region (95). The antisense RNA is transcribed from the 3' LTR, can span the entire *env* coding sequence and, based on 3' RACE, is polyadenylated due to a functional polyA signal in the *pol* region (76). Stable coexpression of a portion of this antisense RNA efficiently inhibited HIV-1 replication in several different cell lines (133). While this RNA has been shown to encode a protein *in vitro* that can be detected by HIV-1+ patient sera, cell lines expressing an antisense RNA with a mutated ATG start site still efficiently inhibited HIV-1 replication (133, 140). In addition to HIV-1, antisense transcripts have been described in cells infected with Human T-cell Lymphotropic Virus-1 (HTLV-1) and Feline Immunodeficiency Virus (FIV), suggesting that antisense transcripts may modulate retroviral gene expression and latency (13, 16).

In addition to retroviruses, several antisense transcripts have been described for cellular RNAs, including WT1 and p15, which regulate expression of their complementary RNAs (30, 156). In the case of p15, a cyclin-dependent kinase inhibitor, antisense transcript levels were increased in leukemia patient cell lines and led to the downregulation of p15 promoter activity. Intriguingly, this activity persisted in Dicer -/- mouse embryonic stem cells, demonstrating that the process is Dicer-independent (156).

Another example implicates natural antisense transcripts in the control of X inactivation during development. Xist is a non-coding RNA that associates with the inactive X chromosome and is required for X inactivation to occur (25). Tsix

is an antisense transcript of Xist expressed from both X chromosomes prior to X inactivation, but whose expression is associated with the future active chromosome during X inactivation (77). Recently, Ogawa *et al.* demonstrated that Xist and Tsix RNAs form duplexes *in vivo* that are processed into small RNAs by a Dicer-dependent mechanism (103). This suggests that the active X chromosome might prevent inactivation by inducing the degradation of Xist:Tsix RNA duplex. Paradoxically, in the absence of Dicer, Xist RNA failed to accumulate on the inactive X chromosome, suggesting that Dicer plays a more complex role in maintaining both the active and inactive X chromosomes.

These studies suggest that regulation by antisense RNA may be a conserved mechanism for modulating gene expression, regardless of whether it is a Dicer-dependent or –independent mechanism. Retroviruses could potentially use this mechanism to regulate latency and the surprising efficiency of the antisense construct used in these studies may be a result of the fact that it is mimicking a natural control mechanism. An additional function of the natural retroviral antisense could be that the double-stranded region formed could become subject to ADAR editing, which would generate a greater diversity of Env proteins, as discussed above.

In addition to the length of antisense RNA, other elements of the expression system could contribute to antisense inhibition. A recent study demonstrated that a long hairpin RNA targeting HIV-1 was more effective when produced from an HIV-1 LTR-driven vector, compared to an EF1α promoter or a

Tet-inducible promoter (72). However, it is not clear whether this effect is due to promoter function or the presence of the HIV-1 packaging signal (ψ). The authors used a 300 bp sequence targeting *tat*, *rev*, and *nef*, but did not attempt long-term passaging. Whether a resistant mutant would eventually develop remains to be seen.

Project Rationale

We were intrigued by the surprising ability of the VIRxSYS antisense construct targeting HIV-1 *env* sequence to both effectively inhibit HIV-1 replication and avoid evasion by resistant viruses (86). In this study, we specifically examined whether efficient inhibition of HIV-1 requires the antisense RNA to be trafficked through the Rev-RRE pathway. To do this, we constructed HIV-1-based plasmids that express antisense RNA containing either an HIV-1 RRE, MPMV CTE or no transport element. The effect of expression of these RNAs on HIV-1 expression was then examined in experiments that included studies on the effects of antisense RNA on target RNA trafficking and expression.

We wanted to determine if the potent antisense effect was due to Rev-RRE activity. In addition, we wanted to define the mechanism by which the antisense construct inhibits HIV-1 replication. Both of these points could have a significant impact on antisense vector design and lead to improved targeting of cellular as well as viral factors.

Chapter 2- Materials and Methods

Antisense constructs and nomenclature

To facilitate identification, all plasmids used in this study were indexed as

numbers in the form of pHRXXXX. Plasmids used in this study are listed in Table

2. Sequences from 3 different pNL4-3-derived proviral clones (pHR1272,

pHR1498 and pHR2772) were used to make constructs expressing HIV-1

antisense RNA. All of the resulting constructs contain the 5' and 3' LTR as well

as the HIV-1 packaging signal. pNL4-3(nef-) (pHR1272) contains a 150 bp

deletion at the start of *nef* that prevents Nef expression. pNL4-3(rev-)(RRE-)

(CTE) (pHR1498) contains a *rev* with two point mutations that prevent Rev

expression, as well as multiple third-base mutations in the RRE that prevent its

function, but maintains the Env amino acid sequence (161). It also contains a

copy of the MPMV CTE cloned into *nef*. pNL4-3(RRE-)(nef-) (pHR2772) contains

the third-base mutations in the RRE as well as the 150 bp deletion in *nef* that is

also present in pHR1272. Antisense constructs were assembled by digesting

pHR1272, pHR1498 or pHR2772 with NsiI (digesting at pNL4-3 nt 1249),

repairing with Klenow Fragment, followed by digestion with NheI (pNL4-3 nt

7252). The resulting plasmid backbones lacked HIV-1 sequences from pNL4-3 nt

1249 to 7252, which contained *gag/pol, vif, vpu, vpr* as well as the first exon of *tat*

and *rev* and regions of *env* 5' to the RRE. A PCR-generated fragment

Table 2: List of plasmids constructed for this study
Hamrek archive number takes the format of pHRXXXX for ease of identification.
A brief description of each plasmid is given in the second column.

Hamrek archive #	Description
pHR16	CMV expression plasmid
pHR30	CMV-Rev expression plasmid
pHR1145	pNL4-3 HIV-1 provirus
pHR1146	pNL4-3 Rev-
pHR1272	pNL4-3 Nef-
pHR1371	pNL4-3 Rev- RRE- MPMV CTE+
pHR1498	pNL4-3 Rev- RRE- MPMV CTE+
pHR2128	pCMV-Tap
pHR2155	pCMV-RevM10-Tap
pHR2208	pCMV-FLAG-Sam68
pHR2415	pCMV-Nxt1
pHR2643	CMV-ß-globin
pHR3473	RRE-driven antisense
pHR3474	CTE-driven antisense
pHR3475	No element antisense
pHR3476	RRE-driven sense
pHR3477	CTE-driven sense
pHR3478	No element sense
pHR3603	pNL4-3-deltaE-EGFP (pNLEGFP)
pHR3742	pGPmyr-pro- cl. 1 (HXB2 w/ myr- pro- frameshift muts)
pHR3744	HXB2 cl. 1
pHR3746	pNLEGFP cl. 1 (pNL4-3 w/ Env-EGFP fusion)
pHR3748	pNLdsRed (pNL4-3 w/ Env-dsRed fusion)
pHR3749	pNLGFP-Hygro cl. 1 (pHR3603 w/ Hygro in *nef*)
pHR3753	pBS-GFP
pHR3754	pBLG-4 (LTR-driven GFP)
pHR3755	RRE-driven antisense GFP
pHR3756	CTE-driven antisense GFP
pHR3757	No element antisense GFP
pHR3758	RRE-driven sense GFP
pHR3759	CTE-driven sense GFP
pHR3760	No element sense GFP

corresponding to the same 937 base region of *env* (pNL4-3 nts 6602 to 7538)

that was expressed in VIRxSYS antisense vector was then inserted into these

backbones. The primers used to generate this fragment incorporated stop

codons in the 5' end of the fragment to prevent any protein expression from the

insert region and an XbaI site in the 3' end for cloning. The fragment was ligated

to the backbone sequences in the antisense orientation, resulting in the following

plasmids: RRE-driven antisense (pHR3476) derived from pHR1272, CTE-driven

antisense (pHR3477) derived from pHR1498 and no element antisense

(pHR3478) derived from pHR2772. These plasmids will be shown in Chapter 3,

Figure 8A. As a control, we also made a similar construct, RRE-driven sense

(pHR3473), containing the RRE with the insert in the sense orientation.

Oligonucleotides used to generate the sense and antisense vectors:

Antisense vectors:

Oligo 1533: 5' aattatgcattgagcggccgcagtttaaagtgcactg 3'

Oligo 1534: 5' atatctagaactagtgtccactgatggggag 3'

Sense vectors:

Oligo 1535: 5' atatctagaactagtagtttaaagtgcactg 3'

Oligo 1536: 5' aattatgcattgagcggccgcgtccactgatgggag 3'

     A similar strategy was used to generate antisense constructs targeting

EGFP, except that the primers amplified a 721 nt fragment containing the EGFP

ORF (Clontech pEGFP-N1, pHR1976). The primers incorporate either a SpeI or

NotI restriction site. The PCR product and backbone vectors were digested with

SpeI and NotI and the EGFP fragment was used to replace the *env* sequence in

pHR3476 and pHR3477 to generate RRE-driven (pHR3755) and CTE-driven

(pHR3756) EGFP antisense constructs.

Oligonucleotides used to construct EGFP sense and antisense vectors:

Antisense vectors:

Oligo 1726: 5' actagtatggtgagcaagggcgag 3'

Oligo 1727: 5' atagcggccgctttacttgtacagctc 3'

Sense vectors:

Oligo 1728: 5' gcggccgctggtgagcaagggcgag 3'

Oligo 1729: 5' ataactagttttacttgtacagctcgtcc 3'

HIV-1 proviral constructs and CMV expression vectors

All of the pNL4-3-derived proviruses that were used in this study contained either

one or two point mutations in the Rev ORF (an AUG mutation and a nonsense

mutation at Rev amino acid 12) that prevent Rev expression. pNL4-3(Rev-)

(pHR1146) contains a functional RRE with a single mutation in Rev at amino acid

12 (11). pNL4-3 (Rev-)(RRE-)(CTE) (pHR1371) contains multiple third-base

mutations in the RRE that prevent its function, but has the MPMV CTE cloned

into *nef*. In some experiments an HXB2-derived provirus containing mutations in the myristylation site, frameshift region and protease active site (pHR1320) was utilized. This was obtained from Casey Morrow (106). CMV-Rev (pHR30), CMV-Tat (pHR136), CMV-RevM10Tap (pHR2155) and CMV-Nxt1 (pHR2415), which express Rev, Tat, RevM10-Tap fusion protein and Nxt1 have been described previously (51, 130). pCMV (pHR16) is the empty backbone vector for these expression constructs. The CMV-ß-globin construct (pHR2643) expressing mouse ß-globin RNA was obtained from Lynne Maquat (U. of Rochester) (159).

The LTR-driven EGFP construct was cloned by digesting pBluescirpt and pEGFP-N1 (Clontech, pHR1976) with HindIII and NotI. The backbone vector from pBluescript and EGFP ORF were gel purified and ligated, resulting in pBS-GFP (pHR3753). pBS-GFP was digested with ClaI and repaired using Klenow Fragment followed by digestion with HindIII. pNL4-3 (pHR1145) was digested with PstI and repaired with Klenow Fragment followed by digestion with HindIII, resulting in a fragment that contained the HIV-1 5' LTR. Following gel purification, the backbone and LTR fragment were ligated, resulting in pLTR-EGFP (pHR3754).

Cheap 'n Easy plasmid minipreps

1 mL overnight culture was harvested in a microfuge tube. After spinning at maximum speed for 1 min., media was removed and the bacteria resuspended in residual media. After adding 300 μL TENS (1X TE, 0.1 M NaOH, 0.5% SDS),

lysate was mixed gently by rocking 3-6 times. Lysis was neutralized by adding

150 μL 3 M NaOAc, pH 5.2 and mixing gently by rocking 3-6 times. After

centrifuging at max. speed 15 min. at 4 ˚C, supernatant was transferred to a new

tube. 900 μL 100% ethanol was added and and centrifuged at max. speed 15

min. at 4 ˚C. After decanting the supernatant, the pellet was rinsed with 1 mL

70% ethanol. Tubes were centrifuged at max. speed 5 min, the ethanol was

decanted and the pellet was air-dried on the benchtop. The pellet was

resuspended in 20 μL 1X TE (10 mM Tris, 1 mM EDTA) and 2 μL RNase A (10

mg/mL). After incubating at 37 ˚C 10 min, DNA was analyzed by agarose gel

electrophoresis. Resulting plasmid DNA was clean enough for restriction

enzyme digestion and sequencing.

Purification of plasmid DNA by cesium chloride gradient centrifugation

A 500 mL flask of Terrific Broth (recipe in next section) was inoculated with a 5

mL LB starter culture and incubated at the appropriate temperature (37 ˚C for

regular plasmids, 30 ˚C for proviral plasmids) with shaking overnight. The culture

was poured into a 1 L spin bottle and centrifuged at 3000 rpm, 20-30 minutes.

After decanting the media back into the culture flask, the bacterial pellet was

resusupended in 70 mL Solution I (recipe in next section) (per 500 mL culture).

After adding 40 mL Solution I/lysozyme (recipe in next section) and incubating on

ice 15 minutes, 100 mL Solution II (recipe in next section) was added, mixed well

and incubated on ice 15 minutes. 75 mL Solution III was added, mixed well and incubated on ice 10 minutes. The cell lysate was centrifuged at 3000 rpm, 30 minutes and the supernatant was poured over gauze into a 500 mL spin bottle. 180 mL isopropanol was added and incubated at room temperature (RT), 10 minutes. The sample was centrifuged in a GS-3 rotor at 7000 rpm, 20-30 minutes. After decanting the supernatant, the pellet was resuspended in 15-16 mL of TE (10 mM Tris, 1 mM EDTA) or enough to make the final volume 16 mL. Exactly 16 mL of resuspended plasmid was transferred to a 50 mL conical tube containing 17.6 g CsCl. The solution was vortexed to dissolve the CsCl and 1.6 mL EtBr (10 mg/mL) was added. The DNA/CsCl/EtBr mixture was transferred to 16 x 67 mm OptiSeal centrifuge tubes (Beckman, Palo Alto, CA), and placed into an NVT65 rotor (Beckman) followed by centrifugation overnight at 50,000 rpm.

The tubes were removed from the rotor and the plasmid band was marked. A piece of transparent tape was placed over and just below the plasmid band to prevent leaking while removing the plasmid band. The plasmid band was removed using an 18-guage needle attached to a 3-5 mL syringe to draw the plasmid band into the syringe, taking care not to draw up the chromosomal band. After transferring the plasmid band to a 13x51 mm Quikseal tube (Beckman), the tube was topped off with TE/CsCl/EtBr mix and sealed. The tubes were placed in an NVT100 rotor (Beckman) and centrifuged 4-6 hours at 75,000 rpm at room temperature (24 ˚C). The tubes were removed from the rotor, and the plasmid band was extracted using a needle and syringe as described above. After

transferring the band to a 15 mL conical tube, the volume was increased to 5 mL

with TE and extracted 10 times with N-butanol. The DNA solution was transferred

to a 50 mL conical tube and 2 volumes of TE and 6 volumes of 100% ethanol

were added. After incubating at –80 ˚C, 30 minutes- 1 hour, the tubes were

centrifuged at 3000 rpm, 30 min. at 4 ˚C. The pellet was washed with 10 mL

70% ethanol and centrifuged at 3000 rpm, 5 min. at 4 ˚C. After decanting the

ethanol, the pellet was resuspended in 5 mL TE and extracted with 5 mL

phenol/chloroform/isoamyl (2.5 mL phenol, pH 8.0, 2.5 mL CHISAM). After

centrifugation at 3000 rpm, 5 min. at 4 ˚C, the aqueous layer was transferred to a

50 mL conical tube and 0.1 volume of 3 M NaOAc (500 μL) and 2 volumes of

100% ethanol (10 mL) were added. After incubating at –80 ˚C, 30 min. and

centrifugation at 3000 rpm, 30 min at 4 ˚C, the pellet was washed with 5 mL 70 %

ethanol. Following a spin at 3000 rpm 5 min. at 4 ˚C, the pellet was air-dried and

resuspended in 250 μL- 1 mL of TE.

Reagent recipes:

Terrific Broth (1 L): 12 g Bacto-tryptone, 24 g yeast extract, 4 mL glycerol in 900

mL water. Autoclave, cool and add 100 mL (for 1 L) 10X salts and selective

agent.

10X Salts (1 L): 23.1 g KH_2PO_4 (monobasic), 125.4 g K_2HPO_4 (dibasic), 1 L total

volume water. Filter sterilize before using. Do not autoclave 10X salts.

Solution I (1 L): 9 g D-glucose, 25 mL 1 M Tris, pH 8.0, 20 mL 0.5 M EDTA, 955 mL water. Combine ingredients, dissolve glucose and autoclave before use.

Solution I + Lysozyme: 10 mg/mL lysozyme dissolved in Solution I.

Solution II (500 mL): 50 mL 10% SDS, 10 mL 10 N NaOH, 440 mL water. Combine ingredients, use sterile water.

Solution III (1 L): 294 g Potassium acetate, 115 mL glacial acetic acid, to 1 L with water. Combine ingredients and autoclave.

TE/CsCl/EtBr Solution (220 mL): 200 mL TE (10 mM Tris, 1 mM EDTA), 220 g Cesium chloride, 20 mL 10 mg/mL ethidium bromide. Combine and store at 4 ˚C. Protect from light.

Cell lines and transfections

293T/17 cells were maintained in Iscove's minimal essential medium supplemented with 10% bovine calf serum and 0.1% Gentamicin. Transient transfections were performed using the calcium phosphate method (47). For analysis of RNA stability, cells were treated with 5 μg/mL Actinomycin D (Sigma, St. Louis, MO) for 0, 3 or 6 hours (83), followed by harvest of total RNA using TriReagent (Molecular Research Center, Cincinnati, OH) according to the manufacturer's instructions.

p24 ELISA

The p24 levels of transfection supernatants were measured by an in house p24 ELISA. The ELISA was performed using a p24 monoclonal antibody (cat# 1513) and pooled human anti-HIV-1 immunoglobulin G (cat# 3957) that were obtained from the AIDS Research and Reference Reagent Program and following a protocol developed by Bruce Chesebro (National Institute of Allergy and Infectious Diseases, Rocky Mountain Laboratories) (146).

A 96 well plate was incubated overnight at 37 °C containing 100μl of the primary antibody (monoclonal IgG p24) in each well. The next day the plate was washed with 1x PBS. 250 μl of blocking buffer (PBS with 5% BSA) was added to each well and the plate incubated at 37 °C for 1 hour. The plate was then washed with 1x PBS with 0.5% Tween-20. 10 μl of lysis buffer (1x PBS with 10% Triton X-100 and 0.05% Trypan Blue) was added to each well except for the blanks. In BL3 conditions, samples were diluted 100- to 1000-fold in tissue culture media before applying to the ELISA plate. 100 μl of standard or sample dilutions were added to appropriate wells. The plate was then incubated at 37 °C for at least 2 hours. The plate was washed with 1x PBS with 0.5% Tween-20. 100 μl of biotinylated secondary antibody diluted 1:800 in assay buffer (PBS with 10% Bovine Calf Serum and 0.5% Triton X-100) was added to all wells except the blanks. The plate was incubated at 37 °C for 1 hour. The plate was washed with 1x PBS with 0.5% Tween. 100 μl of peroxidase-streptavidin diluted 1:4000

in assay buffer was added to all the wells except the blanks. The plate was incubated at 37 °C for 30 minutes. The plate was washed with 1x PBS with 0.5% Tween-20. 100 μl of peroxidase substrate (OPD) was added to every well. The plate was incubated at room temperature protected from light for 30 minutes. 50 μl of 2M H_2SO_4 stop solution was added to each well and the optical density was measured at 492nm. The p24 values (ng/ml) were calculated by the comparison of the measured intensity values to the standard curve factoring in the dilution of the samples.

RNA fractionation for Northern blot analysis

For the isolation of cytoplasmic RNA for use in Northern Blot analysis, six 15 cm plates of 293T cells were transfected per condition by the calcium phosphate method. Sixty-five hours post-transfection, cells were harvested by washing 2X in cold PBS and scraping the cells into 15 ml conical tubes, pooling the cells from the six plates. The cells were pelleted at 1500 rpm and 4 ˚C for 5 min (Sorvall RT-6000B), and any residual PBS was aspirated. The cells were resuspended in 3 ml cold RSB (10 mM Tris, pH 7.4, 10 mM sodium chloride, 1.5 mM magnesium chloride) and incubated on ice for 10 minutes. NP-40 was added drop-wise to the cell suspension to 0.1% final concentration (300 μl 1% solution) with gentle mixing. The nuclei were centrifuged out by two gentle spins, the first at 1600 rpm and 4 ˚C for 5 minutes, and the second at 1200 rpm and 4 ˚C for 5 minutes. To

the supernatant, an equal volume (~3 ml) of 2X Proteinase K buffer (200 mM Tris, pH 7.5, 25 mM EDTA, 300 mM sodium chloride, 2% SDS, 400 µg/ml Proteinase K) was added left to react at 37 ˚C for 30 minutes with shaking. The lysate was then extracted once with one volume of phenol:Chisam (25:24:1 phenol:chloroform:isoamyl alcohol) and twice with one volume Chisam (24:1 chloroform:isoamyl alcohol). Sodium acetate was added to 300 mM (3 M, pH 5.2), and the RNA was precipitated by the addition of 2.5 volumes cold ethanol and left at –20 ˚C overnight. The RNA was pelleted at 2500 rpm and 4 ˚C for one hour (Baxter 6000) and resuspended in 10 mM Tris, pH 7.4, 10 mM EDTA, 0.2% SDS with heating at 65 ˚C for 5 minutes. Sodium chloride was added to 0.5 M final concentration (630 µl 5 M NaCl/10 ml starting lysate). This material was then subjected to oligo d(T) selection.

Total RNA was extracted using TriReagent (Molecular Research Center, Cincinatti, OH) according to the manufacturer's instructions. Briefly, the tissue culture supernatant from a 15 cm plate of transfected cells was removed and 5 mL of TriReagent was added. Cells were collected in a 15 mL conical tube and 500 μL of Bromo chloropropane (Molecular Research Center) was added. After vortexing, tubes were centrifuged at 3000 rpm at 4 ˚C for 30 minutes. The aqueous layer was collected and 2.5 mL isopropanol was added. The tubes were incubated at room temperature and centrifuged at 3000 rpm at 4 ˚C for 30 minutes. The RNA pellet was washed with 75% ethanol and air-dried briefly before resuspending the pellet in binding buffer for oligo d(T) selection.

Polyribosome analysis

Forty-eight hours post-transfection, 100 mg/ml cycloheximide was added to each plate (50 μg/ml final concentration) and incubated at 37 $^\circ$C for 30 min. Cycloheximide is an inhibitor of protein biosynthesis in eukaryotic organisms and exerts its effect by interfering with peptidyl transferase on the 60S ribosome, thus blocking translational elongation. Addition of cycloheximide "freezes" the ribosomes to the mRNA, preventing them from completing translation and falling off the RNA during the polyribosome extraction procedure, thus giving a "snapshot" in time of translating polyribosomes. Also, after this step, all procedures were performed on ice, as the cold temperature helped slow down translation elongation and RNase activity.

To harvest polysomes, the growth medium was aspirated, and the cells were washed twice with 10 ml of ice-cold PBS containing 50 μg/ml of cycloheximide. The cells were scraped and transferred to a 1.5 ml microcentrifuge tube and centrifuged at 4000 rpm for 1 min. The residual PBS was aspirated. The cells were resuspended in 250 μl RSB + inhibitors [10 mM Tris, pH 7.4, 10 mM sodium chloride, 1.5 mM magnesium chloride, 100 U RNasin Plus (40 U/μl; Promega), 1X Proteinase Inhibitor Cocktail (Sigma), 1X Phosphatase Inhibitor Cocktail I (Sigma), 1X Phosphatase Inhibitor Cocktail II (Sigma)] with vortexing. The cells were lysed by adding 250 μl of 2X

polyribosome extraction buffer (10 mM Tris, pH 7.4, 10 mM sodium chloride, 1.5

mM magnesium chloride, 1% Triton X-100, 1% deoxycholate, 2% Tween 20),

and mixed quickly by inversion. The solution was left to incubate on ice for 10

min, and then spun for 10 sec to pellet nuclei. The cytoplasmic extract was

transferred to a new microcentrifuge tube and spun at 10,000X g for 10 min at 4

°C to pellet any remaining cellular debris.

The cleared cytoplasmic lysate was layered onto the top of a 10-50%

continuous sucrose gradient, which was prepared as follows: Sucrose solutions

were prepared using Ultrapure sucrose (Invitrogen) as 10% and 50%

concentrations in 75 mM potassium chloride, 10 mM Tris, pH 7.4, 1.5 mM

magnesium chloride. The solutions were boiled for 10 minutes and then filtered

through a 0.45 μm membrane. The 50% sucrose was used to underlay the 10%

sucrose by gently inserting the tip of a blunt end stainless steel needle to the

bottom of the tube (open top polyclear centrifuge tube, 14X89 mm, Seton

Scientific, Los Gatos, CA) and slowly releasing 5.5 ml 50% sucrose solution from

the syringe to displace the 5.5 ml phase of 10% sucrose solution. Each tube was

closed with a Biocomp cap and placed in the Biocomp gradient master (model

107ip, BioComp Instruments, Inc. New Brunswick, Canada,

http://www.biocompinstruments.com). The gradient parameter was set to long

caps, 10-50%. When the gradient formation finished, the caps were carefully

removed, and the tubes were transferred to an SW41Ti rotor basket. An

additional 500 μl of 10% sucrose was carefully layered on top of the gradient, and

the cytoplasmic lysate was layered on top of this. When EDTA was used to disrupt the polysomes, 30 μl of 250 mM EDTA was added to 470 μl of the cleared cytoplasmic extract (15 mM final EDTA concentration), before layering the extract on top of the gradient. SW41Ti rotor baskets were placed on the SW41Ti rotor and centrifuged in a Baxter ultracentrifuge at 36,000 rpm for 2 h at 4 °C.

Following centrifugation, the rotor baskets were removed and kept on ice until fractions from each tube were collected. From each gradient,19-20 fractions (20 seconds collections at a piston-lowering speed of 0.2 mm/sec) were collected into 1.5-ml microcentrifuge tubes on ice using the Piston gradient fractionator (BioComp Instruments, Inc. New Brunswick, Canada) that was equipped with a UV monitor (Monitor UV-M II, GE Health, Amersham Biosciences, Piscataway, NJ), concomitantly measuring absorbance at 254 nm. The volume of each fraction was approximately 550 μl. Fractions were then analyzed for protein (using either immunoprecipitation for a specific protein or nonspecific isopropanol precipitation to concentrate the samples and to remove the sucrose for better loading and resolution on the SDS-PAGE) or RNA (next section). Immediately after fractionation, 10 ng of a 267-nucleotide long fragment of *in vitro* transcribed gag RNA was added to each fraction used in Northerns as a control for recovery. These were treated with Proteinase K (to each fraction, 60 μl of 10% SDS and 12 μl of 10 mg/ml Proteinase K were added and incubated for 30 min at 42 °C), and then stored at −80 °C until analysis.

Three hundred μl of each Proteinase K-treated fraction was transferred to a new microcentrifuge tube and on ice, extracted twice with an equal volume of phenol/chloroform/isoamyl alcohol and once with an equal volume of chloroform/isoamyl alcohol. The supernatants were transferred to new microcentrifuge tubes, and RNA from each fraction was precipitated by the addition of 1/10 volume 3 M sodium acetate (pH 5.2) and 2.5 volumes 100% ethanol with incubation at –80 °C. The RNA was pelleted by centrifuging at 13000 rpm for 20 min at 4 °C and washed with 1 ml 75% ethanol. The supernatant was carefully aspirated from each tube, and the RNA pellet was air dried briefly.

Northern blot analysis

The RNA pellets from sucrose gradient fractions were resuspended in 4 μl of DEPC-treated water and 15.5 μl of RS buffer (0.0258 M MOPS, 8.35% formaldehyde, 64.5% formamide). The RNA pellets from total and cytoplasmic cell fractions were resuspended in 9 μL of DEPC-water and 31 μL of RS buffer. The samples were incubated at 55 °C for 10 min, cooled on ice, and loaded onto a formaldehyde agarose gel [1% agarose, 0.02 M MOPS (3-[N-morpholino] propanesulfonic acid), pH 7.0, 5 mM sodium acetate, 0.1 mM EDTA, 16.2% formaldehyde]. The gel was run in MOPS Electrophoresis Buffer (0.02 M MOPS, pH 7.0, 5 mM sodium acetate, 0.1 mM EDTA, 8% formaldehyde) at 120 volts for 3-4 hrs. with a peristaltic pump that recirculated the running buffer between the electrodes.

Following electrophoresis, the gel was soaked in 250 ml of autoclaved water for 15 minutes with gentle rocking. The water was replaced three times and incubated for 15 minutes each. The gel was denatured by complete immersion in 50 mM sodium hydroxide for 20 minutes, and then neutralized in 100 mM Tris-HCl (pH 7.0-7.6) for 20 minutes. The gel was then equilibrated in 10X SSC (1.5 M sodium chloride, 0.15 M sodium citrate, pH 7.0) for 15 minutes. Positively charged nylon membrane (BrightStar-Plus; Ambion) was cut to the size of the gel and soaked in 100 ml 10X SSC.

Capillary transfer was performed by setting up the following: 3 inches of cut-to-size paper towels were stacked in a 9X13X2 inch Pyrex tray; 3 pieces of Whatman paper soaked in 10X SSC for 3 minutes were placed on top of the paper towels; the nylon membrane was placed on top of the Whatman paper; the gel with the top-side facing upward was placed on the membrane taking care that any bubbles between the gel and the membrane were removed; and 3 pieces of Whatman paper soaked in 10X SSC for 3 minutes were placed on top of the gel. 100 mL 20X SSC (3.0 M sodium chloride, 0.3 M sodium citrate, pH 7.0) was added to two reservoirs and placed on each side of the Pyrex tray. A long piece of Whatman paper was soaked in 20X SSC for use as a wick. The wick was placed upon the 3 topmost pieces of Whatman paper with the wick ends submerged in the reservoirs. A plastic or glass plate was placed on top of the wick, and the whole set-up was weighted with 4 plastic bottles, each containing 100 ml of water. The RNA was allowed to transfer overnight.

At the end of the transfer period, the nylon membrane was removed from the transfer set-up and rinsed briefly in 10X SSC. The nylon membrane was placed on a clean, dry piece of Whatman paper with the RNA side facing upwards, and the RNA was cross-linked to the nylon membrane using a UV cross-linker (Stratagene UV Stratalinker 2400) at 120 mjoules/cm^2.

The membrane was placed in a heat-sealable bag (2.5 mm thick, 1 pint size; Kapak). Pre-hybridization solution (0.9 M sodium chloride, 0.06 M sodium phosphate monobasic, 0.006 M EDTA, 0.1% SDS, 0.0004% polyvinylpyrrolidone, 0.0004% Ficoll 400 and 0.0004% bovine serum albumin, pH 7.4) was added to the bag, and the bag was sealed. The membrane was incubated at 43 $^{\circ}$C for 1-4 hours in a slowly shaking water bath.

Specific radiolabelled DNA probes to detect GagPol and antisense RNA were generated by PCR incorporating [α-^{32}P] dCTP (Perkin Elmer Life Sciences). The probe template was derived from the pNL4-3 *gag* region and recognized an approximately 500 bp sequence that is present in the 5' portion of both the GagPol viral RNA and the antisense RNA. The probe used to detect mouse ß-globin mRNA was generated by PCR incorporating [α-^{32}P] dCTP, using a template corresponding to exon 3 of the ß-globin mRNA.

The pre-hybridization solution in the heat-sealable bag was replaced with hybridization solution (50% formamide, 0.9 M sodium chloride, 0.06 M sodium phosphate monobasic, 0.006 M EDTA, 0.1% SDS, 0.002% polyvinylpyrrolidone, 0.002% Ficoll 400, 0.002% bovine serum albumin, and 0.1 mg/ml tRNA, pH 7.4).

The probe was denatured by placing it in a boiling water bath for 5 minutes followed by snap cooling on ice. The probe was briefly centrifuged, then added to the bag and sealed. Hybridization occurred overnight in a 43 °C water bath with slow agitation.

The nylon membrane was removed from the bag and rinsed briefly twice in an 11X7X2 inch Rubbermaid container with 6X SSC (0.9 M sodium chloride, 0.09 M sodium citrate) plus 0.1% SDS. The membrane was washed three additional times for 15 minutes each at room temperature, then once at 43 °C for 15 minutes. The membrane was then washed 2-3 more times with 0.1X SSC (0.015 M sodium chloride, 0.0015 M sodium citrate) plus 0.1% SDS at room temperature for 15 minutes each. The background of the membrane was checked using a Geiger Counter, and if the background was high, the blot was continued to be washed with 0.1X SSC plus 0.1% SDS at 43 C for 15 minutes per wash and repeated until the background was low using the Geiger Counter.

The membrane was wrapped with Saran wrap and placed onto a PhosphorImager cassette against a PhosphorImager screen. Visualization and quantitation was performed using a Molecular Dynamics PhosphorImager and ImageQuant software.

Western blot analysis

Proteins were separated using SDS-8% PAGE (acrylamide:bisacrylamide, 37.5:1) and western blot analysis was performed essentially as previously described (54). Proteins were transferred to Immobilon-FL membrane (Millipore) by electrotransfer and blocked using 5% milk in phosphate buffered saline (PBS). Antibodies used for western blotting are listed in Table 3. Mouse monoclonal antibodies were used to detect Pr160 (cat# 1513, AIDS Research and Reference Reagent Program) and Nef (provided by Bernhard Meier) (87). A commercial polyclonal antibody to human ß-tubulin (Abcam, Cambridge, MA) was used to detect cellular ß-tubulin as a loading control. Following incubation with secondary antibody (IRDye800 anti-mouse or AlexaFluor680 anti-rabbit antibodies, Rockland Immunochemicals, Gilbertsville, PA), blots were visualized using the Odyssey Infrared Imaging System (Li-Cor Biosciences, Lincoln NE) and analyzed using the Odyssey software package.

Table 3: Antibodies used in studies, animal source, working dilution and supplier.

Antibody	Source	Working Dilution	Supplier
p24 Gag 183.P3	Mus	1:500	AIDS Research and Reference Reagent Repository
Anti-Env 1D6	Mus	1:500	AIDS Research and Reference Reagent Repository
Anti-Nef SN20	Mus	1:1000	Bernhard Meier
Anti-ß-tubulin	Rabbit	1:10,000	Abcam
Anti-mouse IRDye800	Goat	1:20,000	Rockland Immunochemicals
Anti-rabbit AlexFluor680	Goat	1:50,000	Rockland Immunochemicals

Chapter 3- Efficient antisense targeting of HIV-1 requires the RRE and Rev protein

Introduction

In this chapter, we specifically examine whether efficient inhibition of HIV-1 requires the antisense RNA to be trafficked through the Rev-RRE pathway. To do this, we constructed HIV-1-based plasmids that express antisense RNA containing either an RRE, CTE or no transport element. The effect of expression of these RNAs on HIV-1 expression was then examined in experiments that include studies on the effects of antisense RNA on target RNA trafficking and expression.

Results

Vector construction and RNA expression levels in 293T cells

To test whether the Rev/RRE pathway is important for efficient antisense inhibition of HIV-1, we constructed identical plasmids that express antisense RNA targeting the *env* region of HIV-1, but which differ only in the export element they contain (RRE, CTE or no specific export element, see Materials & Methods). These plasmids were all based on sequences from the pNL4-3 provirus and contain the 5' and 3' LTR, a portion of *gag* sequence, and a fragment from the *env* gene in the antisense orientation which targets a 937 bp region of pNL4-3. The antisense construct targets the 3' UTR of the GagPol RNA and the coding sequence of Env RNA. This is the same region that was targeted by the

previously described VIRxSYS lentivirus vector (86). The no element plasmid is identical to the CTE plasmid, except that no CTE was inserted. As a control, we also made a similar RRE- containing construct that had the target sequence in the "sense" orientation. A schematic diagram of these plasmids is shown in Figure 8A.

We first compared the level of RNA expression from the three different "antisense" plasmids in the absence of an HIV-1 target. To do this, 293T cells were transfected in triplicate with the antisense constructs containing no element, the CTE or the RRE together with CMV promoter-driven plasmids expressing the HIV-1 Tat and Rev proteins. Tat protein is essential for high expression from the HIV-1 LTR promoter and Rev was provided to ensure good expression from the plasmid containing the RRE. A CMV-ß-globin plasmid was also cotransfected to serve as a normalization control. After 48 hours, total RNA was harvested using TriReagent. Oligo d(T) selection was performed and the isolated polyA+ RNA was analyzed on northern blots (Figure 8B). The experiment was performed in triplicate. Quantitation of the blots, with normalization to the ß-globin signal, demonstrated that the no element and the RRE-containing antisense RNA were expressed at similar levels (Figure 8C). The CTE-containing antisense RNA ran slightly slower on the gel, due to the insertion of the CTE, and the levels of this RNA were about 2-fold higher. Thus, our results show that the plasmids produce a reasonable amount of the expected antisense RNA.
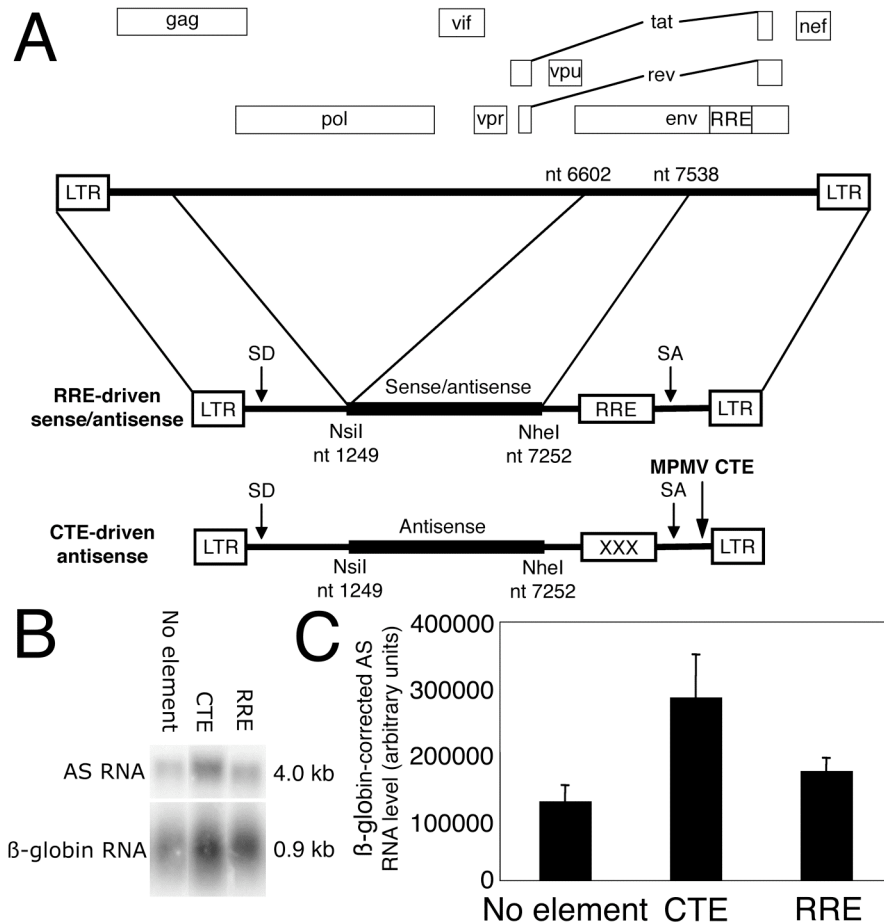
Figure 8: Construction and expression of HIV-1-derived antisense plasmids.

(A) Schematic of the antisense RNA plasmids. The plasmids contain the 5' and 3' long terminal repeats (LTR), a splice donor (SD) and acceptor (SA), a 937 bp portion of HIV-1 *env* (nts 6602-7538) in the sense or antisense orientation, the Rev Response Element (RRE) or the MPMV Constitutive Transport Element (CTE). The restriction enzyme sites utilized for construction with their pNL4-3 nucleotide coordinates are indicated below each construct. Stop codons were inserted between the *gag* and *env* sequence to prevent Env expression. (B) Northern blot analysis of antisense (AS) RNA. 10^7 293T cells were transfected with 5 µg antisense (AS) vector, 500 ng pCMV-Rev (pHR30) and 500 ng pCMV-Tat (pHR136). 5 µg pCMV-ß-globin (pHR2643) was cotransfected as a normalization control. At 48 hours post-transfection, total RNA was harvested, oligo d(T)-selected and analyzed by Northern blot using specific radiolabelled DNA probes to detect ß-globin and antisense RNAs. Blots were analyzed using a Molecular Dynamics Phosphorimager and ImageQuant software. The panel shows representative lanes from the Northern blot that was used to determine RNA expression levels. (C) Quantitation of antisense (AS) level. Antisense (AS) signal was normalized to ß-globin signal to control for recovery. Three independent samples were analyzed and the standard deviation is shown.

Inhibition of particle production from pNL4-3-derived proviruses by the antisense constructs

In order to assess the ability of the antisense to inhibit HIV-1 production, we co-transfected 293T cells with a pNL4-3 provirus containing a nonfunctional Rev gene, a plasmid expressing functional Rev (pCMV-Rev) and the indicated amounts of antisense plasmids. This allowed us to determine a dose-response range for antisense inhibition. In this experiment, we used a Rev- provirus and supplied Rev *in trans* to allow direct comparison with the Rev- provirus containing the CTE that was used as a target in later experiments. Virus production was measured by analyzing the levels of p24 in the medium supernatants of the transfected cells at 48 h post-transfection. The experiment was performed in triplicate.

As shown in Figure 9A (where levels of p24 are shown relative to control cultures in the absence of antisense RNA), the RRE-driven antisense construct efficiently inhibited HIV-1 production at a very low target/antisense molar ratio (5:1). At a ratio of 5:1, the levels of p24 were only about 20% of that in control cultures, at a ratio of 1:1, they were only about 3% and at a ratio of 1:5, they were only about 0.3%. In contrast, the CTE-driven antisense did not significantly inhibit particle production from the provirus, even at a 1:5 molar ratio, despite the fact it expressed more antisense RNA per μg of plasmid (see Figure 8C). The antisense plasmid with no export element also failed to inhibit particle production. These data indicate that the presence of an RRE in the antisense RNA is

Figure 9
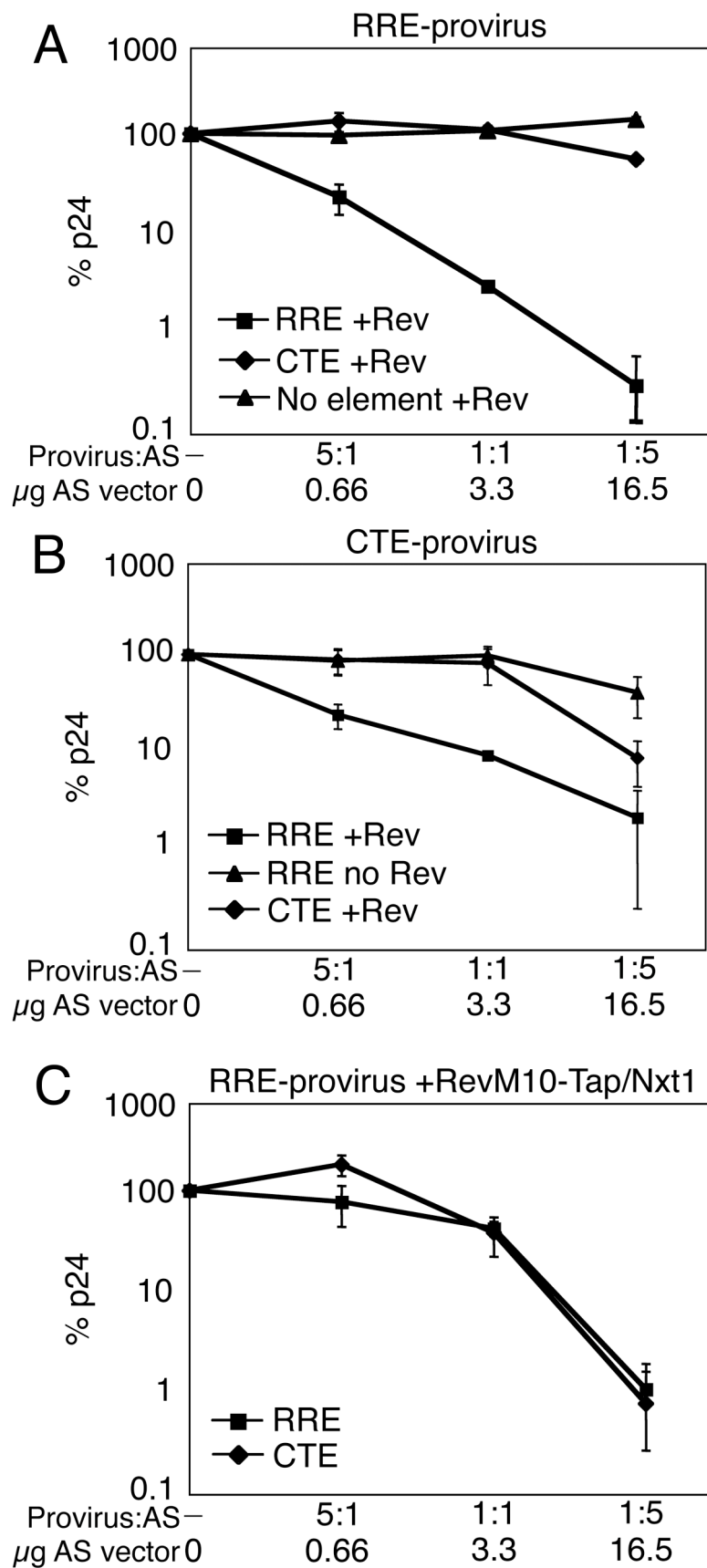
Figure 9: Inhibition of particle production from HIV-1 proviruses by antisense.

(A) Inhibition of particle production from an RRE-driven provirus. 10^6 293T cells were transfected with 5 μg pNL4-3 provirus containing a nonfunctional Rev gene (pHR1146), 500 ng pCMV-Rev (pHR30) and increasing amounts of no element (pHR3475), CTE-driven (pHR3474) or RRE-driven (pHR3473) antisense construct (AS). After 48 hours, p24 expression was assayed by ELISA and plotted as the percentage of p24 expression from the provirus alone. The molar ratio of provirus to antisense plasmid and microgram amount of antisense plasmid is indicated on the X-axis. Transfections were performed in triplicate. The p24 level for 100% was 837 -/+ 31.1 ng/mL. (B) Inhibition of particle production from a Rev-independent CTE-driven provirus. 10^6 293T cells were transfected with 5 μg of a pNL4-3 provirus containing a nonfunctional RRE and Rev gene and the MPMV CTE cloned into the *nef* region (pHR1371) together with 500 ng pCMV-Rev and increasing amounts of RRE- or CTE-driven antisense construct (AS). In the no Rev sample, pCMV was substituted for pCMV-Rev. Transfections, ELISAs and analysis were performed as in (A). The p24 level for 100% was 20.8 -/+ 7.11 ng/mL (C) Inhibition of particle production from an RRE-driven provirus in the presence of RevM10-Tap and Nxt1. 10^6 293T cells were transfected with 5 μg of the pNL4-3 proviral clone lacking a functional *rev* gene (pHR1146), 500 ng pCMV-RevM10-Tap (pHR2155), 500 ng pCMV-Nxt1 (pHR2415) and increasing amounts of RRE- (pHR3473) or CTE-driven antisense construct (pHR3474) (AS). Transfections, ELISAs and analysis were performed as in (A). The p24 level for 100% was 145 -/+8.54 ng/mL.

essential for efficient antisense inhibition and that the CTE fails to substitute for the RRE.

Since the target virus utilized in Figure 9A contained the RRE and was Rev-dependent, the efficient inhibition observed with the RRE-antisense plasmid compared to the other antisense plasmids could simply reflect co-targeting of target and antisense RNA to the same cellular compartment, making antisense/ target RNA association more efficient. To further address this, we analyzed the effects of the antisense constructs on particle production from a provirus that was Rev-independent and that utilized a different export pathway. This provirus carries mutations in *rev* that make it nonfunctional and also contains a nonfunctional RRE with synonymous mutations that do not alter the overlapping Env protein sequence. To overcome the block to RNA export that would otherwise be present, the provirus has the MPMV CTE cloned into the *nef* region. This allows full length and singly spliced viral mRNA to be exported via the MPMV CTE pathway. The provirus has previously been shown to be replication competent (11).

We cotransfected the CTE-containing provirus with different amounts of the RRE-driven antisense plasmid (with or without pCMV-Rev), or with different amounts of CTE-driven antisense plasmid. As before, this experiment was performed in triplicate. As can be seen in Figure 9B, the CTE-driven antisense was still rather inefficient at inhibiting p24 production, although significant inhibition (about 80%) could be seen at higher concentrations (Figure 9B). This

suggests that co-targeting is a factor for the CTE-driven antisense RNA, at these higher concentrations, since the antisense RNA would now be expected to traffic along the same pathway as the provirus, in contrast to the experiment shown in Figure 9A. However, surprisingly, the RRE-driven antisense was still much more efficient in inhibiting the CTE-driven provirus than was the CTE-antisense RNA, when Rev was supplied (square symbols). This cannot be attributed to co-targeting, since the antisense and target RNA utilized different export pathways. However, antisense inhibition by the RRE-driven antisense was less efficient on the CTE-virus (Figure 9B) compared to the RRE-virus (Figure 9A), suggesting that co-targeting may also play a role in this case. No significant inhibition of virus production was observed with the RRE-driven antisense when Rev was not supplied (Figure 9B, triangle symbols). These results demonstrate that both Rev and the RRE are important for efficient inhibition by the RRE-containing antisense even when the RNA produced from the target provirus does not utilize the Rev pathway.

The RevM10 protein is a Rev mutant that contains a mutation in the Nuclear Export Signal (NES), but maintains the ability to bind the RRE (90). Previously, we showed that an RRE-containing RNA can be redirected from the Rev pathway to the Tap/Nxf1pathway when a RevM10-Tap fusion protein in conjunction with the Tap co-factor Nxt1 is utilized in place of Rev (51). This allows the RevM10-Tap protein to still bind to the RRE, but its export is mediated by the Tap/Nxf1 portion of the protein. RevM10-Tap-mediated RNA export is not

sensitive to LMB inhibition (51), demonstrating that it does not use the Crm1 export pathway that is essential in the case of Rev/RRE (40, 148).

To further test the hypothesis that the Rev-RRE pathway is essential for efficient antisense inhibition, we cotransfected the pNL4-3 proviral clone lacking a functional *rev* gene, plasmids expressing RRE- or CTE-driven antisense, a plasmid expressing the RevM10-Tap fusion protein and a plasmid expressing the Nxt1 protein. As can be seen in Figure 9C, this significantly reduced the inhibition that was obtained with RRE-antisense, especially at lower antisense to target ratios (compare with Figure 9A, square symbols). Furthermore, in this experiment the inhibition curves obtained with the CTE- and RRE-driven antisense constructs were virtually overlapping. This result is not unexpected, since both of the antisense RNAs, as well as the target RNA now use the Tap/Nxf1 pathway and the CTE-driven antisense inefficiently inhibits particle production. Taken together, these results clearly demonstrate that trafficking of the antisense RNA along the Rev-RRE pathway is essential for the efficient antisense inhibition that has been observed using HIV-1 vectors, independent of a co-targeting component.

Cytoplasmic localization of target RNA

We next performed an experiment to determine the localization of the antisense RNA and if expression of antisense RNA resulted in nuclear retention

and/or significant degradation of the proviral target RNA. To do this, we cotransfected the pNL4-3 proviral clone lacking a functional *rev* gene with pCMV-Rev and the RRE or CTE antisense constructs at a 5:1 molar ratio. At this molar ratio, the RRE-driven antisense inhibits about 80% of particle production (see Figure 9A). As a control, we also performed a similar experiment using an RRE-containing plasmid with the target region in the "sense" orientation, since this RNA does not inhibit particle production (data not shown). In all of these experiments, a CMV-ß-globin plasmid was cotransfected to provide a normalization control. To control for the quality of subcellular fractionation, we also transfected the provirus with or without pCMV-Rev in the absence of sense/antisense constructs. Since the GagPol RNA produced from the provirus requires Rev for export, in the absence of Rev, GagPol RNA would not be expected to be found in the cytoplasmic fractions (90).

At 65 hours post-transfection, total and cytoplasmic RNA was extracted from the transfected cells, oligo d(T)-selected and analyzed by northern blotting for GagPol, sense/ antisense vector and ß-globin RNA. For this analysis, we compared total and cytoplasmic RNA levels in the control cells transfected with the sense RNA vector to the levels of RNA in cells transfected with the antisense vectors. A probe that detected sequences in the GagPol region in HIV-1 that is shared between the provirus and the sense/antisense plasmids was used for the GagPol and sense/antisense plasmids and a separate probe was also included

to detect ß-globin RNA (see Materials & Methods). The results from this experiment are shown in Figure 10.

Analysis of the data in Figure 10 shows that the levels of total and cytoplasmic GagPol RNA in the presence of antisense were within 2-fold of the GagPol levels in the presence of sense RNA (see GagPol RNA). The total and cytoplasmic levels of the CTE- and RRE- antisense RNAs were also similar (see Vector RNA). The presence of significant amounts of this RNA in the cytoplasm indicates that both the RRE- and CTE-antisense RNA are efficiently exported to the cytoplasm. Figure 10C shows proper fractionation during preparation of cell extracts, since in the absence of Rev, GagPol RNA did not localize to the cytoplasm. Thus, this experiment demonstrates that significant nuclear retention or degradation of target HIV-1 RNA in the presence of antisense RNA does not occur and that considerable amounts of antisense RNA can be found in the cytoplasm.

Antisense RNA does not alter the stability of target RNA

To more directly determine if expression of RRE-driven antisense RNA had any effects on the stability of GagPol RNA and whether antisense RNA was degraded in the presence of target RNA, we cotransfected 293T cells with the pNL4-3 proviral clone lacking a functional *rev* gene, pCMV-Rev and RRE-driven antisense plasmid at a 5:1 molar ratio of provirus and antisense vector, which causes an 80% reduction in p24 levels (Figure 9A). To be able to compare the fate of sense and antisense RNAs in the presence and absence of target, we

Figure 10
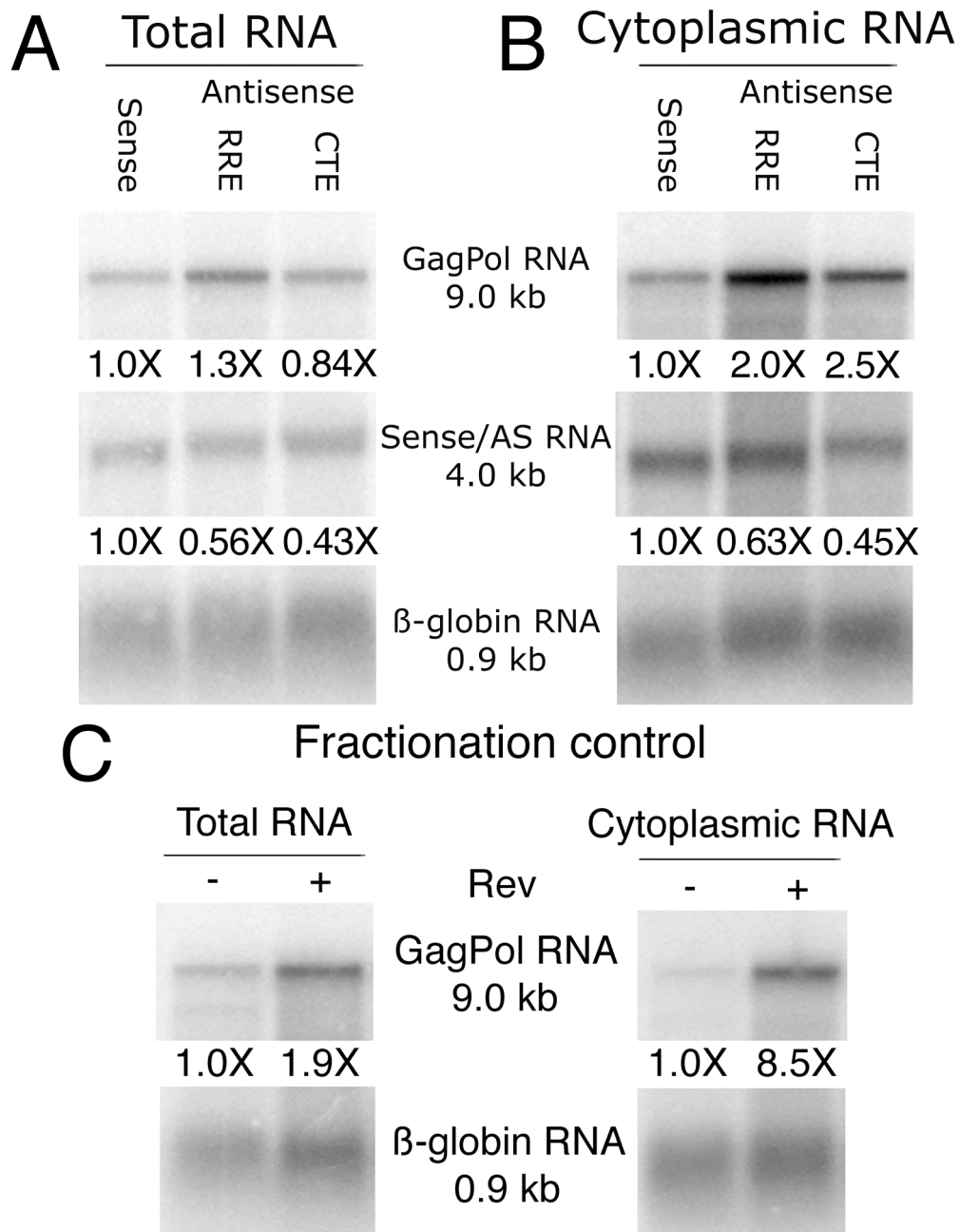
Figure 10: GagPol and sense or antisense RNA levels from total and cytoplasmic cell fractions.

(A) 10^7 293T cells were transfected with 5 μg of the pNL4-3 proviral clone lacking a functional *rev* gene (pHR1146), 500 ng pCMV-Rev (pHR30) and 660 ng RRE-driven sense (pHR3476) or antisense constructs (AS, pHR3473) at a 5:1 DNA molar ratio of provirus and vector. 5 μg CMV-ß-globin (pHR2643) was cotransfected as a normalization control. (B) 293T cells were transfected as in (A), but cytoplasmic RNA was harvested, oligo d(T)-selected and analyzed by Northern blotting. (C) Cell fractionation control for total and cytoplasmic Northern analysis. 10^7 293T cells were transfected with 5 μg of the pNL4-3 proviral clone lacking a functional *rev* gene (pHR1146), 5 μg CMV-ß-globin (pHR2643) and 500 ng of either pCMV (pHR16) or pCMV-Rev (pHR30) to ensure the quality of cellular fractionation. Total and cytoplasmic RNA was isolated and analyzed as in (A and B). After 65 hours, total RNA was harvested, oligo d(T)-selected and analyzed by Northern blotting. Specific radiolabelled DNA probes were used to detect GagPol, sense or antisense (AS) or ß-globin RNA. Blots were analyzed using a Molecular Dynamics Phosphorimager and ImageQuant software. For A and B, the numbers below each lane indicate fold-expression level of GagPol or antisense (AS) RNA relative to their levels in the RRE-driven sense sample after normalization to the ß-globin RNA. For C, the numbers below each lane indicate fold-expression level relative to their levels in the absence of Rev. Values are the mean from three independent experiments.

also performed a separate experiment in which the same amount of sense or antisense plasmid was co-transfected with only pCMV-Rev and pCMV-Tat. In all cases, a CMV-ß-globin plasmid was cotransfected for normalization. After 48 hours, cells were treated with 5 μg/mL Actinomycin D for zero, three or six hours to inhibit RNA pol II transcription. The cells were then harvested for total RNA and oligo d(T)- selected RNA was prepared and analyzed by northern blotting (Figures 11A and C) (83). The GagPol and antisense (vector) RNA levels present in each sample were then quantitated using ImageQuant software after normalization to ß-globin RNA levels (Figures 11B, D and E).

The results show that in the absence of target RNA, both the antisense RNA and sense RNA were not significantly degraded relative to ß-globin RNA (Figure 11A and B). There also was no significant change in the stability of the antisense RNA in the presence of target GagPol RNA, and GagPol RNA also was stable (see Figure 11C, D and E). Taken together, these results demonstrate that antisense, in combination with target expression, does not lead to an apparent degradation of either antisense or target RNA. These results argue against RNA degradation as a contributing factor to the observed antisense effects.

Expression of RRE-antisense RNA inhibits GagPol protein production, but does not inhibit expression of Nef
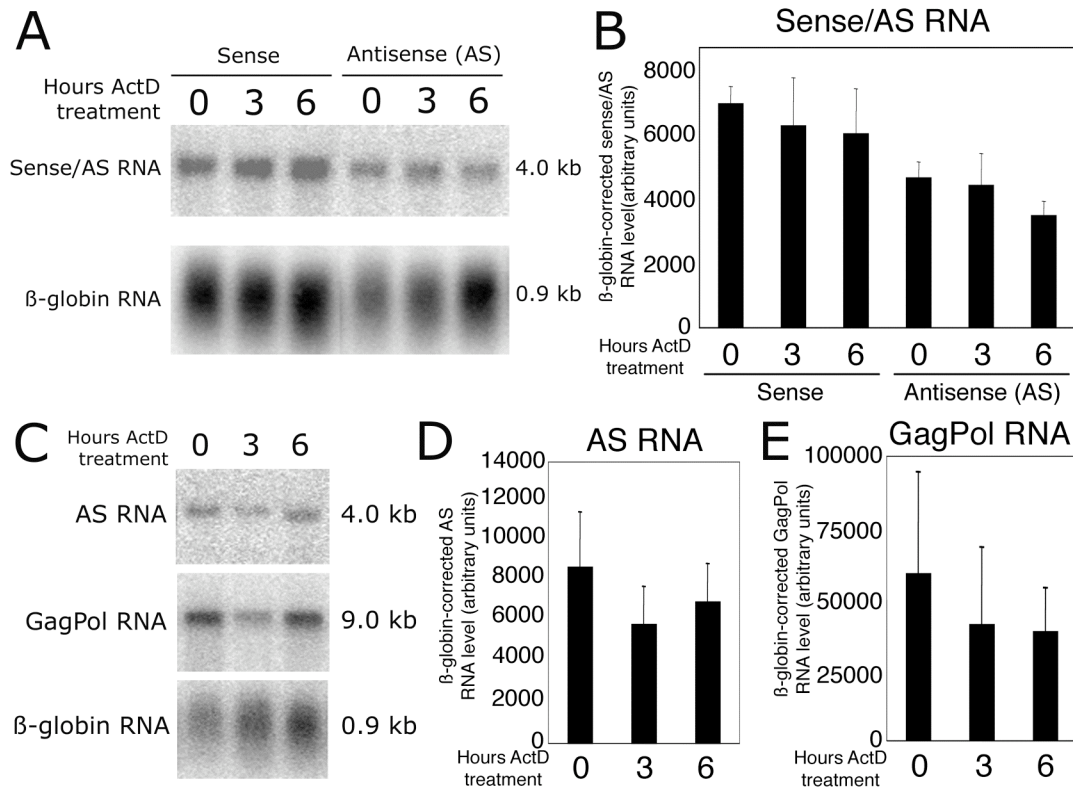
Figure 11: Stability of HIV-1 and sense/AS RNA after Actinomycin D treatment.
(A) Stability of sense/AS RNA in the absence of target RNA. 10^7 293T cells were transfected with 660 ng RRE-driven sense (pHR3476) or antisense plasmid (AS, pHR3473), 500 ng pCMV-Rev (pHR30) and 500 ng pCMV-Tat (pHR136). 5 μg CMV-ß-globin (pHR2643) was cotransfected for a normalization control. Transfections and Actinomycin D treatments were performed in duplicate. After 48 hours, cells were treated with 50 μg/mL Actinomycin D for 0, 3 or 6 hours and harvested for total RNA. RNA was oligo d(T)-selected and analyzed by Northern blotting for sense/AS and ß-globin RNA using specific radiolabelled DNA probes. Blots were visualized using a Molecular Dynamics Phosphorimager and ImageQuant software. (B) Quantitation of sense/AS and ß-globin RNA levels. RNA levels were quantitated after normalization to ß-globin RNA using ImageQuant software. (C) Stability of GagPol and AS RNA. 10^7 293T cells were transfected with 5 μg of the pNL4-3 proviral clone lacking a functional *rev* gene (pHR1146), 500 ng pCMV-Rev and 660 ng RRE-driven antisense (AS) plasmid. 5 μg CMV-ß-globin was cotransfected for a normalization control. After 48 hours, cells were treated, harvested and analyzed as in (A). (D) Quantitation of AS RNA level in the presence of target RNA. AS and ß-globin RNA levels were quantitated as in (B). (E) Quantitation of GagPol RNA level in the presence of vector RNA. GagPol and ß-globin RNA levels were quantitated as in (B).

The results from the RNA analysis indicated that the presence of the RRE-driven antisense RNA, which led to a significant reduction of p24 in the tissue culture supernatant, did not reduce the GagPol mRNA levels in the cytoplasm of transfected cells. Since p24 is expressed from the GagPol RNA, this suggests that the presence of RRE-driven antisense RNA results in either the expression of low levels of protein from the GagPol mRNA or interference with later steps in virus particle assembly or release. To distinguish between these two possibilities, we used a modified HIV-1 proviral clone (pHR1320), derived from the HIV-1 HXB2 isolate, as a target. This clone contains a glycine to alanine myristylation site mutation, a deletion at the GagPol frameshift sites and an inactivating mutation in the protease active site. The result of these three mutations is that the clone produces a GagPol precursor protein (Pr160) that cannot target to the membrane and is trapped within the cell (106). Since the protein is not processed further, its levels can be easily measured and represent a more direct readout of GagPol mRNA translation efficiency than the processed p24 protein. The nucleotide sequences targeted by antisense RNA in pNL4-3 and HXB2 are over 98% identical and we have shown that the antisense constructs inhibit particle production from a wildtype HXB2 proviral clone to the same extent as pNL4-3 (Figure 12).

To examine total GagPol Pr160 production, we cotransfected 293T cells with the mutant HXB2 proviral construct, pCMV-Rev and the RRE-driven sense or antisense plasmids, using a range of provirus:antisense plasmid molar ratios
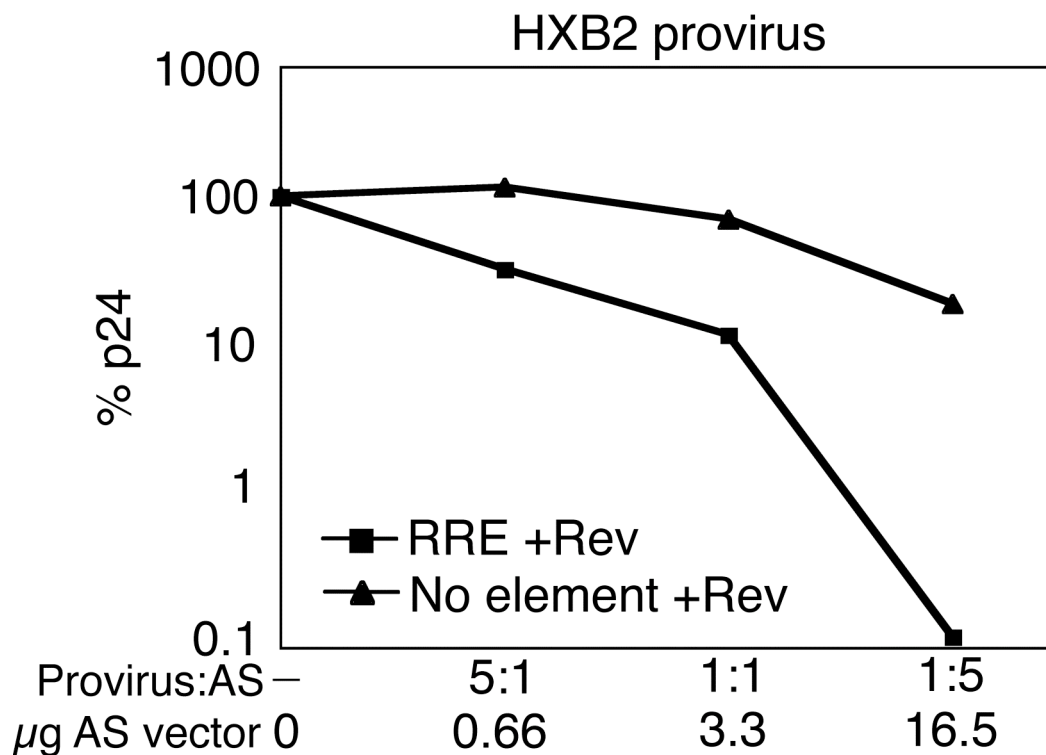
Figure 12: Inhibition of particle production from an HIV-1 HXB2 provirus by antisense.

10^6 293T cells were transfected with 5 μg HXB2 provirus (pHR3744), 500 ng pCMV-Rev (pHR30) and increasing amounts of No element (pHR3478) or RRE-driven antisense (pHR3473) construct (AS). After 48 hours, p24 expression was assayed by ELISA and plotted as the percentage of p24 expression from the provirus alone. The molar ratio of provirus to antisense (AS) plasmid and microgram amount of antisense (AS) plasmid is indicated on the X-axis. The p24 level for 100% was 570 ng/mL.

between 50:1 and 1:1. After 48 hours, cells were harvested, lysed and the extracts were run on SDS- polyacrylamide gels followed by electrotransfer and western blotting with antibodies to the p24 CA portion of Pr160 and ß-tubulin (to provide a loading control) (Figure 13A). The blot was then scanned and quantitated using the Odyssey Infrared Imaging System, and GagPol Pr160 levels were normalized to ß-tubulin. The results are shown in Figure 13A and B.

The data show that expression of RRE-driven antisense RNA efficiently reduced Pr160 levels, even at an extremely low 25:1 target:antisense molar ratio. In contrast, the RRE-driven sense construct did not reduce Pr160 levels at all, except at the highest concentration used. The reduction of intracellular Pr160 levels by the RRE-driven antisense was similar to the observed inhibition of particle production measured by p24 in the supernatant in previous experiments (Figure 9A). Thus, these results indicate a direct effect of antisense on protein levels rather than an effect on virus particle assembly or release.

To exclude the possibility that the reduction of Pr160 levels was the result of non-direct effects of the antisense vectors on the cell, such as interferon induction, we examined the effects of the antisense RNA on the HIV-1 Nef protein, which is made from an mRNA that does not contain the antisense target. The HIV-1 Nef accessory protein is encoded by a multiply spliced RNA in which the antisense target sequence has been removed by splicing. Thus the RNA encoding Nef would not be expected to be directly affected by antisense RNA

Figure 13
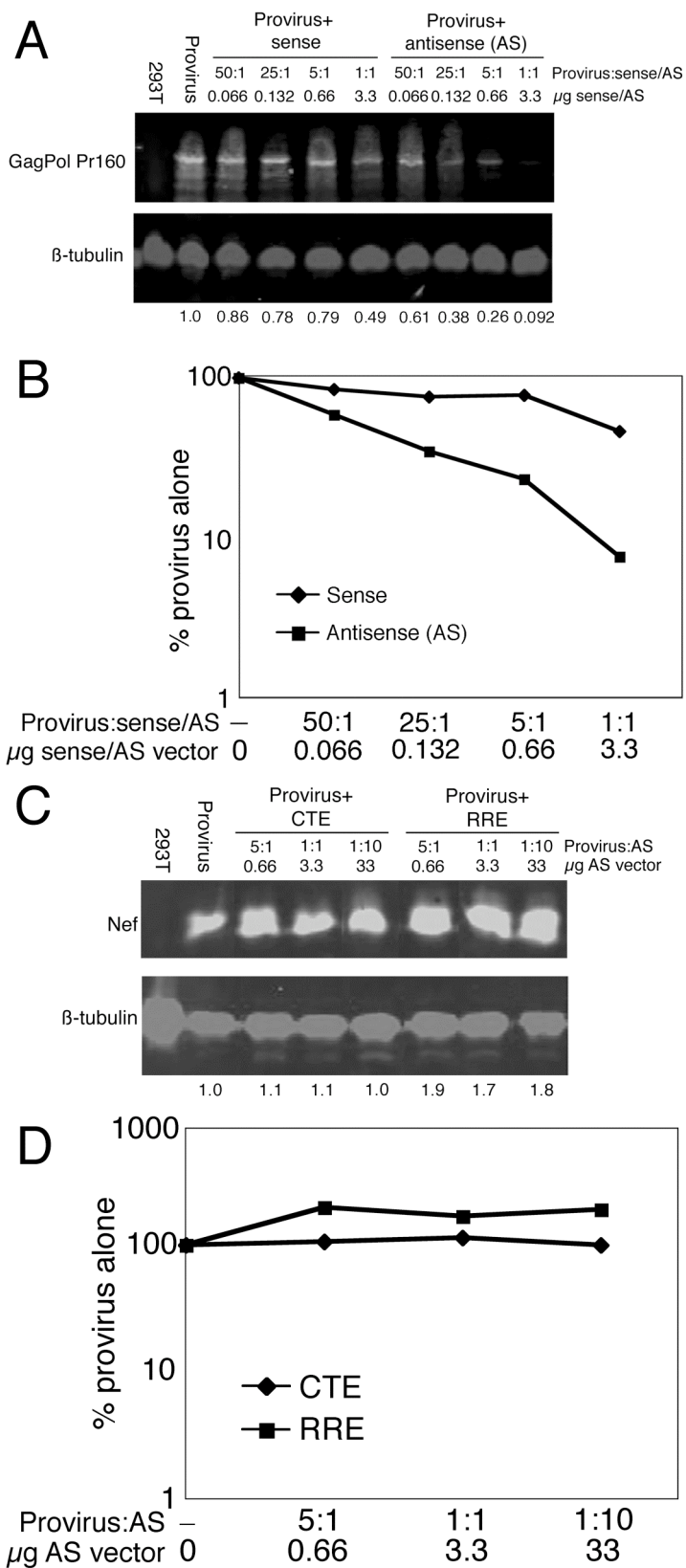
Figure 13: GagPol Pr160 and Nef production in the presence of sense or antisense vector.

(A) Pr160 production in the presence of RRE-driven sense or antisense vector. 10^6 293T cells transfected with 5 μg HXB2-derived provirus (pHR1320), 500 ng pCMV-Rev (pHR30) and increasing amounts of RRE-driven sense (pHR3476) or antisense constructs (AS, pHR3473). The HXB2 provirus contains a nonfunctional myristilation signal, GagPol frameshift and nonfunctional protease. Cells were harvested after 48 hours and extracts were run on an 8% polyacrylamide-SDS gel followed by electrotransfer to Immobilon FL. Blots were probed with a monoclonal antibody to the p24 CA portion of Pr160 (183-H12-5C) and a commercial polyclonal antibody to ß-tubulin (Abcam). The molar ratio of provirus and sense or antisense (AS) vector and microgram amount of vector is indicated above each lane. GagPol Pr160 expression level relative to provirus alone is indicated below each lane. (B) Quantitation of Pr160 production in the presence of RRE-driven sense or antisense vector. Pr160 levels were normalized to cellular ß-tubulin using the Odyssey Imaging System. The Pr160 level is expressed as a percentage of Pr160 produced from the provirus alone. (C) HIV-1 Nef production in the presence of CTE- or RRE-driven antisense constructs (AS). 10^6 293T cells were transfected with 5 μg of the pNL4-3 proviral clone lacking a functional *rev* gene (pHR1146), 500 ng pCMV-Rev (pHR30) and increasing amounts of CTE- (pHR3474) or RRE-driven antisense construct (pHR3473) (AS). Cells were harvested, blotted and analyzed as described in (A) except that an HIV-1 Nef monoclonal antibody (SN20) was used in place of the p24 monoclonal antibody. (D) Quantitation of Nef production in the presence of CTE- or RRE-driven antisense construct. Nef expression levels were measured as described for Pr160 in (B).

expression, unless the antisense RNA targeted the Nef mRNA in the nucleus prior to splicing.

To determine if expression of antisense RNA had any effects on Nef protein levels, we cotransfected 293T cells with the pNL4-3 proviral clone lacking a functional *rev* gene, pCMV-Rev and increasing amounts of either the RRE or CTE-driven antisense construct. After 48 hours, cells were harvested, lysed and the extracts were separated on SDS-polyacrylamide gels followed by electrotransfer and western blotting with antibodies to Nef and ß-tubulin (Figure 13C). The blot was then scanned and quantitated using the Odyssey Infrared Imaging System and Nef levels were normalized to ß-tubulin levels. As can be seen in Figure 13D, Nef protein levels remained constant in the presence of either the CTE- or RRE-driven antisense constructs (Figure 13D). This result demonstrates that the antisense effect is specific for mRNA that contains the target sequence and speaks against non-specific effects on protein production or degradation. It also suggests that the antisense RNA does not target RNA prior to splicing.

Polyribosome localization of GagPol and vector RNA

Although our results clearly indicate that the target RNA reaches the cytoplasm, the lack of stable protein expression could potentially indicate that in the presence of antisense RNA, the RNA traffics to a compartment away from the translation machinery, such as P-bodies (107). This would lead to a failure of the

RNA to appear in polyribosome complexes. To determine if the HIV-1 GagPol

mRNA localized to the polyribosome in the presence of antisense RNA, we

cotransfected 293T cells with the pNL4-3 provirus lacking a functional *rev* gene,

pCMV-Rev and the RRE-driven sense or antisense plasmids. The provirus and

sense or antisense plasmids were transfected at the same 5:1 molar ratio of

provirus and vector used in most of our other experiments. After 48 hours, cells

were harvested for cytoplasmic RNA and extracts were applied to a sucrose

gradient, which was subjected to ultracentrifugation as previously described (8).

During fractionation, the gradient was continuously analyzed using a BioComp

Gradient Master equipped with a UV monitor, which recorded absorbance at 254

nm. *In vitro* transcribed Gag RNA (IVT Gag) was added to each fraction to control

for recovery during subsequent analysis. RNA was then isolated from the

collected fractions and analyzed by northern blotting for GagPol, vector, ß-globin,

and IVT Gag RNA. Northern blots were analyzed and quantitated using

ImageQuant software. The blots are shown in Figure 14A and B and the

quantitation is shown in Figure 14E. To confirm that antisense inhibition was

effective in this experiment, we also assayed cell supernatants for particle

production. The p24 levels are indicated above the UV traces (Figure 14A and

B). As indicated, p24 levels were 53 ng/mL in the presence of antisense RNA,

versus 385 ng/mL in the control experiment. Thus, the 84% inhibition observed

was consistent with earlier experiments.

Figure 14

RRE-driven provirus +sense

A

80S
60S
40S

48 hr p24= 385 +/- 67.1 ng/mL

RRE-driven provirus +antisense (AS)

B

80S
60S
40S

48 hr p24= 53.3 +/- 3.84 ng/mL

Fraction number 1 2 3 4 5 6 7 8 9 10 11 12 13 14 15 16 17 18 19

GagPol RNA 9.0 kb

Sense/AS RNA 4.0 kb

IVT Gag RNA 0.7 kb

Fraction number 1 2 3 4 5 6 7 8 9 10 11 12 13 14 15 16 17 18 19

ß-globin RNA 0.9 kb

RRE-driven provirus +sense +EDTA

C

60S
40S

RRE-driven provirus +antisense (AS) +EDTA

D

60S
40S

Fraction number 1 2 3 4 5 6 7 8 9 10 11 12 13 14 15 16 17 18 19

GagPol RNA 9.0 kb

Sesne/AS RNA 4.0 kb

IVT Gag RNA 0.7 kb

Fraction number 1 2 3 4 5 6 7 8 9 10 11 12 13 14 15 16 17 18 19

ß-globin RNA 0.9 kb

E

GagPol RNA

Sense
Antisense

% total GagPol RNA

Polysome fraction

F

GagPol RNA +EDTA

Sense
Antisense

% total GagPol RNA

Polysome fraction

Figure 14: Polyribosome analysis of GagPol and vector RNA by sucrose gradient centrifugation.

(A and B) 10^7 293T cells were transfected with 5 μg of the pNL4-3 proviral clone lacking a functional *rev* gene (pHR1146), 500 ng pCMV-Rev (pHR30) and 660 ng RRE-driven sense (pHR3476)(A) or antisense (AS, pHR3473)(B) vector at a 5:1 molar ratio of provirus and sense/AS. 5 μg CMV-ß-globin (pHR2643) was cotransfected as a control. 48 hours post-transfection, cytoplasmic extracts were prepared and separated by centrifugation through a sucrose gradient. Gradients were fractionated while monitoring UV absorbance at 254 nm. RNA was purified from fractions after the addition of *in vitro* transcribed Gag (IVT Gag) RNA for a recovery control. RNA from fractions were analyzed by Northern blotting and probed with specific radiolabelled DNA probes to GagPol, sense/AS, ß-globin and IVT Gag RNA. Blots were analyzed using a Molecular Dynamics Phosphorimager and ImageQuant software. (C and D) Polyribosome analysis of GagPol and vector RNA after EDTA treatment and sucrose gradient centrifugation. Transfected cells were harvested and processed as described in (A and B) except that prior to sucrose gradient centrifugation, cytoplasmic extracts were treated with 15 mM EDTA. (E) Quantitation of GagPol RNA localization in a sucrose gradient in the presence of sense or antisense RNA. GagPol RNA levels were normalized to IVT Gag and plotted as a percentage of the total GagPol RNA present in the gradient. (F) Quantitation of GagPol RNA localization in a sucrose gradient in the presence of sense or antisense RNA after treatment with 15 mM EDTA. Analysis was carried out as in (E).

As can be seen in Figures 14A, B and E, the GagPol mRNA showed a similar localization to fractions containing polyribosomes in the presence of either sense or antisense RNA. The sense and antisense RNAs were also localized to the polyribosome region of these gradients. Although these results suggested that, in the presence of antisense RNA, the target RNA still associates in polyribosome complexes in the absence of stable Gag protein levels, it was possible that this reflected association with a non-ribosomal complex that cosediments with polyribosomes. It has previously been demonstrated that treatment with 15 mM EDTA disrupts polyribosomes without disrupting most non-ribosomal RNA-protein complexes (14, 63). For this reason, we also treated cell lysates with 15 mM EDTA prior to fractionation (Figure 14C and D). The loss of polyribosomal complexes in the presence of EDTA can be observed in the UV trace (Figure 14C and D). In the presence of EDTA, GagPol, vector and ß-globin RNA all localized only to fractions that sedimented more slowly than the normal position of polyribosomes and again, the GagPol target RNA showed a similar localization both in the presence and absence of antisense RNA (Figure 14F). These results suggest that the target RNA is indeed localized to polyribosomes in the presence of antisense RNA. However, based on the results described above, it is clear that this association does not result in normal amounts of stable Gag protein.

Discussion

In this chapter, we present experiments demonstrating efficient inhibition of HIV-1 by unmodified antisense RNA that targets the 3' UTR of the GagPol RNA. Our data clearly show that the expression of an antisense RNA targeting a region in *env* is able to significantly reduce particle production, even at very low ratios of antisense to target HIV-1 RNA. Although this was an unexpected finding based on many previous studies showing the inefficiency of similar approaches to target viruses and cellular genes (56, 80), it confirms the recent studies by VIRxSYS targeting HIV-1 using a similar RRE-containing antisense RNA (86).

Our data show that efficient targeting requires trafficking of the antisense RNA along the Rev/RRE pathway. In support of this conclusion, we demonstrated that the inhibition of HIV-1 was virtually abolished when the antisense RNA lacked an RRE or when Rev was not provided. In addition, the efficiency of antisense inhibition was significantly reduced when the RRE-containing antisense RNA was redirected to the Tap/Nxf1 pathway that normally is used to export CTE-containing RNA and many cellular mRNAs. We conclude that the efficient inhibition achieved using HIV-1-derived lentiviral vectors can be explained by the specific RNA trafficking pathway utilized by HIV-1.

Co-targeting of the antisense and HIV-1 target RNA to the same cellular compartment in the nucleus has recently been proposed as a possible mechanism for the efficiency of the VIRxSYS vector that is currently in clinical trials (117). It was proposed that this would trigger extensive adenosine deamination of the HIV-1-antisense duplex, resulting in nuclear retention of the

resulting dsRNA complexes (75, 160). However, our results show that, although co-targeting may contribute to antisense efficiency, it is clearly not essential, since an HIV-1 proviral clone that was altered to use an MPMV CTE, rather than an RRE, was also efficiently inhibited by the RRE-driven antisense RNA in the presence of Rev. In this case, the antisense RNA used the Rev/RRE pathway, whereas the HIV-1 target RNA was exported through the Tap/Nxf1 pathway. Previous work from many laboratories have shown that these export pathways are separate and use different cellular factors (40, 51, 105).

If co-targeting were the dominant reason for the observed antisense inhibition, the efficiency would also have been expected to remain the same when RevM10-Tap was used to replace Rev in the export of the HIV-1 target and antisense RNA. Instead, the inhibition was significantly reduced, demonstrating that trafficking through the Rev pathway is a major determinant of efficient antisense inhibition. However, nuclear co-targeting may still contribute to antisense inhibition, as the CTE-driven antisense more efficiently targeted the RRE-virus that was forced to use the Tap/Nxf1 pathway. Additionally, trafficking of both RRE and CTE-driven antisense RNAs and targets on this pathway also led to nearly identical inhibition profiles.

Our results clearly demonstrate that nuclear retention of HIV-1 target RNA did not contribute to the antisense inhibition that was achieved with the RRE-driven antisense RNA in the presence of Rev. Even when p24 levels were efficiently reduced, the GagPol RNA was still exported to the cytoplasm and

present in polyribosomal complexes. We showed that the reduction of p24 was not due to a general effect on protein synthesis, since Nef protein levels remained normal. Additionally, our experiments with a proviral HIV-1 clone that did not give rise to virus particles demonstrated that the inhibition did not occur at the level of particle assembly or release. Thus, the antisense effects are manifested at the cytoplasmic level, after the association of the mRNA with the translation machinery, but before particle assembly.

We also clearly showed that the reduction in p24 was not due to a general effect on protein synthesis, since Nef protein levels were unaffected by antisense expression. This specificity of inhibition for the HIV-1 target was somewhat surprising, since in mammalian cells, long double-stranded RNAs often activate protein kinase R and 2'5'-oligoadenylate synthetase, which leads to the interferon response and a general downregulation of translation and RNA degradation (58, 120). This suggests that trafficking of the antisense RNA through the Rev/RRE pathway somehow allows the interferon response to be bypassed. An analogous bypass mechanism has been suggested for inhibition by some siRNAs (33, 120). However, activation of the interferon response and subsequent downmodulation of Nef expression needs to be demonstrated in order to unequivocally prove that the interferon response is not induced by the target and antisense RNA duplex.

Although in most cases, appearance of an RNA in polyribosome complexes leads to production of protein, a reduction in the rate of initiation concomitant with a decrease in the rate of elongation can give rise to significantly

reduced levels of protein ("ribosome stalling") that could explain the reduced GagPol protein levels seen (129). Alternatively, the high molecular weight complexes could represent complexes which are EDTA sensitive and appear to be polyribosomes, but are actually newly described pseudo polyribosomal complexes (138). Another possibility is that protein is produced, but rapidly degraded. Both of these mechanisms have been proposed to function in miRNA mediated translation inhibition (102). Further experiments will be needed to distinguish between these possibilities.

Independent of the detailed mechanism utilized, our results clearly point to a novel, previously unknown, mechanism for antisense inhibition. Our current model is that Rev and the RRE allow the target/antisense RNA to be exported to the cytoplasm, where the antisense RNA functions to inhibit protein production. Intriguingly, there have been several reports that some complex retroviruses produce natural antisense transcripts (13, 16, 76, 89, 95). The best characterized of these RNAs in HIV-1 appears to initiate from multiple transcription start sites 5' of the 3' LTR and extend into the *pol* region, where a novel polyadenylation site has recently been described (76). While additional studies are needed to validate the presence of antisense RNA in HIV-1-infected cells, the evidence for the existence of an antisense strand transcript in the HTLV-I retrovirus is much more compelling (16, 119, 139). In light of our finding that antisense transcripts can be potent inhibitors of gene expression in the HIV-1 system, further studies on the role of these natural transcripts in the regulation of HIV-1 and other

retroviruses seem warranted. In this regard, it would be of interest to determine if antisense transcripts similar to the ones we have described, but driven by the HTLV-I Rex protein and RexRE, would work as potently as those that utilize the Rev protein and RRE.

Although we do not know if a similar mechanism of antisense inhibition normally operates in the host cell to function in gene regulation, recent evidence indicates that expression of natural antisense RNA to normal gene transcripts may be a common occurrence (22, 44). Although most mRNAs probably do not traffic down the Crm1 pathway used by Rev and the RRE, this pathway has been reported to be utilized by some mRNAs (74, 121). Thus, it is possible that similar mechanisms to the one we have described are utilized to regulate expression of cellular mRNAs.

In the case of cellular, as well as viral mRNA, it has been shown that regions of double stranded RNA, resulting from the presence of inverted sequences in the RNA or association with antisense RNA are subject to deamination by ADAR, leading to multiple inosines in the RNA (4). Such RNAs are normally retained in the nucleus through interaction with nuclear matrix proteins and eventually degraded (75, 110, 160). However, a previous study using the Xenopus oocyte export model, showed that edited RNA was exported to the cytoplasm if the RNA contained an RRE and Rev was provided *in trans* (160). Additionally, a previous study by Lu *et al.* using the VIRxSYS lentivirus antisense vector reported that HIV-1 RNA recovered from cells expressing

antisense RNA showed multiple mutations in the antisense target region of the

HIV-1 genome that were consistent with ADAR activity (86). These results

suggest that at least some of the genomic RNA, which was complexed with

antisense RNA and edited as a result of formation of dsRNA, was eventually

exported to the cytoplasm and packaged. Therefore, it seems possible that

editing activity plays a role in antisense inhibition. It also follows that naturally

occurring antisense could help provide retroviruses with an additional pathway for

sequence diversification.

However, to date, RT-PCR sequencing of cytoplasmic RNA in cells

transfected with proviral clones and plasmids expressing antisense RNA have

failed to detect any mutations indicating ADAR editing (data not shown). Thus,

we do not believe that editing is directly connected to the reduced protein levels

we observe. Also, the target region is downstream of the GagPol ORF and

mutations in the target region, the 3' UTR, will not affect the GagPol protein *per

se*. However, editing of even a small amount of the RNA could potentially lead to

the production of miRNA from the antisense RNA (104). Inhibition by a miRNA-

mediated mechanism would be consistent with the efficient inhibition we observe,

and miRNA often exerts its effect at the translation level (107).

Irrespective of the mechanism utilized for antisense inhibition, our results

are of importance for future development in the gene therapy field. The data

suggest that it will be advantageous to ensure that any long antisense RNA

designed to combat HIV-1 contains the RRE, to allow trafficking along the

Rev/RRE pathway, as this will likely significantly increase the efficiency of antisense inhibition. Our data also show that an RRE-driven antisense RNA, in combination with Rev, is able to efficiently inhibit a target that utilizes the CTE pathway. This raises the possibility that Rev/RRE trafficking of antisense RNA can also be exploited to make antisense RNA inhibition more efficient for non-HIV-1 applications.

Chapter 4- Mechanistic studies and alternative target RNAs

Introduction

The following experiments extend the results presented in the previous chapter by exploring additional aspects of antisense inhibition and its mechanism of action. For instance, while we clearly established the ability of the RRE-driven antisense construct to inhibit particle production from an RRE-driven provirus by examining p24 levels in tissue culture supernatant (Figure 9A), it was not clear what effect the antisense construct had on Env expression from the provirus. The antisense constructs target Env as well as GagPol mRNA, thus it was of interest to determine if Env expression was also inhibited.

As also shown in the previous chapter, we observed inefficient inhibition of particle production by the CTE-driven antisense construct, even when a CTE-driven provirus was targeted (Figure 9B). Since Tap/Nxf1 and Sam68 have been demonstrated to improve polyribosomal localization of CTE-containing RNAs, we wanted to determine if inhibition by the CTE-driven antisense could be improved by overexpression of CTE cofactors such as Tap/Nxf1 and Nxt1 or Sam68.

We also performed experiments to determine if antisense inhibition could be competed out by increasing amounts of sense RNA. We hoped that this could provide some insight into the mechanism of antisense inhibition, specifically in distinguishing whether the antisense-target duplex remains intact or is processed into small effector RNAs. Finally, we examined the ability of the antisense

vectors to inhibit expression from non-HIV-1 sequences. We targeted EGFP expression from both a pNL4-3-derived provirus containing the EGFP sequence and a minimal LTR-driven EGFP expression construct.

Results

Envelope expression in the presence of antisense constructs

The RRE-driven antisense construct efficiently inhibited particle production, which is dependent on the expression of the Gag and GagPol proteins. All HIV-1 RNAs are derived from the GagPol RNA through alternative splicing and the Gag and GagPol proteins are encoded by the unspliced mRNA. In the context of the GagPol mRNA, the antisense construct targets sequence in the 3' UTR. The Env protein, on the other hand, is encoded by a singly spliced RNA. Env is translated into the gp160 precursor protein, which is cleaved intracellularly into gp120 (SU) and gp41 (TM) prior to incorporation into the virion (144, 147). In the context of the Env mRNA, the antisense construct targets the Env coding sequence. Since the target sequence is in a different context and functions as an ORF, we wanted to determine if the antisense constructs could inhibit Env expression. 293T cells were transfected with pNL4-3 provirus and increasing amounts of CTE- or RRE-driven sense or antisense construct in a range of molar ratios of 1:1 to 1:5 of provirus and vector. In these experiments, the pNL4-3 provirus contained a functional *rev* gene. The experiment in Figure 15A was performed without cotransfection of the pCMV-Rev expression plasmid.

Cells were harvested after 48 hours, run on a 12% low-bis SDS polyacrylamide

gel and electrotransferred to Immobilon FL. Blots were probed for HIV-1

Envelope using the Env 1D6 mouse monoclonal antibody (NIH AIDS Research

and Reference Reagent Repository). Blots were visualized using the Odyssey

Infrared Imaging System (Figure 15A).

Western blotting demonstrated that the RRE-driven antisense construct

efficiently inhibited Env production, whereas the CTE-driven antisense construct

did not inhibit Env production. Neither the RRE- driven sense or CTE-driven

antisense constructs altered Env expression.

The experiment in Figure 15B was performed with 500 ng of co-

transfected pCMV-Rev. We cotransfected pNL4-3 provirus, pCMV-Rev and the

RRE-driven sense or antisense using a range of molar ratios from 8:1 to 2:1 of

provirus and vector. This range of molar ratios uses less antisense vector than in

the previous experiment in order to determine the effective range for inhibition of

Env production. Across this range of molar ratios, the RRE-driven antisense

construct efficiently inhibited Env expression, whereas the RRE-driven sense

construct had no obvious effect on Env expression (Figure 15B). Together with

the previous p24 ELISA data (Figure 9A), these results demonstrate that the

RRE-driven antisense efficiently inhibits protein expression from HIV-1 RNAs

containing the target sequence. In addition, it demonstrates that the location of

the target sequence, whether in the 3' UTR or within an ORF, is not a major

determinant of efficient antisense inhibition.
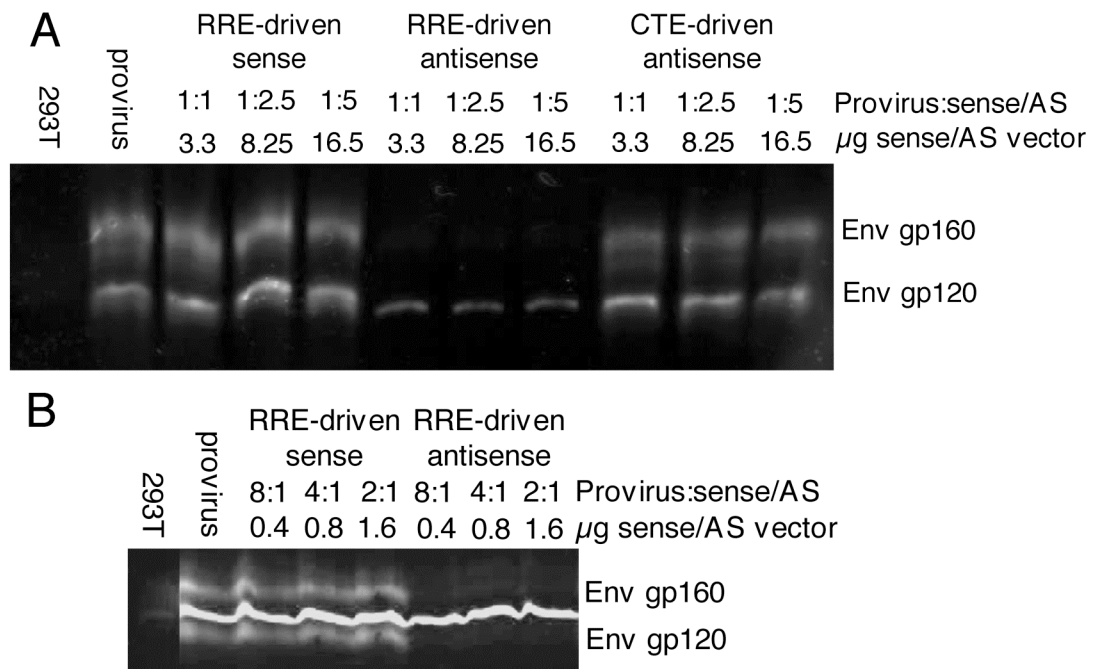
Figure 15: Inhibition of Env production from an HIV-1 provirus in the presence of antisense construct

(A) 10^6 293T cells were transfected with 5 μg pNL4-3 provirus (pHR1145) and increasing amounts of RRE-driven sense (pHR3476) or RRE- (pHR3473) or CTE-driven antisense (AS) construct (pHR3474). After 48 hours, cells were harvested and run on a low-bis 12% polyacrylamide-SDS gel and electrotransferred to Immobilon FL. Blots were probed with a monoclonal antibody to Env gp120 (Env 1D6). The molar ratio and microgram amount of sense or antisense (AS) vector is indicated above each lane. The blot was visualized using the Odyssey Infrared Imaging System. (B) 10^6 293T cells were cotransfected with 5 μg pNL4-3 provirus (pHR1145), 500 ng pCMV-Rev (pHR30) and different molar ratios of RRE-driven sense (pHR3476) or antisense (AS) vector (pHR3473). After 48 hours, cells were harvested and analyzed as in (A).

Effect of Tap/Nxf1 coexpression on CTE-driven antisense inhibition

The CTE-driven antisense construct poorly inhibited particle production, regardless of whether the target RNA used the RRE or CTE pathway. We have demonstrated that coexpression of the Tap/Nxf1 and Nxt1 proteins enhanced nuclear export of CTE-containing RNAs and increased the localization of CTE-containing RNAs in the polyribosome (51, 62). It is possible that coexpression of Tap/Nxf1 and Nxt1 could improve antisense inhibition by increasing cytoplasmic or polyribosomal localization of the antisense RNA. In order to test this, 293T cells were cotransfected with a pNL4-3 derived provirus containing a nonfunctional *rev* gene, pCMV-Rev and CTE-driven sense or antisense vector in two molar ratios (1:1 and 1:5 of provirus and antisense) that demonstrated no inhibition (1:1) or 50% inhibition (1:5) of particle production in the absence of exogenous Tap/Nxf1 (Figure 9A). Cells were cotransfected with equivalent amounts of pCMV or pCMV-Tap and pCMV-Nxt1 plasmids. After 48 hours, tissue culture supernatants were assayed for particle production.

We found that Tap/Nxf1 and Nxt1 significantly improved antisense inhibition by the CTE-driven antisense vector, compared to CTE-driven antisense in the absence of exogenous Tap and Nxt1 (Figure 16). However, the improved inhibition was still not as efficient as when the RRE-driven antisense construct was utilized. For example, Figure 9A in Chapter 3 showed that at a 1:1 molar ratio, the RRE-driven antisense inhibited particle production to 3% of provirus
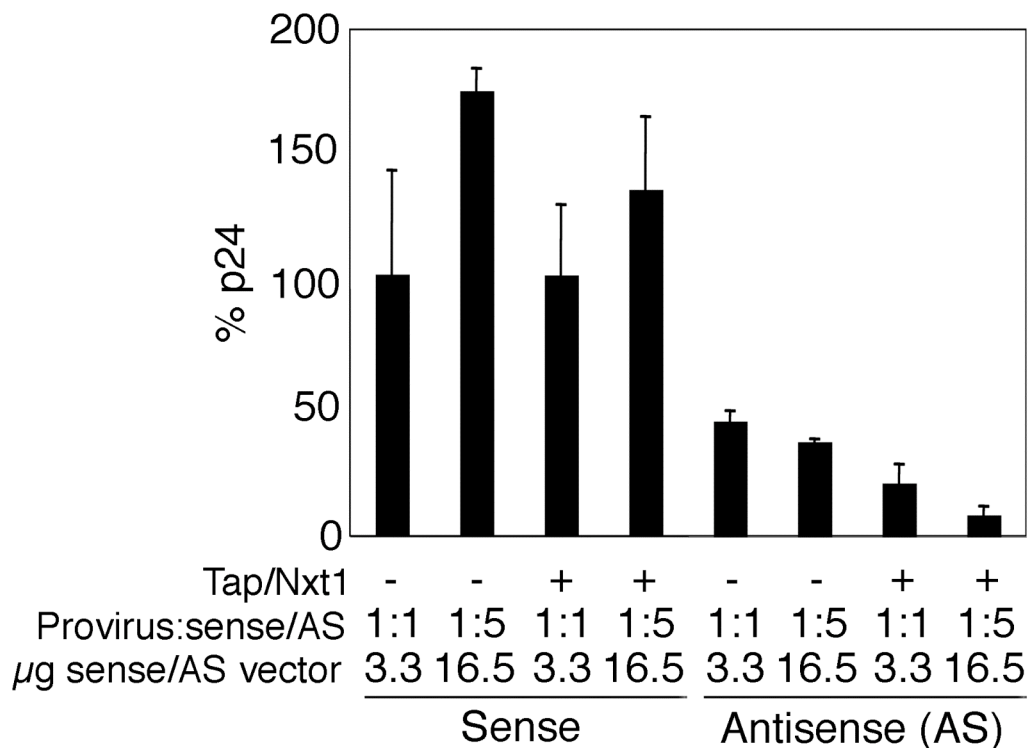
Figure 16: Effect of Tap/Nxf1 and Nxt1 coexpression on antisense inhibition by a CTE-driven vector

10^6 293T cells were transfected with a pNL4-3 provirus containg a nonfunctional *rev* gene (pHR1146), pCMV-Rev (pHR30) and CTE-driven sense (pHR3477) or antisense (AS, pHR3474) at a 1:1 or 1:5 molar ratio of provirus and sense/AS. Cells were cotransfected with either 1 μg pCMV (pHR16) or 500 ng pCMV-Tap (pHR2128) and 500 ng pCMV-Nxt1 (pHR2415), as indicated on the plot. After 48 hours, p24 expression was assayed by ELISA and plotted as a percentage of p24 expression from the provirus alone. The molar ratio and microgram amount of sense or antisense (AS) vector are indicated on the X-axis. Three independent transfections were performed on different days and standard deviation is indicated. The mean p24 value for 100% was 436 ng/mL.

alone, whereas the CTE-driven antisense, at the same molar ratio and in the

presence of Tap/Nxf1, inhibited only to 19.5%. In addition, at a 1:5 molar ratio,

the RRE-driven antisense inhibited to 0.3% of provirus alone, whereas the CTE-

driven antisense, in the presence of Tap/Nxf1 inhibited to 8.4%. Results are

representative of three independent experiments. These results suggest that

exogenous Tap/Nxf1 enhances CTE-driven antisense inhibition of particle

production from an RRE-driven provirus.

Effect of Sam68 coexpression on CTE-driven antisense inhibition

The CTE-driven antisense construct poorly inhibited particle production,

regardless of whether the target RNA used the RRE or CTE pathway (Figure 9A

and B). We have demonstrated that coexpression of Sam68 significantly

improves localization of CTE-containing RNAs to the polyribosome (28). It is

possible that coexpression of Sam68 could improve antisense inhibition by

increasing polyribosomal localization of the antisense RNA. In order to test this,

we cotransfected 293T cells with a pNL4-3 provirus containing a nonfunctional

rev gene, pCMV-Rev and CTE-driven sense or antisense vector in a range of

molar ratios from 1:1 to 1:10 of provirus and antisense, which demonstrated

approximately 50% inhibition in previous experiments. We cotransfected

equivalent amounts of either pCMV or pCMV-Sam68. After 48 hours, tissue

culture supernatants were assayed for particle production.
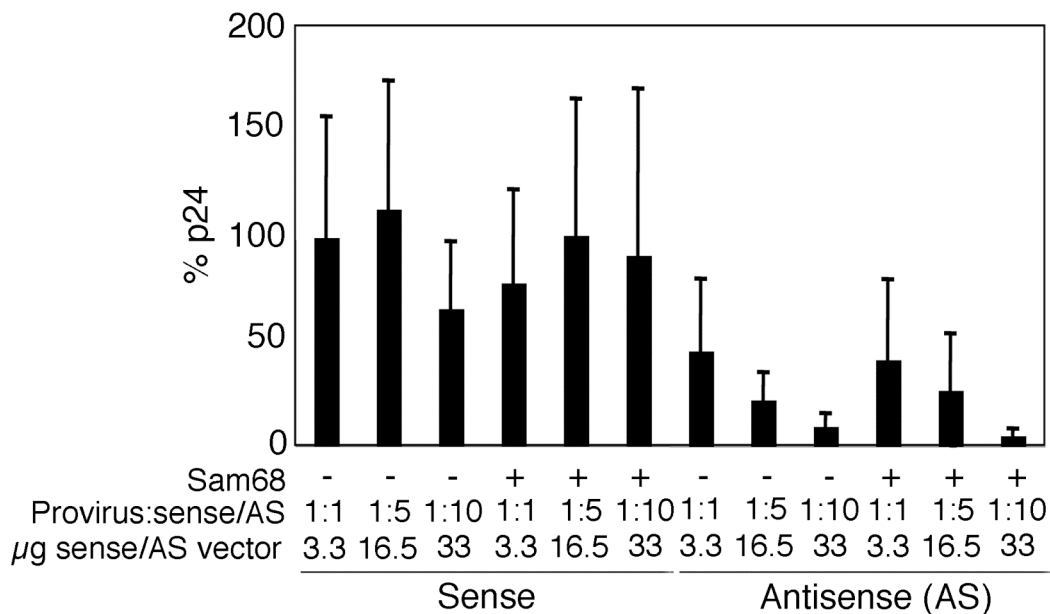
Figure 17: Effect of Sam68 coexpression on antisense inhibition by a CTE-driven vector

10^6 293T cells were transfected with 5 μg pNL4-3 provirus lacking a functional *rev* gene (pHR1146), 500 ng pCMV-Rev (pHR30) and increasing amounts of CTE-driven sense (pHR3477) or antisense (AS) vector (pHR3474). Cells were cotransfected with 500 ng pCMV (pHR16) or pCMV-Sam68 (pHR2208), as indicated on the plot. After 48 hours, p24 expression was assayed by ELISA and plotted as a percentage of p24 expression from the provirus alone. The molar ratio and microgram amount of sense or antisense (AS) vector are indicated on the X-axis. Three independent transfections were performed on three different days and the standard deviation is indicated. The mean p24 value for 100% was 517 ng/mL.

We found that coexpression of Sam68 did not significantly improve antisense inhibition by the CTE-driven antisense vector (Figure 17). Results are representative of three independent experiments. These results suggest that exogenous Sam68 does not enhance CTE-driven antisense inhibition of particle production from an RRE-driven provirus, in contrast to the previous result demonstrating that exogenous Tap/Nxf1 enhances CTE-driven antisense inhibition. Whether the function has to do with nuclear export or translation remains to be determined.

Competition assays for RRE-driven antisense construct

There are two known mechanisms that can be envisaged to explain the inhibition of protein production from a targeted RNA by antisense. In the first mechanism, one target RNA is bound by one antisense RNA in order to inhibit protein expression. This relies on binding of the antisense RNA to its target and stimulation of RNase H activity. Antisense oligonucleotides are thought to use this mechanism to inhibit protein expression from targeted RNAs. Alternatively, the formation of double-stranded RNA is subject to editing by ADAR, which leads to nuclear retention due to the presence of inosine residues. In the second mechanism, the antisense and target RNA duplex could be processed by Dicer enzyme into small effector RNAs, which can inhibit translation or induce the cleavage of complementary RNAs via the RISC complex. Long double-stranded RNAs are Dicer substrates *in vitro* and the generation of multiple small RNAs

could explain the efficiency of antisense inhibition. In order to distinguish between these mechanisms, we attempted to compete out the antisense effect by cotransfecting increasing amounts of complementary sense plasmid. We reasoned that if the antisense effect could be competed out, then the antisense construct was probably using a RNase H-dependent, "classical" antisense mechanism. This implies that one antisense RNA would inhibit one target RNA and then either be recycled or degraded in the process. If there was no difference or an additional reduction of particle production, then it was possible that the antisense-target RNA duplex was processed by Dicer. The additional double-stranded RNAs would generate many siRNAs and amplify the observed antisense effect. In addition, they would access a more complex regulatory pathway involving the RISC complex and Argonaute family of proteins.

We cotransfected 293T cells with a pNL4-3 provirus lacking a functional *rev* gene, pCMV-Rev, RRE-driven antisense and increasing amounts of RRE-driven sense. The provirus and antisense were cotransfected at a 5:1 molar ratio, respectively, where about 80% of particle production is inhibited. RRE-driven sense was cotransfected in a range of molar ratios up to 25-fold greater than the RRE-driven antisense. After 48 hours, we assayed for particle production and found that there was no significant effect on antisense inhibition, except at the highest concentration of RRE-driven sense (Figure 18A). When the experiment was repeated, there was no significant change in antisense inhibition, except at the highest concentration of RRE-driven sense, but the change was the
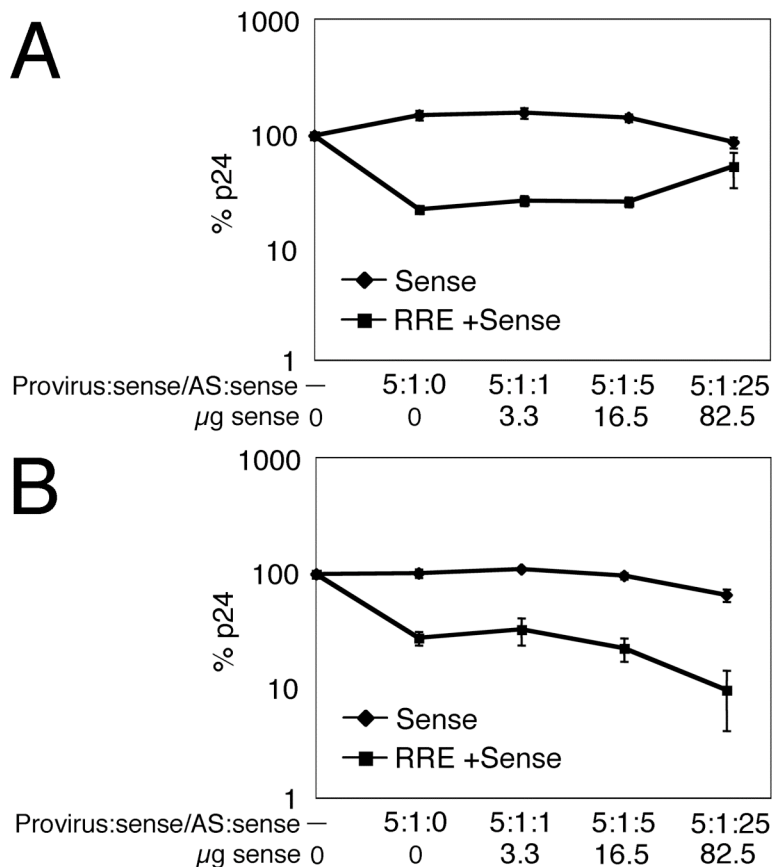
Figure 18: Effect of competitor RNA on RRE-driven antisense inhibition

(A) 10^6 293T cells were transfected with 5 μg pNL4-3 provirus lacking a functional *rev* gene (pHR1146), pCMV-Rev (pHR30) and RRE-driven sense (pHR3476) or antisense vector (AS, pHR3473) at a 5:1 molar ratio of provirus and sense/AS, and increasing amounts of RRE-driven sense vector (pHR3476). After 48 hours, p24 expression was assayed by ELISA and plotted as a percentage of p24 expression from provirus alone. The molar ratio of antisense vector (AS), provirus and sense vector are indicated on the X-axis as well as the microgram amount of sense vector. Transfections were performed in triplicate and standard deviation is indicated. The mean p24 value for 100% was 609 ng/mL. (B) Duplicate assay to test the effect of competitor RNA on RRE-driven antisense (AS) inhibition. Transfections, assay and analysis were performed as in (A). The mean p24 value for 100% was 60.6 ng/mL.

 opposite of the previous experiment (Figure 18B). Although we cannot explain

this anomaly, overall, these results demonstrate that the antisense effect cannot

be competed out and implies that the mechanism of antisense inhibition does not

rely on one antisense RNA inhibiting one target RNA.

Competition assay for CTE-driven antisense construct

        The CTE-driven antisense construct inefficiently inhibited particle

production, even when the target and antisense RNA used the CTE pathway.

We wanted to determine if the mechanism of CTE-driven antisense inhibition

relied on the "classical" antisense pathway or accessed the siRNA pathway.

Similarly to the previous competition assay, we reasoned that if there was a

reduction in antisense inhibition in the presence of increasing amounts of sense

RNA, then the CTE-driven antisense might be accessing the "classical" antisense

pathway. Alternatively, if there was no change or a significant improvement in

antisense inhibition in the presence of increasing amounts of sense RNA, then

the CTE-driven antisense might be accessing an siRNA-mediated pathway.

        We cotransfected 293T cells with a pNL4-3 provirus containing a

nonfunctional *rev* gene and the MPMV CTE cloned into the *nef* region, CTE-

driven antisense and increasing amounts of CTE-driven sense vector. Provirus

and CTE-driven antisense were cotransfected at a 1:5 molar ratio, respectively,

where approximately 80% of particle production is inhibited (Figure 9B). We

cotransfected up to 2-fold more CTE-driven sense than CTE-driven antisense to

test for derepression. After 48 hours, we assayed for particle production and found that there was no significant difference in the level of antisense inhibition with increasing amounts of CTE-driven sense vector (Figure 19). These results suggest that the CTE-driven antisense might not access the "classical" antisense pathway, similar to the RRE-driven antisense (Figure 18), though additional experiments need to be performed to confirm these results.

Effect of EGFP antisense constructs on p24 and EGFP expression from pNLEGFP

Our results clearly demonstrated that the Rev-RRE pathway was required for efficient antisense inhibition of a target region in HIV-1 *env* (Figure 9). To determine if this effect could be extended to other non-HIV-1 related target regions, we replaced the *env*-derived antisense sequence with an EGFP-derived antisense sequence in the CTE-driven, RRE-driven and no element antisense constructs. The EGFP antisense sequence was 721 nt in length as compared to the 927 nt *env* antisense. These were then analyzed in conjunction with a pNL4-3-derived proviral clone containing the EGFP coding sequences in *env.* This provirus produces a truncated Env-EGFP fusion protein that is retained in the endoplasmic reticulum and produces non-infectious virus particles (158).

We cotransfected 293T cells with the pNL4-3 provirus with the EGFP sequence in *env*, pCMV-Rev and increasing amounts of RRE-driven, CTE-driven or no element antisense contructs targeting EGFP. After 48 hours, p24 levels in
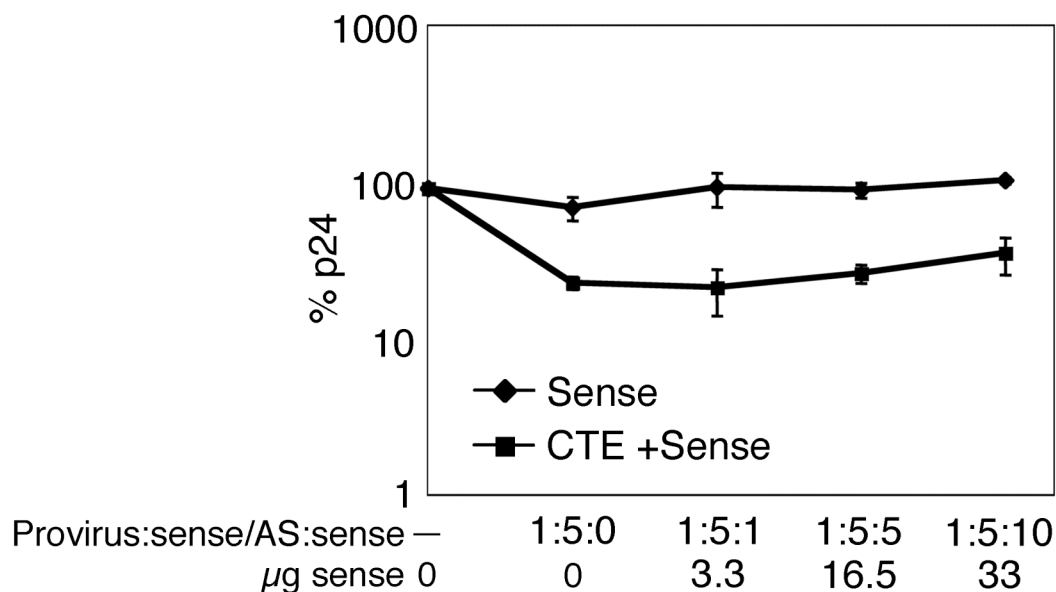
Figure 19: Effect of competitor RNA on CTE-driven antisense inhibition

10^6 293T cells were transfected with a pNL4-3 provirus containing a nonfunctional RRE and *rev* gene and the MPMV CTE cloned into the *nef* region (pHR1371) and CTE-driven sense (pHR3477) or antisense vector (AS, pHR3474) at a 1:5 molar ratio of provirus and vector, and increasing amounts of CTE-driven sense vector (pHR3477). After 48 hours, p24 expression was assayed by ELISA and plotted as a percentage of p24 expression from provirus alone. The molar ratio of antisense vector (AS), provirus and sense vector are indicated on the X-axis as well as the microgram amount of sense vector. Transfections were performed in triplicate. The mean p24 value for 100% was 9.18 ng/mL.

tissue culture supernatant were measured by p24 ELISA. Based on this analysis, we demonstrated that the RRE antisense was superior to the CTE and no element antisense in inhibiting virus production as assayed by p24 ELISA (Figure 20). However, in this case, the CTE and no element antisense showed a better inhibition than what we observed in the case of the original constructs. The reason for this discrepancy is unclear. However, these results demonstrate that the Rev-RRE pathway promotes efficient antisense inhibition independent of the target and antisense sequences.

The RRE-driven EGFP antisense construct efficiently inhibited particle production from the pNLEGFP provirus. This provirus produces a truncated Env-EGFP fusion protein that is retained in the endoplasmic reticulum and produces non-infectious virion. The EGFP sequence is similar in length to the *env* target sequence and is cloned into pNL4-3 in almost the same location as the *env* target sequence. Since Gag, which gives rise to p24, is expressed from an unspliced RNA and EGFP is expressed from a singly spliced RNA, we wanted to determine if the antisense effect extended to EGFP.

293T cells were transfected with pNLEGFP, pCMV-Rev and increasing amounts of CTE-, RRE- or No element-containing antisense construct in a range of molar ratios from 10:1 to 1:10 of provirus and antisense. After 48 hours, cells were harvested, run on an 8% SDS-polyacrylamide gel and electrotransferred to Immobilon FL. Protein expression was analyzed using a commercial mouse monoclonal antibody to EGFP (Covance) and a commercial polyclonal antibody
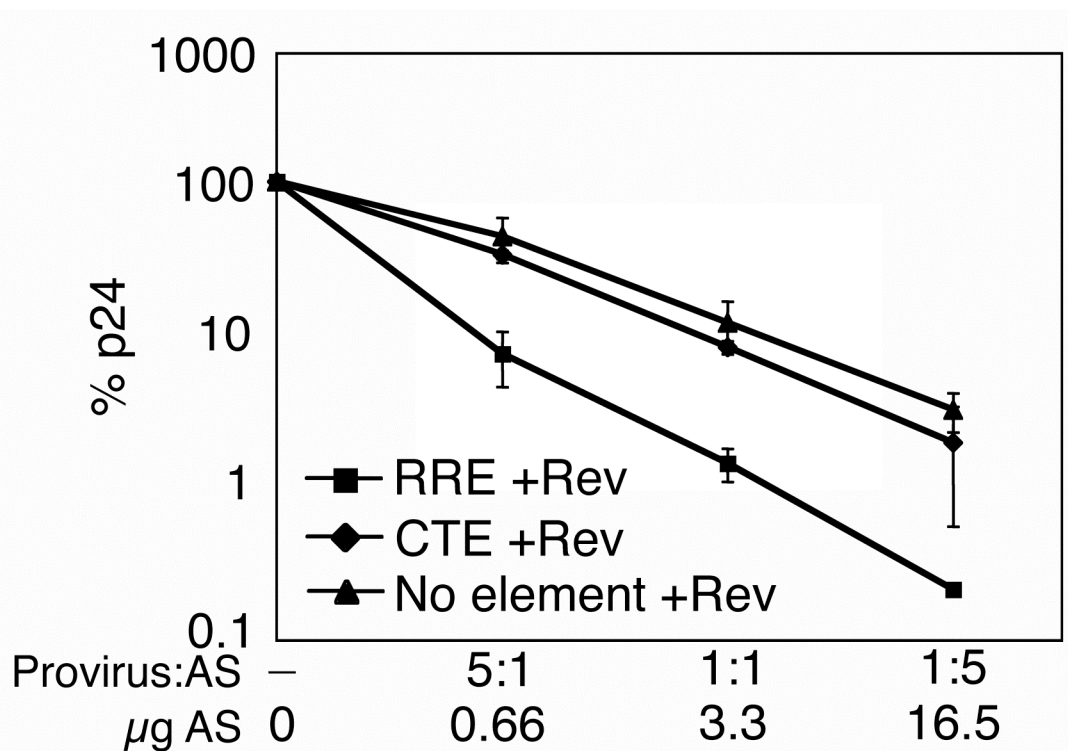
Figure 20: Inhibition of particle production from an RRE-driven provirus containing an EGFP target sequence.

10^6 293T cells were transfected with a 5 μg pNL4-3 provirus containing the EGFP sequence in *env*, 500 ng pCMV-Rev and increasing amounts of RRE- or CTE-driven EGFP antisense vector (AS). The antisense vectors are the same as those used in previous analyses except the *env* antisense sequence has been replaced with an EGFP antisense sequence. After 48 hours, p24 expression was assayed by ELISA and plotted as the percentage of p24 expression from the provirus alone. The molar ratio of provirus to antisense plasmid (AS) and microgram amount of antisense plasmid (AS) is indicated on the X-axis. Transfections were performed in duplicate. The p24 level at 100% was 839 -/+ 58.7 ng/mL.

to ß-tubulin (Abcam). Blots were visualized using the Odyssey Infrared Imaging System (Figure 21A).

Samples were quantitated and normalized to cellular ß-tubulin. EGFP expression was expressed as the percentage of EGFP expression from the provirus alone (Figure 21B). We found that expression of the Env-EGFP fusion protein was not inhibited by the RRE-, CTE- or no element antisense. However, the quality of the blot is questionable and the experiment warrants repeating before drawing any conclusions regarding inhibition of EGFP expression from this construct.

Effect of EGFP antisense constructs on expression from an LTR-driven EGFP construct

Our results demonstrated that an RRE-driven antisense construct targeting EGFP sequence could efficiently inhibit particle production from a provirus that contains the EGFP target sequence in Env. In this context, the target RNA is Rev-dependent and the target sequence is in the 3' UTR. In order to test whether the EGFP antisense constructs could inhibit EGFP expression from a Rev-independent RNA that is an ORF, we constructed an EGFP expression vector that uses the HIV-1 5' LTR as a promoter in order to mimic transcription from a provirus (LTR-EGFP). This construct does not contain splice sites and is expected to generate only one RNA transcript. In addition, it is not known to contain additional elements that control RNA splicing or stability.
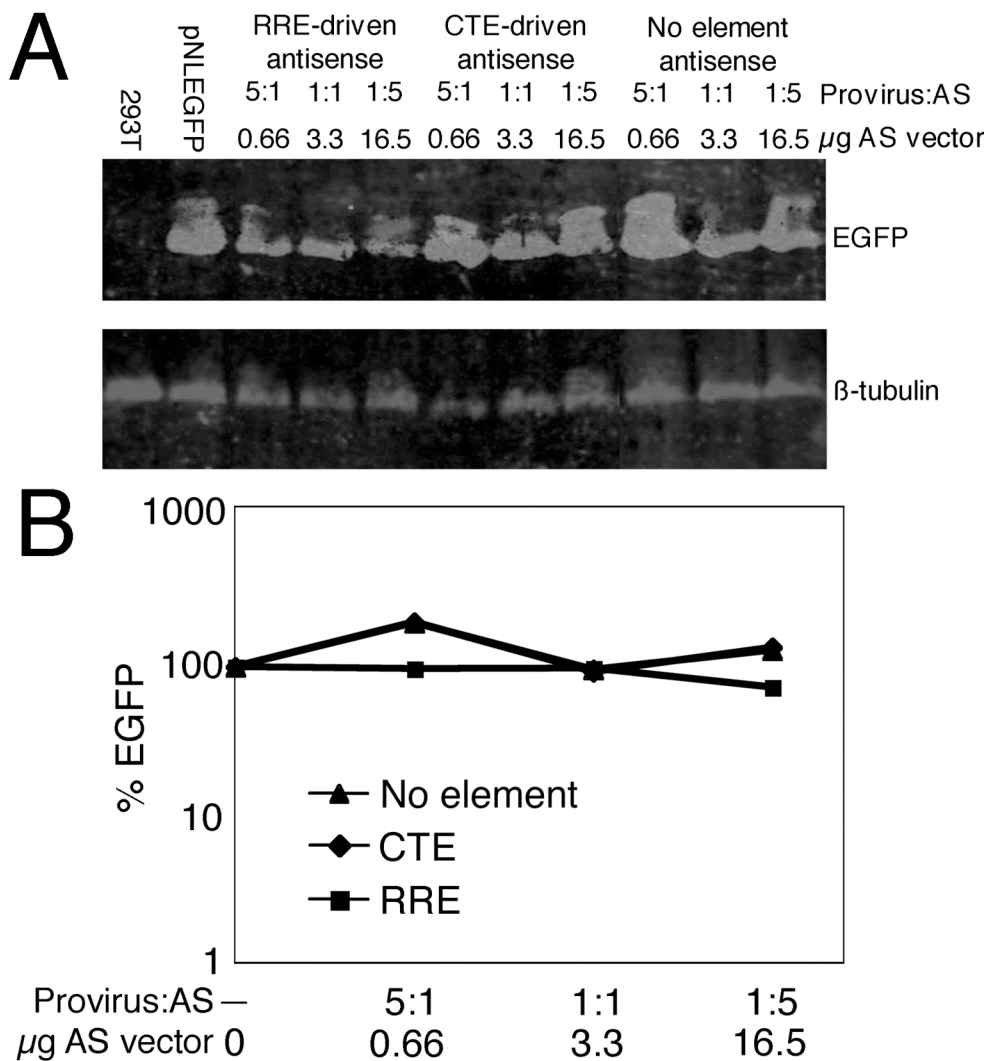
Figure 21: Antisense inhibition of EGFP expression from a provirus

10^6 293T cells were transfected with 5 μg pNL4-3 provirus containing the EGFP sequence in *env* (pHR3603), 500 ng pCMV-Rev (pHR30) and increasing amounts of RRE- (pHR3755) or CTE-driven EGFP antisense (AS) vector (pHR3756). Cells were harvested after 48 hours, run on an 8% polyacrylamide-SDS gel and transferred to Immobilon FL. Blots were probed with a commercial monoclonal antibody to EGFP (Covance) and a commercial polyclonal antibody to ß-tubulin (Abcam). Blots were visualized using the Odyssey Infrared Imaging System. The molar ratio of provirus and antisense plasmid (AS) and microgram amount of antisense plasmid (AS) is indicated above each lane. (B) Quantitation of EGFP expression from a provirus. EGFP expression levels were quantitated using the Odyssey software package and normalized to cellular ß-tubulin. EGFP expression level is expressed as a percentage of EGFP expression from the provirus alone.

293T cells were transfected with LTR-EGFP, pCMV-Rev and increasing amounts of sense or antisense vector in a range of molar ratios of 5:1 to 1:5 of LTR-EGFP and vector. The amounts of antisense plasmid differ from other experiments due to the difference in size of the LTR-EGFP (5 kb) and the proviruses (15 kb). After 48 hours, cells were harvested, run on a 10% SDS-polyacrylamide gel and electrotransferred to Immobilon FL. Protein expression was analyzed using a commercial mouse monoclonal antibody to EGFP (Covance) and a commercial polyclonal antibody to ß-tubulin (Abcam). Blots were visualized using the Odyssey Infrared Imaging System (Figure 22A).

Following normalization to cellular ß-tubulin, EGFP expression was plotted as a percentage of LTR-EGFP expression in the absence of sense or antisense vector. Quantitation demonstrated that the RRE-driven antisense inhibited EGFP expression from the LTR-EGFP construct (Figure 22B). However, inhibition was not as efficient as that observed in experiments measuring particle production. In addition, the RRE-driven sense construct appeared to inhibit some EGFP expression, again in contrast to previous experiments. It would be prudent to repeat the experiment again, as this represents a single experiment.
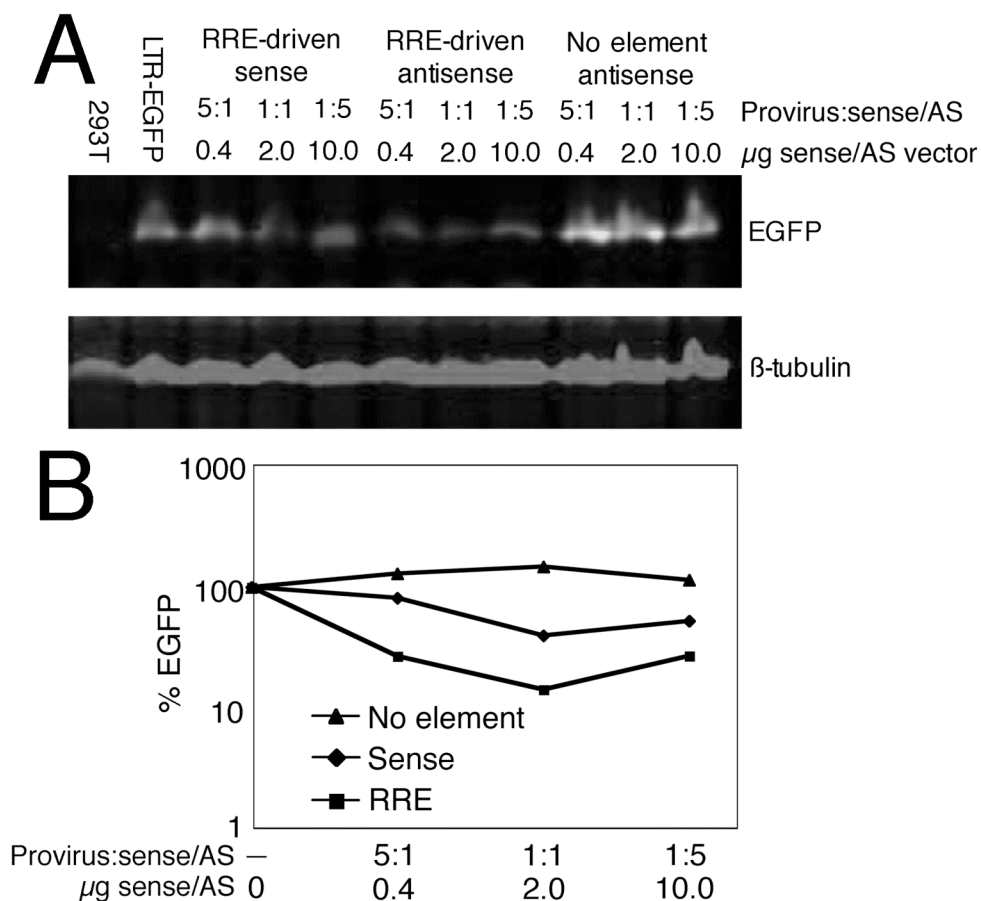
Figure 22: Antisense inhibition of EGFP expression from an LTR-driven EGFP plasmid

(A) 10^6 293T cells were transfected with 5 μg LTR-driven EGFP plasmid that expresses EGFP under the control of the 5' HIV-1 LTR from pNL4-3 (pHR3754). This plasmid was cotransfected with 500 ng pCMV-Rev (pHR30), 500 ng pCMV-Tat (pHR136) and increasing amounts of RRE-driven EGFP sense (pHR3758) or RRE-driven EGFP antisense (pHR3755), or no element EGFP antisense vector (pHR3757) (AS). Cells were harvested after 48 hours, run on an 8% polyacrylamide-SDS gel and transferred to Immobilon FL. Blots were probed with a commercial monoclonal antibody to EGFP (Covance) and a commercial polyclonal antibody to ß-tubulin (Abcam). Blots were visualized using the Odyssey Infrared Imaging System. The molar ratio of provirus and antisense plasmid (AS) and microgram amount of antisense plasmid (AS) is indicated above each lane. (B) Quantitation of EGFP expression from the LTR-EGFP construct. EGFP expression levels were quantitated using the Odyssey software package and normalized to cellular ß-tubulin. EGFP expression level is expressed as a percentage of EGFP expression from the construct alone.

Discussion

Results in Chapter 3 demonstrated that particle production was efficiently inhibited by the RRE-driven antisense vector. Gag and Pol proteins are translated from an unspliced HIV-1 RNA, whereas the Env protein is translated from a singly spliced HIV-1 RNA. The antisense construct targets *env*, so in the context of GagPol expression, the target sequence lies in the 3' UTR. For Env expression, the target sequence lies within the ORF. It is possible that differences in the context of target sequence could affect the efficiency of antisense inhibition. Our results demonstrate that, in addition to particle production, the RRE-driven antisense vector efficiently inhibited Env production. In contrast, the CTE-driven antisense construct did not efficiently inhibit Env production, similar to its effect on particle production. These results demonstrate that antisense inhibition by the RRE-driven vector is of similar efficiency whether the target sequence lies in the 3' UTR or within an ORF.

The CTE-driven antisense inefficiently inhibits both particle production and Env expression from an RRE-driven provirus. Additional results demonstrated that the GagPol and antisense RNAs localize to the cytoplasm and the polyribosome. Tap/Nxf1 has been shown to enhance cytoplasmic localization of CTE-containing RNAs (48, 51). The Tap/Nxf1 and Sam68 proteins have been shown to increase polyribosomal localization of CTE-containing RNAs (28, 62). It is possible that enhancing cytoplasmic or polyribosomal localization of the CTE-driven antisense RNA could enhance antisense inhibition. To test this, we

cotransfected an RRE-driven provirus with different amounts of CTE-driven

sense or antisense vector in the absence or presence of Tap/Nxt1 or Sam68

expression plasmids. We found that coexpression of Tap/Nxf1 significantly

improved CTE-driven antisense inhibition of particle production from an RRE-

driven provirus, whereas coexpression of Sam68 did not significantly improve

CTE-driven antisense inhibition. These results suggest that Tap/Nxf1 accesses

a cellular compartment or factor that contributes to efficient antisense inhibition.

Sam68 does not access this compartment or factor, but it is not clear whether

Tap/Nxf1 and Rev are accessing the same cellular compartment or factor. In

addition, it is not clear whether enhanced antisense inhibition is due to the

nuclear export or polyribosomal localization phenotype established for Tap/Nxf1.

Additional experiments are required to determine the precise role of Tap/Nxf1 in

CTE-driven antisense inhibition.

We wanted to distinguish whether a single antisense RNA inhibits a single

target or whether the antisense-target duplex is processed into small effector

RNAs, like siRNAs, which can act on multiple targets. We tested this by

cotransfecting increasing amounts of the RRE- or CTE-driven sense constructs

and testing their ability to compete out RRE- or CTE-driven antisense inhibition,

respectively. If "classical" antisense inhibition, of one antisense and one target

RNA, was the mechanism, we expected that the antisense effect would be

competed out. If the duplexes were processed into small effector RNAs, then we

would not expect to be able to compete out the antisense inhibition, since it

would result in increasing amounts of effector RNA. We found that both RRE-
and CTE-driven antisense inhibition could not be competed out. Thus, we cannot
rule out that the duplexes may be processed into small effector molecules by
Dicer.

An RRE-driven EGFP-targeted antisense construct efficiently inhibited
particle production from an RRE-driven provirus containing the EGFP target
sequence in *env*. In this provirus, EGFP has been cloned into the *env* gene and
generates an Env-EGFP fusion protein containing the KDEL ER retention signal
(158). GagPol expression generates the proteins required for particle formation
and the antisense target sequence lies within the 3' UTR of GagPol RNA. In the
context of the Env-EGFP fusion protein, the antisense target sequence lies in the
ORF of the coding RNA. It is possible that the *env* sequence is somehow
sensitive to antisense inhibition, especially by the RRE-driven antisense vector.
In order to rule out this possibility, we used the EGFP provirus and EGFP-
targeting antisense vectors to determine if protein expression was inhibited
similarly by EGFP-targeted antisense constructs. Preliminarily, we found that
EGFP levels were not significantly reduced by either the CTE-, RRE- or no
element-containing antisense construct, but the experiment was not of good
quality and needs to be repeated. This result contrasts with earlier results
demonstrating that Env expression was efficiently inhibited by the RRE-driven
antisense construct. However, particle production was efficiently inhibited by the

RRE-driven antisense vector, suggesting that the *env* sequence is not significantly more sensitive to antisense inhibition than other sequences.

We wanted to determine if EGFP expression could be inhibited by the antisense constructs in a non-proviral context. It is possible that the presence of additional control elements that regulate splicing or stability could influence sensitivity to antisense inhibition. To address this possibility, we constructed an LTR-driven EGFP expression plasmid that does not contain splice sites or other RNA control elements that might be present in the provirus. We tested the ability of RRE-driven sense or antisense constructs to inhibit EGFP expression from this construct and found that the RRE-driven antisense construct inhibited EGFP expression, though incompletely. In contrast, the no element antisense and RRE-driven sense vectors did not inhibit EGFP expression as efficiently as the RRE-driven antisense vector, demonstrating that the RRE pathway confers an advantage with antisense inhibition. This advantage is apparent even when the target sequence is not in a proviral context and implies that the RRE may be a crucial element to consider in antisense vector design and that the context of the target sequence does not influence its sensitivity to antisense inhibition. However, this conclusion should be considered as a preliminary one since the level of inhibition with the RRE antisense was not as great as when an HIV-1 target was used. EGFP is a relatively stable protein, which allows the possibility that the protein could accumulate in transfected cells before antisense inhibition

can occur (17). It will be necessary to test a variety of reporter constructs before

a firm conclusion can be drawn.

Concluding Remarks and Future Directions

The RRE-driven antisense construct is an effective tool for suppressing HIV-1 replication. It is also a new platform for using antisense inhibition to specifically suppress gene expression. Currently, the therapeutic has only been tested in HIV-1-infected individuals, but the potential of this construct to be used for protection from initial HIV-1 infection has yet to be examined. It would be interesting to see if the antisense construct would prevent initial HIV-1 infection. In this case, healthy individuals would receive cells transduced with the construct. Additional studies have to be performed to establish the safety of the construct for non HIV-1-infected individuals, since lentiviral vectors have not been successfully used in the past. Lentiviruses do not have predictable sites for integration into the host genome, so there is the potential for adverse effects, such as oncogenesis. The potential for inappropriate integration will have to be evaluated before being approved for wider use.

For now, the antisense construct appears to be an effective second-line therapy, reserved for HIV-1-infected individuals who do not respond to traditional anti-HIV-1 therapies. Other second line therapies include entry inhibitors, such as enfuvirtide. Unfortunately, Fuzeon-resistant HIV-1 has already been observed in patients. In contrast, long-term passaging of HIV-1 in cells transduced with the antisense vector did not result in resistant viruses. While it cannot be ruled out that drug resistance could eventually develop, the construct has demonstrated great promise in studies up to now. It will be necessary to perform additional

trials in HIV-1-infected individuals before the potential of developing drug

resistance can be ruled out.

Another interesting use for this construct is to target other viruses or

cellular RNAs. We demonstrated the potential to target EGFP with the antisense,

either in a provirus or expression construct, suggesting that other RNAs could be

effectively inhibited by antisense. An attractive target for antisense inhibition is

HTLV-I, which is another complex retrovirus that can cause T-cell leukemia

(109). HTLV-I relies on an RRE homolog, the RexRE, and Rev homolog, Rex, to

accomplish nuclear export of viral RNAs (82). Since they share Rev/RRE-like

regulatory elements and target similar cell types, HTLV-I would be another target

for antisense inhibition. The use of antisense therapeutics for other viral targets

also needs to be explored.

We have demonstrated that the RRE-driven antisense vector efficiently

inhibits particle production and Env expression from an HIV-1 provirus. We

observed efficient antisense inhibition by the RRE-driven vector with both RRE-

driven and CTE-driven proviruses. It would be interesting to test whether the

RRE homolog from HTLV-I, the RexRE, and the Rev homolog from HTLV-I, Rex,

can substitute for Rev and the RRE for efficient antisense inhibition (82). Rex

uses the Crm1 pathway and can substitute for Rev for RRE-mediated nuclear

export (53). It is possible that trafficking through the Crm1 pathway specifically

confers an advantage for antisense inhibition. This conclusion is supported by

the experiments with the RevM10-Tap fusion protein. Additional experiments are

required to elucidate the precise Rev functions that confer an advantage to the RRE-driven antisense vector.

The precise mechanism by which the construct inhibits gene expression remains to be seen, but our results suggest that antisense inhibition prevents production of stable protein from targeted mRNAs in polyribosomes. It is not clear why both the GagPol and antisense RNA engage the polyribosome or whether this contributes to efficient antisense inhibition. A possible explanation for the antisense RNA engaging the polyribosome is that the vector used in these studies contains the Gag start codon, with coding sequence up to the cloning site used to incorporate the *env* antisense sequence. As a result of this short ORF, the antisense RNA could be recognized as an mRNA and allowed to engage the polyribosome. In contrast, the VIRxSYS antisense construct does not contain the Gag start codon, but its localization to the polyribosome has not been examined. An interesting experiment to test whether the start codon has any contribution to efficient antisense inhibition would be to mutate the start codon in our antisense construct and examine its polyribosomal localization. While both our construct and the VIRxSYS construct have been shown to efficiently inhibit particle production, this could have an impact on defining the mechanism of antisense inhibition.

In addition, it would be interesting to identify factors that contribute to antisense inhibition, either by evaluating Rev interactors for antisense functions or identifying proteins associated with translationally silenced RNAs in the

polyribosome. It is important to determine the precise Rev functions that contribute to efficient antisense inhibition. Such a study would also reveal new details of Rev regulation and the HIV-1 life cycle.

Another intriguing possibility for the mechanism of antisense inhibition is that the target and antisense RNA form a duplex that is processed into small RNAs by Dicer. As discussed in the Introduction, double-stranded RNAs are substrates for Dicer and its role in siRNA metabolism is well established (see Small interfering and other small RNAs). While our experiments examining the stability of both the GagPol and antisense RNAs suggest that degradation is not occurring, Dicer-mediated processing of duplex RNA, even in small amounts, cannot be ruled out. Very low concentrations of siRNA have been shown to have potent effects on gene expression, so the amount of Dicer processing could be below the level of detection by our analysis of RNA degradation. A more informative experiment would be to perform a targeted knockdown of Dicer using siRNAs. If the the efficiency of antisense inhibition was reduced due to Dicer knockdown, it would suggest a role for Dicer in antisense inhibition. To date, our attempts to knockdown Dicer have not been successful. The appropriate use of positive controls and reliable detection of Dicer knockdown are required to draw any conclusions regarding the role of Dicer in this mechanism.

Rev function in nuclear export has been well established, but it may have additional functions that contribute to antisense inhibition. One way to separate the Rev nuclear export function from some other Rev-mediated process is to

construct a Rev or RevM10 fusion protein containing the MS2 RNA binding

domain and a leucine rich NES, possibly by duplicating the Rev NES, and an

antisense construct containing MS2 binding sites. MS2 is a bacteriophage

protein that binds to a stem-loop sequence in phage RNA that has been used in

heterologous gene constructs to examine RNA localization in the cell (115). The

MS2 binding domain could substitute for Rev RNA binding while the NES

conserves the crucial RNA export function in the fusion protein, independent of

the Rev NES. In such an experimental system, extensive mutational analysis

could be used to explore any additional Rev functions that might contribute to

antisense inhibition. Studying these functions could provide great insight into the

mechanism of antisense inhibition, aid vector design and contribute to our

understanding of HIV-1 biology.

While Rev and the RRE can overcome nuclear retention of edited RNA, a

role for the RNA-editing enzyme ADAR in antisense inhibition cannot be ruled

out. It is possible that edited RNA is recognized by a cellular factor in the

cytoplasm that prevents its translation. This factor could act in the polyribosome

or recruit additional factors to the edited RNA. Since the long isoform of ADAR1

is localized to the cytoplasm, it could act as a cytoplasmic equivalent of p54/nrb,

which binds to inosine-containing RNAs in the nucleus. It is not known whether

ADAR has a direct role in translation regulation. It would be interesting to assay

for the presence of ADAR in the polyribosome-associated fractions following

separation of cytoplasmic fractions by sucrose gradient centrifugation. Another

way to test the role of ADAR in antisense inhibition is to overexpress ADAR in the presence of the antisense and target RNAs. If ADAR overexpression enhanced antisense inhibition, this would suggest a role for ADAR.

We demonstrated that the antisense vector specifically inhibited GagPol production and not production of non-targeted proteins, such as Nef. However, this is not a direct demonstration of translation inhibition. A more direct measure of translation inhibition would be to perform a pulse-chase/IP experiment to assay for synthesis of GagPol Pr160 in the presence of antisense. This experiment would establish whether protein synthesis is inhibited, in which case no protein would be immunoprecipitated, or whether the newly synthesized protein is unstable, resulting in a decrease of the Pr160 half-life.

We demonstrated that the GagPol RNA and both sense and antisense vector RNAs localize to the polyribosome. In spite of polyribosomal localization, little GagPol protein is produced in the presence of antisense RNA. Treatment of the cytoplasmic extracts with 15 mM EDTA demonstrated that the localization was specific to the polyribosome and not some other cytoplasmic complex. One possible explanation is that translation of the GagPol RNA is stalled or actively inhibited. Nef is produced in the presence of antisense RNA, implying that there is not a global downregulation of translation. It is possible that there are subsets of polyribosomes that associate with specific factors responsible for maintaining an active or inactive state of translation. It would be interesting to identify these factors, as it would have a profound impact on our understanding of both this

mechanism of antisense inhibition and the regulation of translation in the cell. Another intriguing possibility is that newly synthesized protein is immediately degraded as a result of antisense inhibition. While it is not clear how such a mechanism would be regulated, it has been suggested in the literature as a mechanism of miRNA inhibition (102).

Future experiments should give insight into the precise mechanism of antisense inhibition. With greater understanding of the cellular mechanism behind antisense targeting, additional viral targets for antisense therapeutics can be identified. In addition, research and development of new therapeutics will give us greater insight into basic cell biology. Beyond increasing our understanding of RNA metabolism and viral replication, development of such novel therapeutic strategies for a wide variety of diseases represents an important approach for improving public health.

References

1. **Abbott, A. L., E. Alvarez-Saavedra, E. A. Miska, N. C. Lau, D. P. Bartel, H. R. Horvitz, and V. Ambros.** 2005. The let-7 MicroRNA family members mir-48, mir-84, and mir-241 function together to regulate developmental timing in Caenorhabditis elegans. Dev Cell **9:**403-14.

2. **Adamson, C. S., and E. O. Freed.** 2007. Human immunodeficiency virus type 1 assembly, release, and maturation. Adv Pharmacol **55:**347-87.

3. **Anderson, J. L., A. T. Johnson, J. L. Howard, and D. F. Purcell.** 2007. Both linear and discontinuous ribosome scanning are used for translation initiation from bicistronic human immunodeficiency virus type 1 env mRNAs. J Virol **81:**4664-76.

4. **Bass, B. L.** 2002. RNA editing by adenosine deaminases that act on RNA. Annu Rev Biochem **71:**817-46.

5. **Berger, E. A., P. M. Murphy, and J. M. Farber.** 1999. Chemokine receptors as HIV-1 coreceptors: roles in viral entry, tropism, and disease. Annu Rev Immunol **17:**657-700.

6. **Bishop, K. N., R. K. Holmes, A. M. Sheehy, and M. H. Malim.** 2004. APOBEC-mediated editing of viral RNA. Science **305:**645.

7. **Boden, D., O. Pusch, F. Lee, L. Tucker, and B. Ramratnam.** 2003. Human immunodeficiency virus type 1 escape from RNA interference. J Virol **77:**11531-5.

8. **Bor, Y. C., J. Swartz, A. Morrison, D. Rekosh, M. Ladomery, and M. L. Hammarskjold.** 2006. The Wilms' tumor 1 (WT1) gene (+KTS isoform) functions with a CTE to enhance translation from an unspliced RNA with a retained intron. Genes Dev **20:**1597-608.

9. **Bowerman, B., P. O. Brown, J. M. Bishop, and H. E. Varmus.** 1989. A nucleoprotein complex mediates the integration of retroviral DNA. Genes Dev **3:**469-78.

10. **Bramlage, B., E. Luzi, and F. Eckstein.** 2000. HIV-1 LTR as a target for synthetic ribozyme-mediated inhibition of gene expression: site selection and inhibition in cell culture. Nucleic Acids Res **28:**4059-67.

11. **Bray, M., S. Prasad, J. W. Dubay, E. Hunter, K. T. Jeang, D. Rekosh, and M. L. Hammarskjold.** 1994. A small element from the Mason-Pfizer monkey virus genome makes human immunodeficiency virus type 1 expression and replication Rev-independent. Proc Natl Acad Sci U S A **91:**1256-60.

12. **Briggs, J. A., K. Grunewald, B. Glass, F. Forster, H. G. Krausslich, and S. D. Fuller.** 2006. The mechanism of HIV-1 core assembly: insights from three-dimensional reconstructions of authentic virions. Structure **14:**15-20.

13. **Briquet, S., J. Richardson, C. Vanhee-Brossollet, and C. Vaquero.** 2001. Natural antisense transcripts are detected in different cell lines and

tissues of cats infected with feline immunodeficiency virus. Gene **267:**157-64.

14. **Calzone, F. J., R. C. Angerer, and M. A. Gorovsky.** 1982. Regulation of protein synthesis in Tetrahymena: isolation and characterization of polysomes by gel filtration and precipitation at pH 5.3. Nucleic Acids Res **10:**2145-61.

15. **Caplen, N. J., S. Parrish, F. Imani, A. Fire, and R. A. Morgan.** 2001. Specific inhibition of gene expression by small double-stranded RNAs in invertebrate and vertebrate systems. Proc Natl Acad Sci U S A **98:**9742-7.

16. **Cavanagh, M. H., S. Landry, B. Audet, C. Arpin-Andre, P. Hivin, M. E. Pare, J. Thete, E. Wattel, S. J. Marriott, J. M. Mesnard, and B. Barbeau.** 2006. HTLV-I antisense transcripts initiating in the 3'LTR are alternatively spliced and polyadenylated. Retrovirology **3:**15.

17. **Chalfie, M., Y. Tu, G. Euskirchen, W. W. Ward, and D. C. Prasher.** 1994. Green fluorescent protein as a marker for gene expression. Science **263:**802-5.

18. **Chan, D. C., D. Fass, J. M. Berger, and P. S. Kim.** 1997. Core structure of gp41 from the HIV envelope glycoprotein. Cell **89:**263-73.

19. **Chang, D. D., and P. A. Sharp.** 1989. Regulation by HIV Rev depends upon recognition of splice sites. Cell **59:**789-795.

20. **Chazal, N., G. Singer, C. Aiken, M. L. Hammarskjold, and D. Rekosh.** 2001. Human immunodeficiency virus type 1 particles pseudotyped with envelope proteins that fuse at low pH no longer require Nef for optimal infectivity. J Virol **75:**4014-8.

21. **Chen, H., C. E. Lilley, Q. Yu, D. V. Lee, J. Chou, I. Narvaiza, N. R. Landau, and M. D. Weitzman.** 2006. APOBEC3A is a potent inhibitor of adeno-associated virus and retrotransposons. Curr Biol **16:**480-5.

22. **Chen, J., M. Sun, W. J. Kent, X. Huang, H. Xie, W. Wang, G. Zhou, R. Z. Shi, and J. D. Rowley.** 2004. Over 20% of human transcripts might form sense-antisense pairs. Nucleic Acids Res **32:**4812-20.

23. **Chinnadurai, R., J. Munch, and F. Kirchhoff.** 2005. Effect of naturally-occurring gp41 HR1 variations on susceptibility of HIV-1 to fusion inhibitors. AIDS **19:**1401-5.

24. **Chu, C. Y., and T. M. Rana.** 2006. Translation repression in human cells by microRNA-induced gene silencing requires RCK/p54. PLoS Biol **4:**e210.

25. **Clemson, C. M., J. A. McNeil, H. F. Willard, and J. B. Lawrence.** 1996. XIST RNA paints the inactive X chromosome at interphase: evidence for a novel RNA involved in nuclear/chromosome structure. J Cell Biol **132:**259-75.

26. **Coffin, J.** 1996. Retroviridae: The Viruses and Their Replication, 3rd ed, vol. 2. Lippincott-Raven, Philadelphia.

27. **Coovadia, H. M.** 2000. Access to voluntary counseling and testing for HIV in developing countries. Ann N Y Acad Sci **918:**57-63.

28. **Coyle, J. H., B. W. Guzik, Y. C. Bor, L. Jin, L. Eisner-Smerage, S. J. Taylor, D. Rekosh, and M. L. Hammarskjold.** 2003. Sam68 enhances the cytoplasmic utilization of intron-containing RNA and is functionally regulated by the nuclear kinase Sik/BRK. Mol Cell Biol **23:**92-103.

29. **Crooke, S. T.** 2004. Progress in antisense technology. Annu Rev Med **55:**61-95.

30. **Dallosso, A. R., A. L. Hancock, S. Malik, A. Salpekar, L. King-Underwood, K. Pritchard-Jones, J. Peters, K. Moorwood, A. Ward, K. T. Malik, and K. W. Brown.** 2007. Alternately spliced WT1 antisense transcripts interact with WT1 sense RNA and show epigenetic and splicing defects in cancer. RNA **13:**2287-99.

31. **de Smet, M. D., C. J. Meenken, and G. J. van den Horn.** 1999. Fomivirsen - a phosphorothioate oligonucleotide for the treatment of CMV retinitis. Ocul Immunol Inflamm **7:**189-98.

32. **Desterro, J. M., L. P. Keegan, M. Lafarga, M. T. Berciano, M. O'Connell, and M. Carmo-Fonseca.** 2003. Dynamic association of RNA-editing enzymes with the nucleolus. J Cell Sci **116:**1805-18.

33. **Elbashir, S. M., J. Harborth, W. Lendeckel, A. Yalcin, K. Weber, and T. Tuschl.** 2001. Duplexes of 21-nucleotide RNAs mediate RNA interference in cultured mammalian cells. Nature **411:**494-8.

34. **Ernst, R. K., M. Bray, D. Rekosh, and M. L. Hammarskjold.** 1997. A structured retroviral RNA element that mediates nucleocytoplasmic export of intron-containing RNA. Mol Cell Biol **17:**135-44.

35. **Eulalio, A., E. Huntzinger, and E. Izaurralde.** 2008. GW182 interaction with Argonaute is essential for miRNA-mediated translational repression and mRNA decay. Nat Struct Mol Biol **15:**346-53.

36. **Felber, B. K., M. Hadzopoulou-Cladaras, C. Cladaras, T. Copeland, and G. N. Pavlakis.** 1989. rev protein of human immunodeficiency virus type 1 affects the stability and transport of the viral mRNA. Proc Natl Acad Sci U S A **86:**1495-9.

37. **Feng, Y., C. C. Broder, P. E. Kennedy, and E. A. Berger.** 1996. HIV-1 entry cofactor: functional cDNA cloning of a seven-transmembrane, G protein-coupled receptor. Science **272:**872-7.

38. **Fenton, K. A.** 2007. Changing epidemiology of HIV/AIDS in the United States: implications for enhancing and promoting HIV testing strategies. Clin Infect Dis **45 Suppl 4:**S213-20.

39. **Fire, A., S. Xu, M. K. Montgomery, S. A. Kostas, S. E. Driver, and C. C. Mello.** 1998. Potent and specific genetic interference by double-stranded RNA in Caenorhabditis elegans. Nature **391:**806-11.

40. **Fornerod, M., M. Ohno, M. Yoshida, and I. W. Mattaj.** 1997. CRM1 is an export receptor for leucine-rich nuclear export signals. Cell **90:**1051-60.

41. **Frankel, A. D., and J. A. Young.** 1998. HIV-1: fifteen proteins and an RNA. Annu Rev Biochem **67:**1-25.

42. **Fumagalli, S., N. F. Totty, J. J. Hsuan, and S. A. Courtneidge.** 1994. A target for Src in mitosis. Nature **368:**871-4.

43. **Ganser-Pornillos, B. K., M. Yeager, and W. I. Sundquist.** 2008. The structural biology of HIV assembly. Curr Opin Struct Biol **18:**203-17.

44. **Ge, X., W. S. Rubinstein, Y. C. Jung, and Q. Wu.** 2008. Genome-wide analysis of antisense transcription with Affymetrix exon array. BMC Genomics **9:**27.

45. **George, C. X., and C. E. Samuel.** 1999. Human RNA-specific adenosine deaminase ADAR1 transcripts possess alternative exon 1 structures that initiate from different promoters, one constitutively active and the other interferon inducible. Proc Natl Acad Sci U S A **96:**4621-6.

46. **Giordano, V., D. Y. Jin, D. Rekosh, and K. T. Jeang.** 2000. Intravirion targeting of a functional anti-human immunodeficiency virus ribozyme directed to pol. Virology **267:**174-84.

47. **Graham, F. L., and A. J. van der Eb.** 1973. A new technique for the assay of infectivity of human adenovirus 5 DNA. Virology **52:**456-67.

48. **Gruter, P., C. Tabernero, C. von Kobbe, C. Schmitt, C. Saavedra, A. Bachi, M. Wilm, B. K. Felber, and E. Izaurralde.** 1998. TAP, the human homolog of Mex67p, mediates CTE-dependent RNA export from the nucleus. Mol Cell **1:**649-59.

49. **Guerrier-Takada, C., K. Gardiner, T. Marsh, N. Pace, and S. Altman.** 1983. The RNA moiety of ribonuclease P is the catalytic subunit of the enzyme. Cell **35:**849-57.

50. **Gulick, R. M., J. W. Mellors, D. Havlir, J. J. Eron, C. Gonzalez, D. McMahon, D. D. Richman, F. T. Valentine, L. Jonas, A. Meibohm, E. A. Emini, and J. A. Chodakewitz.** 1997. Treatment with indinavir, zidovudine, and lamivudine in adults with human immunodeficiency virus infection and prior antiretroviral therapy. N Engl J Med **337:**734-9.

51. **Guzik, B. W., L. Levesque, S. Prasad, Y. C. Bor, B. E. Black, B. M. Paschal, D. Rekosh, and M. L. Hammarskjold.** 2001. NXT1 (p15) is a crucial cellular cofactor in TAP-dependent export of intron-containing RNA in mammalian cells. Mol Cell Biol **21:**2545-54.

52. **Hajjar, A. M., and M. L. Linial.** 1995. Modification of retroviral RNA by double-stranded RNA adenosine deaminase. J Virol **69:**5878-82.

53. **Hakata, Y., T. Umemoto, S. Matsushita, and H. Shida.** 1998. Involvement of human CRM1 (exportin 1) in the export and multimerization of the Rex protein of human T-cell leukemia virus type 1. J Virol **72:**6602-7.

54. **Hammarskjold, M. L., J. Heimer, B. Hammarskjold, I. Sangwan, L. Albert, and D. Rekosh.** 1989. Regulation of human immunodeficiency virus env expression by the rev gene product. J Virol **63:**1959-66.

55. **Hardy, H., and P. R. Skolnik.** 2004. Enfuvirtide, a new fusion inhibitor for therapy of human immunodeficiency virus infection. Pharmacotherapy **24:**198-211.

56. **Heidenreich, O., S. H. Kang, X. Xu, and M. Nerenberg.** 1995. Application of antisense technology to therapeutics. Mol Med Today **1:**128-33.

57. **Holmes, R. K., M. H. Malim, and K. N. Bishop.** 2007. APOBEC-mediated viral restriction: not simply editing? Trends Biochem Sci **32:**118-28.

58. **Hovanessian, A. G.** 2007. On the discovery of interferon-inducible, double-stranded RNA activated enzymes: the 2'-5'oligoadenylate synthetases and the protein kinase PKR. Cytokine Growth Factor Rev **18:**351-61.

59. **Huang, J., Z. Liang, B. Yang, H. Tian, J. Ma, and H. Zhang.** 2007. Derepression of microRNA-mediated protein translation inhibition by apolipoprotein B mRNA-editing enzyme catalytic polypeptide-like 3G (APOBEC3G) and its family members. J Biol Chem **282:**33632-40.

60. **Jan, E., C. K. Motzny, L. E. Graves, and E. B. Goodwin.** 1999. The STAR protein, GLD-1, is a translational regulator of sexual identity in Caenorhabditis elegans. EMBO J **18:**258-69.

61. **Ji, J. P., and L. A. Loeb.** 1992. Fidelity of HIV-1 reverse transcriptase copying RNA in vitro. Biochemistry **31:**954-8.

62. **Jin, L., B. W. Guzik, Y. C. Bor, D. Rekosh, and M. L. Hammarskjold.** 2003. Tap and NXT promote translation of unspliced mRNA. Genes Dev **17:**3075-86.

63. **Johannes, G., and P. Sarnow.** 1998. Cap-independent polysomal association of natural mRNAs encoding c-myc, BiP, and eIF4G conferred by internal ribosome entry sites. RNA **4:**1500-13.

64. **Jones, A. R., R. Francis, and T. Schedl.** 1996. GLD-1, a cytoplasmic protein essential for oocyte differentiation, shows stage- and sex-specific expression during Caenorhabditis elegans germline development. Dev Biol **180:**165-83.

65. **Kao, S., M. A. Khan, E. Miyagi, R. Plishka, A. Buckler-White, and K. Strebel.** 2003. The human immunodeficiency virus type 1 Vif protein reduces intracellular expression and inhibits packaging of APOBEC3G (CEM15), a cellular inhibitor of virus infectivity. J Virol **77:**11398-407.

66. **Kato, M., and F. J. Slack.** 2008. microRNAs: small molecules with big roles - C. elegans to human cancer. Biol Cell **100:**71-81.

67. **Kavi, H. H., H. Fernandez, W. Xie, and J. A. Birchler.** 2008. Genetics and biochemistry of RNAi in Drosophila. Curr Top Microbiol Immunol **320:**37-75.

68. **Kearney, M., S. Palmer, F. Maldarelli, W. Shao, M. A. Polis, J. Mican, D. Rock-Kress, J. B. Margolick, J. M. Coffin, and J. W. Mellors.** 2008. Frequent polymorphism at drug resistance sites in HIV-1 protease and reverse transcriptase. AIDS **22:**497-501.

69. **Kim, K., and F. Liu.** 2007. Inhibition of gene expression in human cells using RNase P-derived ribozymes and external guide sequences. Biochim Biophys Acta **1769:**603-12.

70. **Kiriakidou, M., G. S. Tan, S. Lamprinaki, M. De Planell-Saguer, P. T. Nelson, and Z. Mourelatos.** 2007. An mRNA m7G cap binding-like motif within human Ago2 represses translation. Cell **129:**1141-51.

71. **Klimas, N., A. O. Koneru, and M. A. Fletcher.** 2008. Overview of HIV. Psychosom Med **70:**523-30.

72. **Konstantinova, P., W. de Vries, J. Haasnoot, O. ter Brake, P. de Haan, and B. Berkhout.** 2006. Inhibition of human immunodeficiency virus type 1 by RNA interference using long-hairpin RNA. Gene Ther **13:**1403-13.

73. **Kruger, K., P. J. Grabowski, A. J. Zaug, J. Sands, D. E. Gottschling, and T. R. Cech.** 1982. Self-splicing RNA: autoexcision and autocyclization of the ribosomal RNA intervening sequence of Tetrahymena. Cell **31:**147-57.

74. **Kuersten, S., S. P. Segal, J. Verheyden, S. M. LaMartina, and E. B. Goodwin.** 2004. NXF-2, REF-1, and REF-2 affect the choice of nuclear export pathway for tra-2 mRNA in C. elegans. Mol Cell **14:**599-610.

75. **Kumar, M., and G. G. Carmichael.** 1997. Nuclear antisense RNA induces extensive adenosine modifications and nuclear retention of target transcripts. Proc Natl Acad Sci U S A **94:**3542-7.

76. **Landry, S., M. Halin, S. Lefort, B. Audet, C. Vaquero, J. M. Mesnard, and B. Barbeau.** 2007. Detection, characterization and regulation of antisense transcripts in HIV-1. Retrovirology **4:**71.

77. **Lee, J. T., L. S. Davidow, and D. Warshawsky.** 1999. Tsix, a gene antisense to Xist at the X-inactivation centre. Nat Genet **21:**400-4.

78. **Lee, Y., C. Ahn, J. Han, H. Choi, J. Kim, J. Yim, J. Lee, P. Provost, O. Radmark, S. Kim, and V. N. Kim.** 2003. The nuclear RNase III Drosha initiates microRNA processing. Nature **425:**415-9.

79. **Lee, Y. S., and A. Dutta.** 2007. The tumor suppressor microRNA let-7 represses the HMGA2 oncogene. Genes Dev **21:**1025-30.

80. **Lehmann, M. J., V. Patzel, and G. Sczakiel.** 2000. Theoretical design of antisense genes with statistically increased efficacy. Nucleic Acids Res **28:**2597-604.

81. **Levine, B. L., L. M. Humeau, J. Boyer, R. R. MacGregor, T. Rebello, X. Lu, G. K. Binder, V. Slepushkin, F. Lemiale, J. R. Mascola, F. D. Bushman, B. Dropulic, and C. H. June.** 2006. Gene transfer in humans using a conditionally replicating lentiviral vector. Proc Natl Acad Sci U S A **103:**17372-7.

82. **Lewis, N., J. Williams, D. Rekosh, and M. L. Hammarskjold.** 1990. Identification of a cis-acting element in human immunodeficiency virus type 2 (HIV-2) that is responsive to the HIV-1 rev and human T-cell leukemia virus types I and II rex proteins. J Virol **64:**1690-7.

83. **Lim, S. K., C. D. Sigmund, K. W. Gross, and L. E. Maquat.** 1992. Nonsense codons in human beta-globin mRNA result in the production of mRNA degradation products. Mol Cell Biol **12:**1149-61.

84. **Liu, J., M. A. Carmell, F. V. Rivas, C. G. Marsden, J. M. Thomson, J. J. Song, S. M. Hammond, L. Joshua-Tor, and G. J. Hannon.** 2004. Argonaute2 is the catalytic engine of mammalian RNAi. Science **305:**1437-41.

85. **Lu, J., P. Sista, F. Giguel, M. Greenberg, and D. R. Kuritzkes.** 2004. Relative replicative fitness of human immunodeficiency virus type 1 mutants resistant to enfuvirtide (T-20). J Virol **78:**4628-37.

86. **Lu, X., Q. Yu, G. K. Binder, Z. Chen, T. Slepushkina, J. Rossi, and B. Dropulic.** 2004. Antisense-mediated inhibition of human immunodeficiency virus (HIV) replication by use of an HIV type 1-based vector results in severely attenuated mutants incapable of developing resistance. J Virol **78:**7079-88.

87. **Lucchiari, M., G. Niedermann, C. Leipner, A. Meyerhans, K. Eichmann, and B. Maier.** 1994. Human immune response to HIV-1-Nef. I. CD45RO- T lymphocytes of non-infected donors contain cytotoxic T lymphocyte precursors at high frequency. Int Immunol **6:**1739-49.

88. **Luciw, P.** 1996. Human Immunodeficiency Viruses and Their Replication, 3rd ed, vol. 2. Lippincott-Raven, Philadelphia.

89. **Ludwig, L. B., J. L. Ambrus, Jr., K. A. Krawczyk, S. Sharma, S. Brooks, C. B. Hsiao, and S. A. Schwartz.** 2006. Human Immunodeficiency Virus-Type 1 LTR DNA contains an intrinsic gene producing antisense RNA and protein products. Retrovirology **3:**80.

90. **Malim, M. H., S. Bohnlein, J. Hauber, and B. R. Cullen.** 1989. Functional dissection of the HIV-1 Rev trans-activator--derivation of a trans-dominant repressor of Rev function. Cell **58:**205-14.

91. **Malim, M. H., J. Hauber, S. Y. Le, J. V. Maizel, and B. R. Cullen.** 1989. The HIV-1 rev trans-activator acts through a structured target sequence to activate nuclear export of unspliced viral mRNA. Nature **338:**254-7.

92. **Maroney, P. A., Y. Yu, J. Fisher, and T. W. Nilsen.** 2006. Evidence that microRNAs are associated with translating messenger RNAs in human cells. Nat Struct Mol Biol **13:**1102-7.

93. **Martinez-Cajas, J. L., and M. A. Wainberg.** 2008. Antiretroviral therapy : optimal sequencing of therapy to avoid resistance. Drugs **68:**43-72.

94. **Meanwell, N. A., and J. F. Kadow.** 2007. Maraviroc, a chemokine CCR5 receptor antagonist for the treatment of HIV infection and AIDS. Curr Opin Investig Drugs **8:**669-81.

95. **Michael, N. L., M. T. Vahey, L. d'Arcy, P. K. Ehrenberg, J. D. Mosca, J. Rappaport, and R. R. Redfield.** 1994. Negative-strand RNA transcripts are produced in human immunodeficiency virus type 1-infected cells and patients by a novel promoter downregulated by Tat. J Virol **68:**979-87.

96.	**Miller, M. D., C. M. Farnet, and F. D. Bushman.** 1997. Human immunodeficiency virus type 1 preintegration complexes: studies of organization and composition. J Virol **71:**5382-90.

97.	**Morozov, V. A., A. V. Morozov, D. Schurmann, H. Jessen, and C. Kucherer.** 2007. Transmembrane protein polymorphisms and resistance to T-20 (Enfuvirtide, Fuzeon) in HIV-1 infected therapy-naive seroconverters and AIDS patients under HAART-T-20 therapy. Virus Genes **35:**167-74.

98.	**Nelson, P. T., A. G. Hatzigeorgiou, and Z. Mourelatos.** 2004. miRNP:mRNA association in polyribosomes in a human neuronal cell line. RNA **10:**387-94.

99.	**Neville, M., F. Stutz, L. Lee, L. I. Davis, and M. Rosbash.** 1997. The importin-beta family member Crm1p bridges the interaction between Rev and the nuclear pore complex during nuclear export. Curr Biol **7:**767-75.

100.	**Newman, E. N., R. K. Holmes, H. M. Craig, K. C. Klein, J. R. Lingappa, M. H. Malim, and A. M. Sheehy.** 2005. Antiviral function of APOBEC3G can be dissociated from cytidine deaminase activity. Curr Biol **15:**166-70.

101.	**Nishikura, K.** 2006. Editor meets silencer: crosstalk between RNA editing and RNA interference. Nat Rev Mol Cell Biol **7:**919-31.

102.	**Nottrott, S., M. J. Simard, and J. D. Richter.** 2006. Human let-7a miRNA blocks protein production on actively translating polyribosomes. Nat Struct Mol Biol **13:**1108-14.

103.	**Ogawa, Y., B. K. Sun, and J. T. Lee.** 2008. Intersection of the RNA interference and X-inactivation pathways. Science **320:**1336-41.

104.	**Ohman, M.** 2007. A-to-I editing challenger or ally to the microRNA process. Biochimie **89:**1171-6.

105.	**Otero, G. C., M. E. Harris, J. E. Donello, and T. J. Hope.** 1998. Leptomycin B inhibits equine infectious anemia virus Rev and feline immunodeficiency virus rev function but not the function of the hepatitis B virus posttranscriptional regulatory element. J Virol **72:**7593-7.

106.	**Park, J., and C. D. Morrow.** 1992. The nonmyristylated Pr160gag-pol polyprotein of human immunodeficiency virus type 1 interacts with Pr55gag and is incorporated into viruslike particles. J Virol **66:**6304-13.

107.	**Parker, R., and U. Sheth.** 2007. P bodies and the control of mRNA translation and degradation. Mol Cell **25:**635-46.

108.	**Pasquinelli, A. E., R. K. Ernst, E. Lund, C. Grimm, M. L. Zapp, D. Rekosh, M. L. Hammarskjold, and J. E. Dahlberg.** 1997. The constitutive transport element (CTE) of Mason-Pfizer monkey virus (MPMV) accesses a cellular mRNA export pathway. EMBO J **16:**7500-10.

109.	**Poiesz, B. J., F. W. Ruscetti, M. S. Reitz, V. S. Kalyanaraman, and R. C. Gallo.** 1981. Isolation of a new type C retrovirus (HTLV) in primary uncultured cells of a patient with Sezary T-cell leukaemia. Nature **294:**268-71.

110. **Prasanth, K. V., S. G. Prasanth, Z. Xuan, S. Hearn, S. M. Freier, C. F. Bennett, M. Q. Zhang, and D. L. Spector.** 2005. Regulating gene expression through RNA nuclear retention. Cell **123:**249-63.

111. **Purcell, D. F., and M. A. Martin.** 1993. Alternative splicing of human immunodeficiency virus type 1 mRNA modulates viral protein expression, replication, and infectivity. J Virol **67:**6365-78.

112. **Ramezani, A., X. Z. Ma, R. Nazari, and S. Joshi.** 2002. Development and testing of retroviral vectors expressing multimeric hammerhead ribozymes targeted against all major clades of HIV-1. Front Biosci **7:**a29-36.

113. **Rehwinkel, J., I. Behm-Ansmant, D. Gatfield, and E. Izaurralde.** 2005. A crucial role for GW182 and the DCP1:DCP2 decapping complex in miRNA-mediated gene silencing. RNA **11:**1640-7.

114. **Reinhart, B. J., F. J. Slack, M. Basson, A. E. Pasquinelli, J. C. Bettinger, A. E. Rougvie, H. R. Horvitz, and G. Ruvkun.** 2000. The 21-nucleotide let-7 RNA regulates developmental timing in Caenorhabditis elegans. Nature **403:**901-6.

115. **Rodriguez, A. J., J. Condeelis, R. H. Singer, and J. B. Dictenberg.** 2007. Imaging mRNA movement from transcription sites to translation sites. Semin Cell Dev Biol **18:**202-8.

116. **Roizman, B. a. P., P.** 1996. Multiplication of Viruses: An Overview, 3rd ed, vol. 1. Lippincott-Raven, Philadelphia.

117. **Rossi, J. J., C. H. June, and D. B. Kohn.** 2007. Genetic therapies against HIV. Nat Biotechnol **25:**1444-54.

118. **Saito, K., K. M. Nishida, T. Mori, Y. Kawamura, K. Miyoshi, T. Nagami, H. Siomi, and M. C. Siomi.** 2006. Specific association of Piwi with rasiRNAs derived from retrotransposon and heterochromatic regions in the Drosophila genome. Genes Dev **20:**2214-22.

119. **Satou, Y., J. Yasunaga, M. Yoshida, and M. Matsuoka.** 2006. HTLV-I basic leucine zipper factor gene mRNA supports proliferation of adult T cell leukemia cells. Proc Natl Acad Sci U S A **103:**720-5.

120. **Scherer, L. J., and J. J. Rossi.** 2003. Approaches for the sequence-specific knockdown of mRNA. Nat Biotechnol **21:**1457-65.

121. **Schutz, S., J. Chemnitz, C. Spillner, M. Frohme, J. Hauber, and R. H. Kehlenbach.** 2006. Stimulated expression of mRNAs in activated T cells depends on a functional CRM1 nuclear export pathway. J Mol Biol **358:**997-1009.

122. **Schwartz, S., B. K. Felber, E. M. Fenyo, and G. N. Pavlakis.** 1990. Env and Vpu proteins of human immunodeficiency virus type 1 are produced from multiple bicistronic mRNAs. J Virol **64:**5448-56.

123. **Schwartz, S., B. K. Felber, and G. N. Pavlakis.** 1992. Mechanism of translation of monocistronic and multicistronic human immunodeficiency virus type 1 mRNAs. Mol Cell Biol **12:**207-19.

124. **Senserrich, J., E. Pauls, M. Armand-Ugon, I. Clotet-Codina, G. Moncunill, B. Clotet, and J. A. Este.** 2008. HIV-1 resistance to the anti-

HIV activity of a shRNA targeting a dual-coding region. Virology **372:**421-9.

125. **Seraphin, B., and M. Rosbash.** 1989. Identification of functional U1 snRNA-pre-mRNA complexes committed to spliceosome assembly and splicing. Cell **59:**349-58.

126. **Sharmeen, L., B. Bass, N. Sonenberg, H. Weintraub, and M. Groudine.** 1991. Tat-dependent adenosine-to-inosine modification of wild-type transactivation response RNA. Proc Natl Acad Sci U S A **88:**8096-100.

127. **Sheehy, A. M., N. C. Gaddis, J. D. Choi, and M. H. Malim.** 2002. Isolation of a human gene that inhibits HIV-1 infection and is suppressed by the viral Vif protein. Nature **418:**646-50.

128. **Sheehy, A. M., N. C. Gaddis, and M. H. Malim.** 2003. The antiretroviral enzyme APOBEC3G is degraded by the proteasome in response to HIV-1 Vif. Nat Med **9:**1404-7.

129. **Sivan, G., N. Kedersha, and O. Elroy-Stein.** 2007. Ribosomal slowdown mediates translational arrest during cellular division. Mol Cell Biol **27:**6639-46.

130. **Smith, A. J., N. Srinivasakumar, M. L. Hammarskjold, and D. Rekosh.** 1993. Requirements for incorporation of Pr160gag-pol from human immunodeficiency virus type 1 into virus-like particles. J Virol **67:**2266-75.

131. **Stopak, K., C. de Noronha, W. Yonemoto, and W. C. Greene.** 2003. HIV-1 Vif blocks the antiviral activity of APOBEC3G by impairing both its translation and intracellular stability. Mol Cell **12:**591-601.

132. **Stoss, O., M. Olbrich, A. M. Hartmann, H. Konig, J. Memmott, A. Andreadis, and S. Stamm.** 2001. The STAR/GSG family protein rSLM-2 regulates the selection of alternative splice sites. J Biol Chem **276:**8665-73.

133. **Tagieva, N. E., and C. Vaquero.** 1997. Expression of naturally occurring antisense RNA inhibits human immunodeficiency virus type 1 heterologous strain replication. J Gen Virol **78 (Pt 10):**2503-11.

134. **Tang, J., and R. R. Breaker.** 2000. Structural diversity of self-cleaving ribozymes. Proc Natl Acad Sci U S A **97:**5784-9.

135. **Tassie, J. M., S. Grabar, R. Lancar, J. Deloumeaux, M. Bentata, and D. Costagliola.** 2002. Time to AIDS from 1992 to 1999 in HIV-1-infected subjects with known date of infection. J Acquir Immune Defic Syndr **30:**81-7.

136. **Taylor, S. J., M. Anafi, T. Pawson, and D. Shalloway.** 1995. Functional interaction between c-Src and its mitotic target, Sam 68. J Biol Chem **270:**10120-4.

137. **Taylor, S. J., and D. Shalloway.** 1994. An RNA-binding protein associated with Src through its SH2 and SH3 domains in mitosis. Nature **368:**867-71.

138. **Thermann, R., and M. W. Hentze.** 2007. Drosophila miR2 induces pseudo-polysomes and inhibits translation initiation. Nature **447:**875-8.

139. **Usui, T., K. Yanagihara, K. Tsukasaki, K. Murata, H. Hasegawa, Y. Yamada, and S. Kamihira.** 2008. Characteristic expression of HTLV-1 basic zipper factor (HBZ) transcripts in HTLV-1 provirus-positive cells. Retrovirology **5:**34.

140. **Vanhee-Brossollet, C., H. Thoreau, N. Serpente, L. D'Auriol, J. P. Levy, and C. Vaquero.** 1995. A natural antisense RNA derived from the HIV-1 env gene encodes a protein which is recognized by circulating antibodies of HIV+ individuals. Virology **206:**196-202.

141. **Vasudevan, S., Y. Tong, and J. A. Steitz.** 2007. Switching from repression to activation: microRNAs can up-regulate translation. Science **318:**1931-4.

142. **Vella, M. C., E. Y. Choi, S. Y. Lin, K. Reinert, and F. J. Slack.** 2004. The C. elegans microRNA let-7 binds to imperfect let-7 complementary sites from the lin-41 3'UTR. Genes Dev **18:**132-7.

143. **Vernet, C., and K. Artzt.** 1997. STAR, a gene family involved in signal transduction and activation of RNA. Trends Genet **13:**479-84.

144. **Veronese, F. D., A. L. DeVico, T. D. Copeland, S. Oroszlan, R. C. Gallo, and M. G. Sarngadharan.** 1985. Characterization of gp41 as the transmembrane protein coded by the HTLV-III/LAV envelope gene. Science **229:**1402-5.

145. **Wakefield, J. K., A. G. Wolf, and C. D. Morrow.** 1995. Human immunodeficiency virus type 1 can use different tRNAs as primers for reverse transcription but selectively maintains a primer binding site complementary to tRNA(3Lys). J Virol **69:**6021-9.

146. **Wehrly, K., and B. Chesebro.** 1997. p24 antigen capture assay for quantification of human immunodeficiency virus using readily available inexpensive reagents. Methods **12:**288-93.

147. **Willey, R. L., J. S. Bonifacino, B. J. Potts, M. A. Martin, and R. D. Klausner.** 1988. Biosynthesis, cleavage, and degradation of the human immunodeficiency virus 1 envelope glycoprotein gp160. Proc Natl Acad Sci U S A **85:**9580-4.

148. **Wolff, B., J. J. Sanglier, and Y. Wang.** 1997. Leptomycin B is an inhibitor of nuclear export: inhibition of nucleo-cytoplasmic translocation of the human immunodeficiency virus type 1 (HIV-1) Rev protein and Rev-dependent mRNA. Chem Biol **4:**139-47.

149. **Wong, S. K., and D. W. Lazinski.** 2002. Replicating hepatitis delta virus RNA is edited in the nucleus by the small form of ADAR1. Proc Natl Acad Sci U S A **99:**15118-23.

150. **Wu, L., J. Fan, and J. G. Belasco.** 2006. MicroRNAs direct rapid deadenylation of mRNA. Proc Natl Acad Sci U S A **103:**4034-9.

151. **Wyszko, E., M. Z. Barciszewska, R. Bald, V. A. Erdmann, and J. Barciszewski.** 2001. The specific hydrolysis of HIV-1 TAR RNA element

with the anti-TAR hammerhead ribozyme: structural and functional implications. Int J Biol Macromol **28:**373-80.

152. **Yamada, S., and S. Ohnishi.** 1986. Vesicular stomatitis virus binds and fuses with phospholipid domain in target cell membranes. Biochemistry **25:**3703-8.

153. **Yang, W., T. P. Chendrimada, Q. Wang, M. Higuchi, P. H. Seeburg, R. Shiekhattar, and K. Nishikura.** 2006. Modulation of microRNA processing and expression through RNA editing by ADAR deaminases. Nat Struct Mol Biol **13:**13-21.

154. **Yi, R., Y. Qin, I. G. Macara, and B. R. Cullen.** 2003. Exportin-5 mediates the nuclear export of pre-microRNAs and short hairpin RNAs. Genes Dev **17:**3011-6.

155. **Yin, H., and H. Lin.** 2007. An epigenetic activation role of Piwi and a Piwi-associated piRNA in Drosophila melanogaster. Nature **450:**304-8.

156. **Yu, W., D. Gius, P. Onyango, K. Muldoon-Jacobs, J. Karp, A. P. Feinberg, and H. Cui.** 2008. Epigenetic silencing of tumour suppressor gene p15 by its antisense RNA. Nature **451:**202-6.

157. **Zennou, V., C. Petit, D. Guetard, U. Nerhbass, L. Montagnier, and P. Charneau.** 2000. HIV-1 genome nuclear import is mediated by a central DNA flap. Cell **101:**173-85.

158. **Zhang, H., Y. Zhou, C. Alcock, T. Kiefer, D. Monie, J. Siliciano, Q. Li, P. Pham, J. Cofrancesco, D. Persaud, and R. F. Siliciano.** 2004. Novel single-cell-level phenotypic assay for residual drug susceptibility and reduced replication capacity of drug-resistant human immunodeficiency virus type 1. J Virol **78:**1718-29.

159. **Zhang, J., X. Sun, Y. Qian, and L. E. Maquat.** 1998. Intron function in the nonsense-mediated decay of beta-globin mRNA: indications that pre-mRNA splicing in the nucleus can influence mRNA translation in the cytoplasm. RNA **4:**801-15.

160. **Zhang, Z., and G. G. Carmichael.** 2001. The fate of dsRNA in the nucleus: a p54(nrb)-containing complex mediates the nuclear retention of promiscuously A-to-I edited RNAs. Cell **106:**465-75.

161. **Zolotukhin, A. S., A. Valentin, G. N. Pavlakis, and B. K. Felber.** 1994. Continuous propagation of RRE(-) and Rev(-)RRE(-) human immunodeficiency virus type 1 molecular clones containing a cis-acting element of simian retrovirus type 1 in human peripheral blood lymphocytes. J Virol **68:**7944-52.